Dissertation

Submitted to the

combined Faculties for the Natural Sciences and for Mathematics

of the Ruperto-Carola University of Heidelberg, Germany

for the degree of

Doctor of Natural Sciences

presented by

Diplom-Biologin   Kathrin Weißmüller
born in   Weilburg

Oral examination 03.07.2013

Analysis of the function of

histone deacetylases in neuro- and

gliogenesis in embryonic mouse forebrain

Referees:

Prof. Dr. Hilmar Bading

Prof. Dr. Joachim Kirsch

Zusammenfassung

Die Zielsetzung dieses Projektes war die Untersuchung der Rolle von Histondeacetylasen (HDACs) in der Neuro- und Gliogenese im embryonalen Mausvorderhirn.

Wir haben gezeigt, dass in sich differenzierenden neuralen Vorläuferzellen eine Reihe verschiedener HDACs exprimiert werden, und, dass die pharmakologische Hemmung von HDACs der Klassen I und II mittels Trichostatin A zu einer verringerten Neurogenese in den Basalganglien und vermehrter Astrogliogenese führt (Shaked et al. 2008).

Die Expression der meisten HDACs der Klassen I und II konnte im Cortex, den ganglionischen Eminenzen (GE) und im Hippocampus des Embryos nachgewiesen werden. Zum Zwecke eines tieferen Verständnisses der den Effekt von HDACs auf Neuro- und Astrogliogenese vermittelnden Signaltransduktionswege wurde die Expression relevanter Gene in E 15.5 GE-Neurosphärenkulturen untersucht. Dabei habe ich festgestellt, dass im Bmp2/4-Signalweg involvierte Gene transkriptionell durch HDACs reguliert werden, was zu einer Aktivierung dieses Pathways führt. Die astrogliogenen Transkriptionsfaktoren Stat1 und Stat3 wurden nach HDAC-Hemmung verstärkt exprimiert, was mit unserer Beobachtung einer erhöhten Astrogliogenese konsistent ist. In Zusammenarbeit mit Dr. Catharina Scholl wurden die beteiligten Pathways weiter mit Hilfe von Microarray-Genexpressionsanalysen beleuchtet.

Um die spezifische Rolle einzelner HDACs für die Neurogenese zu untersuchen, wurden die entsprechenden Gene mittels RNA-Interferenz reprimiert. Spezifische shRNA gegen HDAC1, -2, -4 und -5 wurde über lentivirale Vektoren in neurale Vorläuferzellen eingebracht und exprimiert. In allen Fällen fand sich unter den getesteten Oligonucleotiden eine Sequenz, die die Transkription um mindestens 50% reduzierte. Allerdings zeigte sich durch Real Time RT-PCR, dass die Oligos unspezifisch auch die Expression anderer HDACs beeinflussten. HDAC2-Knock-down konnte auf der Transkript- und Proteinebene nachgewiesen werden, allerdings ohne beobachtbare Auswirkungen auf Neuro- oder Gliogenese.

In jüngerer Vergangenheit erzeugte HDAC-Knockouts in Mäusen bieten vielfältige Möglichkeiten zur Untersuchung der Effekte einzelner HDACs auf die Bildung von Neuronen und Glia. Die HDACs 4 und 5 werden stark im Gehirn exprimiert, weswegen ich dessen Entwicklung und Morphologie in Mausmutanten untersucht habe, die diese Enzyme nicht mehr exprimieren.

Die detaillierte Analyse der subzellulären Lokalisation von HDAC4 zeigte, dass das Enzym in den neurogenen Regionen des sich entwickelnden Gehirns vorhanden ist, worauf die Zellproliferation in der ventrikulären und subventrikulären Zone (SVZ) von HDAC4-Null-Mäusen weiter untersucht wurde. Im rostralen Cortex konnte ein leichter Anstieg der Proliferation beobachtet werden, nicht jedoch bei den basalen Vorläuferzellen der SVZ.

Da ich festgestellt habe, dass HDAC5 sowohl in der Kortikal- als auch in der Subplatte exprimiert wird, beschloss ich, die kortikale Schichtung der HDAC5-Mutanten zu untersuchen. Hierbei zeigten sich keine Unterschiede in der Expression spezifischer Schichtmarker zwischen dem Wildtyp und der HDAC5-Null-Mutante.

Summary

In this project the role of histone deacetylases (HDACs) in neuro- and gliogenesis in embryonic mouse brain was investigated. We could show that in differentiating neural progenitor cells many different HDACs are expressed and that pharmacological inhibition of class I and II HDACs with trichostatin A led to a decrease in neurogenesis in the basal ganglia and an increase in premature astrogliogenesis (Shaked et al 2008). The expression of most class I and II HDACs could be confirmed in embryonic cortex, GE and hippocampus.

To better understand which signaling pathway is mediating the effect of HDACs on neuro- and astrogliogenesis, a real time RT-PCR analysis of candidate genes was carried out using neurosphere cultures derived from E 15.5 ganglionic eminence (GE). I found genes involved in Bmp2/4 signalling to be transcriptionally regulated upon HDAC inhibition, hints to the assumption that inhibition of HDACs by TSA releases an inhibition of BMP signalling. Stat1 and Stat3, transcription factors known to promote astrogliogenesis, were upregulated upon HDAC inhibition which corresponds to our observation of an increase in premature astrogliogenesis. The analysis of signaling pathways was further complemented by a microarray gene expression study carried out in collaboration with Dr. Catharina Scholl.

In order to understand which HDACs are responsible for the effect on neurogenesis, RNA interference was used to inhibit the expression of individual HDAC genes. ShRNA against HDAC1, -2, -4, and -5 was generated and expressed in neural precursor cultures via lentiviral vectors. For all HDACs examined one shRNA oligo was found which knocked down transcription by at least 50%. However, real time RT-PCR revealed that the oligos also influenced expression of non-target HDACs. Knock-down of HDAC2 could be confirmed on the RNA and protein level, however, no effect on neuro- and gliogensis could be observed upon shRNA knock down of HDAC2.

Recently generated knockout mouse models of individual HDAC genes provide a powerful tool to analyze the effect of individual HDACs on neuro- and gliogenesis.

HDAC4 and -5 show high expression levels in brain tissue, therefore I investigated brain development and morphology in mutant animals deficient in these enzymes.

A detailed analysis of the subcellular localization of HDAC4 revealed the presence of the enzyme in neurogenic regions of the developing brain, therefore proliferation in the ventricular zone and basal progenitors in the SVZ were subsequently examined in Hdac4$^{-/-}$. A slight increase in proliferation in rostral cortex could be observed, but no change in basal progenitors.

I found HDAC5 to be expressed in the cortical plate and subplate and decided to examine cortical layering in HDAC5 mutants. No difference in the expression of specific layer markers could be observed between wildtype and Hdac5 null mouse.

Table of contents

11

Table of Figures

14

List of Abbreviations

ΔCT	Difference between the CT-value of the gene of interest and the control (housekeeping) gene
aHDAC1o1	shRNA directed against HDAC1, oligo number 1
APS	Ammoniumpersulfate
bHLH	Basic helix-loop-helix (transcription factors)
bp	Base pairs
BRE	Bmp-responsive element
BSA	Bovine serum albumin
CaMK	Calcium/calmodulin-dependent protein kinase
CBP	CREB-binding protein, a HAT and coactivator of transcription
cDNA	Copy DNA
CHX	Cycloheximide
CNS	Central nervous system
CP	Cortical plate
CT	Cycle of threshold: cycle of the real time RT-PCR, in which the enzyme-substrate curve changes from the linear to the Plateau-phase)
DAPI	4',6-diamidino-2-phenylindole, fluorescent dye binding AT-rich regions of DNA
DIV	Day *in vitro*
DMEM	Dulbecco's modified Eagle medium
DMSO	Dimethylsulfoxide
dNTP	Deoxyribunucleotide-Triphosphate
dpc	Days post coitum
E	Embryonic day
EDTA	Ethylendiamine-tetraacetate
EGF	Epidermal growth factor
EGFP	enhanced green fluorescent protein
et al.	et alteri
FCS	Fetal calf serum
FACS	Fluorescence activated cell sorting

FGF	Fibroblast growth factor
GABA	Gamma-aminobutyric acid
GE	Ganglionic emineces
GFP	Green fluorescent protein
HAT	Histone acetyltransferase
HDAC	Histone deacetylase
HEK	Human embryonic kidney
HMFM	Hogness modified freezing medium
HRP	Horse radish peroxidise
IKNM	Interkinetic nuclear migration
IPC	Intermediate progenitor cell
LGE	Lateral ganglionic eminence
M	Mol per liter
mA	Milliampere
MEF	Mouse embryonic fibroblast
MEF2	Myocyte enhancer factor 2
MGE	Medial ganglionic eminence
mM	Millimol per liter
MP	Medial pallium
mRNA	Messenger RNA
MZ	Marginal zone
NICD	Intracellular domain of Notch
NP	Neural precursor
NS	Neurosphere
P	Postnatal day
PBS	Phosphate buffered saline
PFA	Paraformaldehyde
PH3	Phospho histone H3
PKD	Protein kinase D
PMSF	Phenylmethylsulfonyl fluoride (serine protease inhibitor)
PP	Preplate
RG	Radial glia

RIPA	Radio immunoprecipitation assay
Rpm	Rounds per minute
RT	Room temperature
RT-PCR	Reverse transcription polymerase chain reaction
SAHA	Suberoylanilide hydroxamic acid (Vorinostat)
SDS	Sodium dodecyl sulfate
shRNA	Short hairpin RNA
SP	Subplate
SVZ	Subventricular zone
TBS	Tris buffered saline
TBST	Tris buffered saline /Tween-20
TRC	The RNA consortium
TSA	Trichostatin A
V	Volt
VPA	Valproic acid
VZ	Ventricular zone

1   Introduction

The central nervous system (CNS) of mammals is composed of the brain and the spinal cord. It is responsible for processing and distributing information, as well as for coordinating and maintaining vital functions of the organism.

The development of the nervous system in mammals is a complex and tightly regulated procedure where several processes need to be adjusted to each other and have to take place in a coordinated manner. Expression of relevant genes has to occur in a coordinated manner. Relevant genes must be expressed in a temporally and spatially regulated pattern in order to ensure correct development, positioning and differentiation of all the cell types of the nervous system. Epigenetic factors are crucial for the regulation of gene expression providing various possibilities to regulate developmental processes.

1.1   Development of the nervous system

Development of the nervous system begins with neural induction, based on inhibition of BMP signals in the ectoderm. Neurulation is induced by signals from the notochord ventral of the neural plate and gives rise to the neural folds and eventually neural tube. The neural tube is patterned along the anterior-posterior axis of the embryo, which leads to establishment of distinct regions with a specific fate: the prosencephalon or forebrain (telencephalon and diencephalon), mesencephalon (midbrain) and rhombencephalon (hindbrain).

The cerebral cortex arises from the dorsal telencephalic neuroepithelium (Bayer 1991). The striatum develops from the ganglionic eminences which are located ventrally in the telencephalic vesicle (Smart 1979).

1.1.1   Cortical neurogenesis

The cerebral cortex is the area of consciousness and cognitive functions in the mammalian brain. It is the most complex structure of the central nervous system and

comprises a large variety of cells organized in a spatially and temporally precisely regulated manner.

Neurons in the neocortex are born by proliferating radial glia cells (Anthony et al 2004, Hartfuss et al 2001, Malatesta et al 2003, Malatesta et al 2000), either directly generated in asymmetric divisions in the ventricular zone or deriving from symmetrically-dividing basal progenitors in the subventricular zone (Figure 1.1).
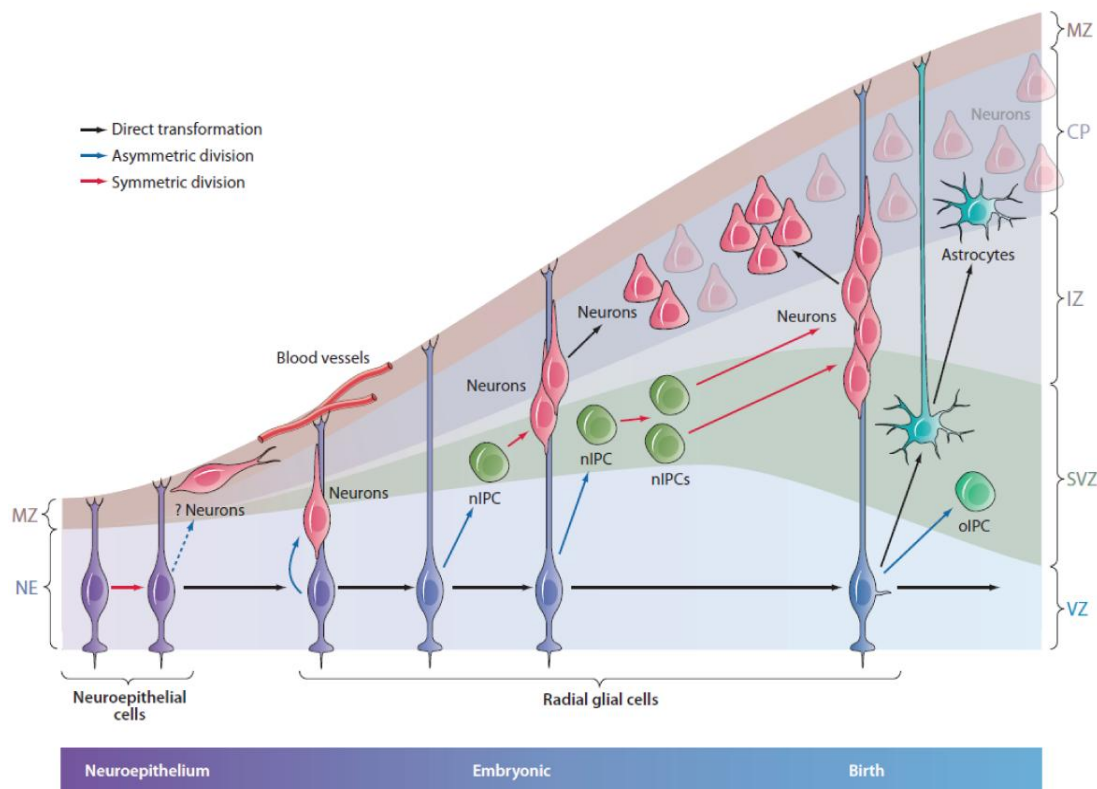
Figure 1.1. Neurogenesis in the embryonic brain. Neurons are born directly from asymmetric cell divisions of radial glia in the ventricular zone of the developing neocortex. These also give rise to intermediate progenitor cells (nIPCs) in the subventricularzone which then divide symmetrically into new neurons, which is considered the indirect mode of neurogenesis. Later in development, radial glia generate macroglial cells (astrocytes and oligodendrocytes) (Kriegstein & Alvarez-Buylla 2009)

The intermediate or basal progenitors (IPs) are also derived from radial glial cells (Haubensak et al. 2004; Miyata et al. 2004; Noctor et al. 2004). Most of them only divide once, generating 2 neuronal daughter cells, only few IPs undergo up to 3 rounds

of proliferation and thereby amplify the output of certain neuron types at specific stages of cortical development (Haubensak, Attardo et al. 2004; Miyata, Kawaguchi et al. 2004; Noctor, Martinez-Cerdeno et al. 2004).

Radial glia and IPs differ in their profile of transcription factor expression. Radial glia express Pax6, which has been shown to be a marker for their neurogenic potential (Gotz et al. 1998; Heins et al. 2002) and Hes family transcription factors (Englund et al 2005, Ohtsuka et al 2001). Intermediate precursors in contrast express, among others, Tbr2, which is considered to be a specific marker for this population (Englund et al 2005), Cux1 and Cux2 (Nieto et al 2004), Ngn2 (Miyata et al 2004), Svet1 (Tarabykin et al 2001) and Insm1 (Farkas et al. 2008). Projection neurons in the cerebral cortex are pyramidal neurons which use glutamate as their transmitter. They send axonal projections to cortical, subcortical and subcerebral targets.

In the adult, cortical neurons are arranged in 6 clearly distinguishable layers (Figure 1.2). The layers are generated in an inside-out manner with the inner cortical layers generated first, whereas the neurons of the outer layers are born later and migrate through the previously formed layers to their final locations (Nowakowski et al 2002, Rakic 1974).

At around Embyronic day (E) 11.5 in mouse, progenitors assume radial glia morphology. In asymmetric division they generate neurons, which migrate to the mantle layers guided by radial glia. The first projection neurons settle within the preplate to form the nascent cortical plate, which will subsequently become layers 2 to 6 of the neocortex. Additional incoming cortical plate neurons then split the preplate into the marginal zone and the subplate. Migration of newborn neurons into the cortical plate occurs in an inside-first, outside-last manner; early-born neurons form the deep layers, whereas later-born neurons migrate past older neurons to form the more superficial layers. The cells of the individual cortical layers display discrete molecular and functional properties (Arlotta et al 2005, Hevner 2006, Hevner et al 2003).

At the end of neurogenesis, around E17.5, neural precursor cells become gliogenic, generating cortical and subependymal zone astrocytes and giving rise to a layer of ependymal cells (Kwan et al. 2012).
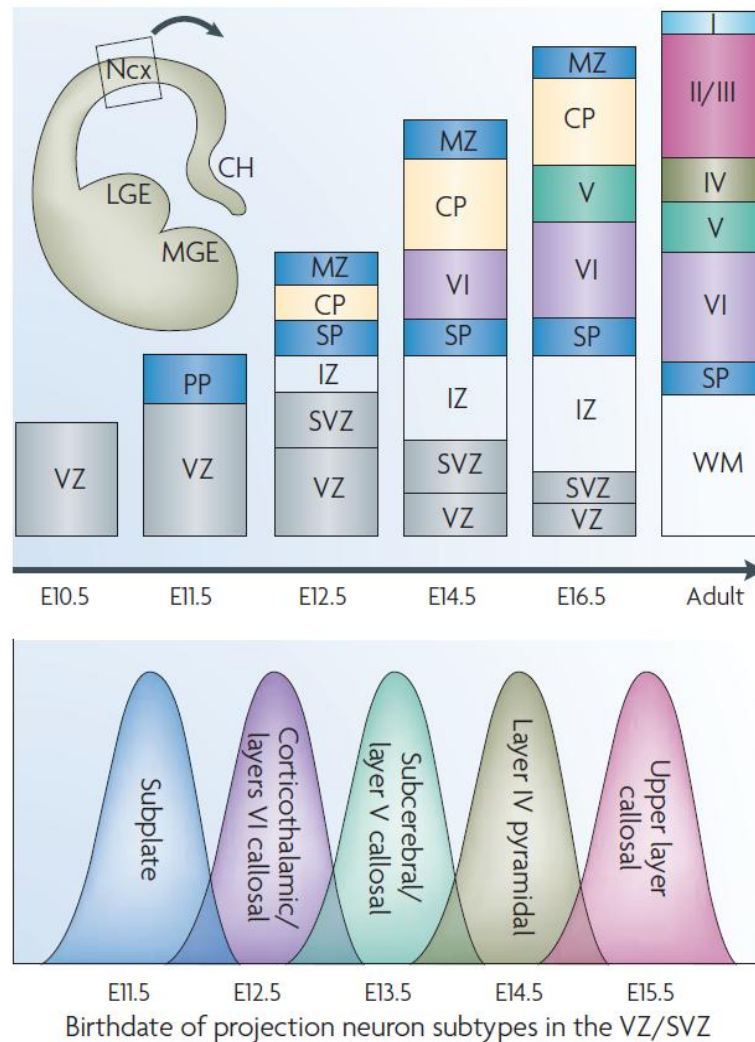
Figure 1.2. Generation of projection neurons in developing mouse cortex in an inside-out-mode. The preplate consists of early born neurons and is divided into marginal zone and subplate. The cortical plate develops between these two layers and generates most layers of the neocortex. Different subtypes of projection neurons are born at different times in cortical development (Molyneaux et al 2007).

1.1.2   Striatal neurogenesis

The mature striatum shows variability between adults of different mammalian species, however, the initial development of the structure is similar. It develops from the ganglionic eminences (GE) which are situated in the ventral telencephalon. The ganglionic eminences are morphologically divided into the lateral ganglionic eminence (LGE) and the medial ganglionic eminence (MGE).

The MGE develops earlier and generates cholinergic interneurons of the striatum, pallidum and basal forebrain (Olsson et al. 1998; Marin et al. 2000). Most striatal interneurons migrate tangentially from the MGE or adjacent preoptic/anterior entopeduncular areas and express the NKX2.1 homeodomain protein (Marin, Anderson et al. 2000).

Neurogenesis in the ventral neuroepithelium takes place in the ventricular and the subventricular zone (Halliday and Cepko 1992) (Figure 1.3).
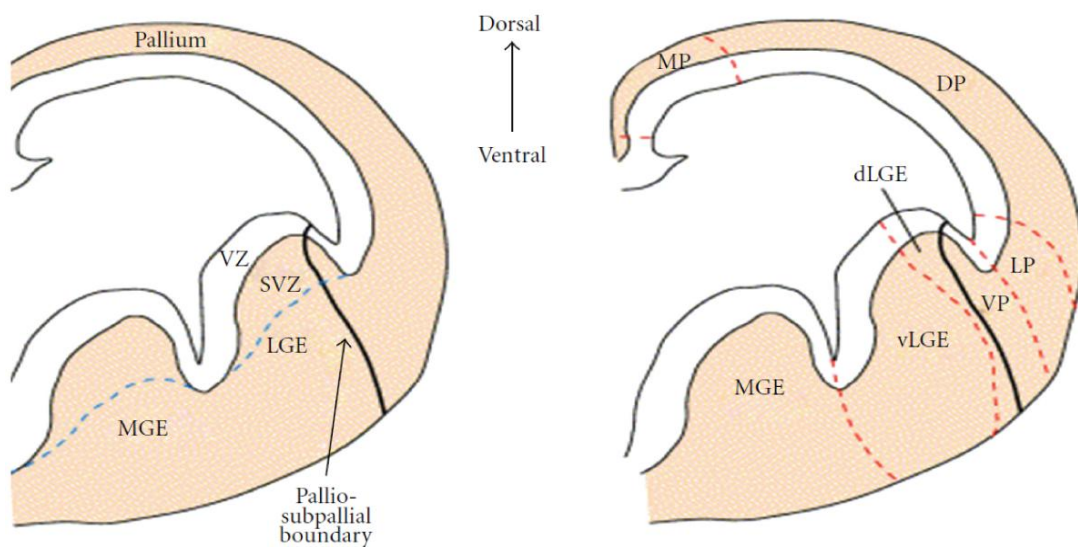
Figure 1.3. Coronal hemisections of E12.5 mouse telencephalon illustrating areas of neurogenesis in the ventral telencephalon. Progenitor cells migrate radially and tangentially from these areas populating their target areas. MGE/LGE: medial/lateral ganglionic eminence; MP: medial pallium; DP: dorsal pallium; LP: lateral pallium; VP: ventral pallium (Olsson et al 1998)

Neuroepithelial cells divide asymmetrically into one neuroblast and another neuroepithelial cell. Neuroblasts exit the cell cycle and migrate laterally into the mantle zone to undergo terminal differentiation. LGE and MGE cells migrate along different routes to populate distinct regions in the developing brain.

Early in development neurons born in the MGE migrate dorsally and invade the developing neocortex through the neocortical subventricular zone. They differentiate into the transient subpial granule neurons in the marginal zone and into a stable

population of GABA-, parvalbumin- or somatostatin-expressing interneurons throughout the cortical plate (Anderson et al 2001, Wichterle et al 2001).

Later in neurogenesis, LGE-derived cells also migrate into the cortex, mainly through the subventricular zone. Some of these LGE-derived cells invade the cortical plate and express GABA, while others remain within the cortical proliferative zone and appear to become mitotically active late in gestation (Anderson et al 2001). LGE neurons also migrate ventrally and anteriorly, and give rise to the projecting medium spiny neurons in the striatum, nucleus accumbens and olfactory tubercle, and to granule and periglomerular cells in the olfactory bulb (Wichterle et al 2001).

Radial glia also contribute to neurogenesis is the ganglionic eminences (Anthony et al 2004). Taken together, striatal neurogenesis is crucial not only for the proper functioning of the basal ganglia, but also of the cerebral cortex.

1.1.3   Differentiation in cortex and GE

The generation of new neurons and macroglial cells (astrocytes and oligodendryocytes) by progenitor cells in the developing vertebrate central nervous system requires a number of precisely orchestrated steps. As stated before, the neurogenic regions in cortex and GE differ in their expression of transcription factors and proneural genes. This reflects the specificity of neurogenesis in both regions.

Progenitors undergo a last cell division and become committed to their post-mitotic fate (Edlund & Jessell 1999). This process is influenced by various transcription factors leading to regional and time-specific differentiation. Post-mitotic neurons migrate out of the neurogenic regions along specific routes and begin to differentiate (reviewed in (Edlund & Jessell 1999, Marin et al 2010)). Proneural transcription factors of the bHLH family are expressed in proliferating progenitors and play an important role regulating the neurogenic differentiation program (Bertrand et al 2002, Powell & Jarman 2008).

Pax6 and Ngn2 are expressed in the dorsal telencephalon and contribute to a cortical differentiation program. Markers for this differentiation are, among others, the transcription factors Math2/3, NeuroD1/2, and Tbr1/2. In the ventral telencephalon

Mash1 and Nkx2.1 are expressed, steering differentiation towards a striatal pattern marked by the expression of the homeobox genes Dlx1/2, Dlx5/6, and Gsh1/2 (Guillemot et al. 2006).

1.1.4   Gliogenesis

There are three types of glial cells in the central nervous system: astrocytes, oligodendrocytes and microglia. Astrocytes and oligodendrocytes are also referred to as macroglia, both deriving from radial glia precursor cells in development. Microglia, the smallest glial cells have a different origin. They are generated by macrophages outside the nervous system.

Astrocytes have a distinct asterisk-like morphology, hence the name. Their processes have broad end-feet. Astrocytes provide structural and metabolic support to neurons. The cell body of oligodendrocytes is comparatively small; their processes however are extensive and form myelin sheaths around axons.

In mammals, macroglial cells are generated by the same precursors as neurons: radial glia. They are first born late in gestation and until after the birth of the animal (Bayer 1991). During neurogenesis, astrogliogenesis is actively repressed by the proneural bHLH transcription factors Ngn2 and Mash1 whose expression is induced by neurogenic factors such as BMPs (Tomita et al. 2000; Nieto et al. 2001).

It is not completely understood how the precursor cell population switches from a neurogenic to a gliogenic programme. Several pathways are known to promote gliogenesis. Notch signaling (Gaiano and Fishell 2002), as well as JAK/STAT signaling (Bhat 1995; Bonni et al. 1997; Barnabe-Heider et al. 2005) are known to induce gliogenesis. Both leukemia inhibitory factor (LIF) and ciliary neurotrophic factor (CNTF) activate the JAK/STAT pathway. Upon activation of the JAK/STAT pathway, Stat proteins are phosphorylated and recruited by transcription factors. The Stat complex is then targeted to promoters of genes involved in gliogenesis.

Another signaling cascade involved in astrogliogenesis is the bone morphogenetic protein (BMP) pathway (Bonaguidi et al 2005, Gross et al 1996)). BMPs activate the

Smad1/5/8 pathway. They also induce the transcription factors Hes5, Id1 and Id3 which antagonize the pro-neurogenic activity of Ngn1 (Nakashima et al 2001). All signaling pathways involved act upon the promoter of glial fibrillary acidic protein (GFAP) (Nakashima et al. 1999) (Figure 1.4).
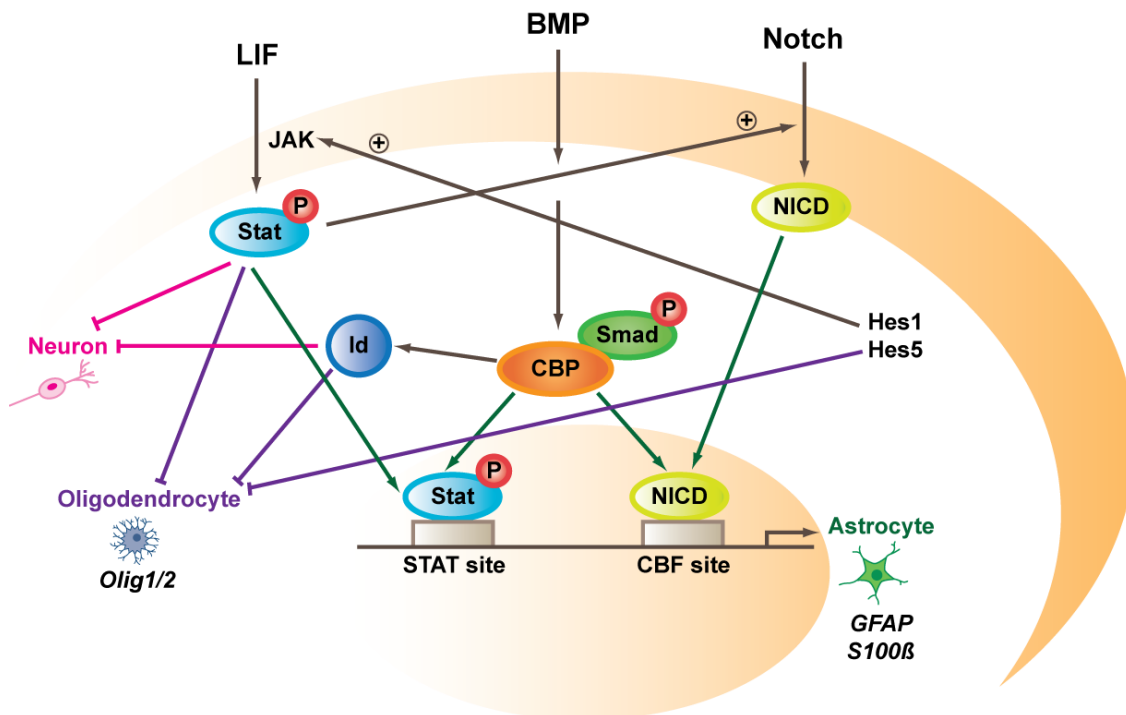
Figure 1.4. Signaling pathways and transcription factors involved in gliogenesis (adapted from (He & Sun 2007))

Just as neurons and astrocytes, oligodendrocytes are generated by multipotent precursor cells throughout the CNS (Casper & McCarthy 2006, Fogarty et al 2005). In ventral telencephalon the Dlx homeobox transcription factors Dlx1 and Dlx2 were found to suppress the generation of Olig2-dependent oliodendrocytes (Petryniak et al 2007)

The first cortical oligodendrocytes are born from Nkx2.1-expressing precursor cells in the ventricular zone of the MGE (Spassky et al 1998, Tekki-Kessaris et al 2001). They can be detected in cortex around E16. The second population is derived from cells in the LGE and migrates dorsally into the cortex (Kessaris et al. 2006). The third population of cortical oligodendrocytes arises within the cortex itself, the cells are detected around embryonic day 18 and are derived from Emx1-positive precursors (Gorski et al. 2002; Kessaris, Fogarty et al. 2006). These cells, in contrast to the ventrally derived ones,

persist until after birth and therefore provide for the majority of cortical oligodendrocytes.

It could be shown that neural progenitors not only generate neurons and microglia in the developing brain, but retain properties of neural stem cells in the postnatal brain (Alvarez-Buylla et al 1990, Doetsch et al 1999).

1.2   Neurosphere cultures as a model system

To determine the influence of histone deacetylases on neuro- and gliogenesis *in vitro*, neurosphere cultures were chosen as a model system to generate a uniform population of precursors which can generate neurons and microglia. Neurospheres are derived from neural stem and progenitor cells from the adult or fetal central nervous system or embryonic stem (ES) cells (Gritti et al. 1996; Tropepe et al. 1999; Tropepe et al. 2001). We used a protocol described by Reynolds and Weiss (Gritti et al 2001, Reynolds & Weiss 1992, Reynolds & Weiss 1996). The cells are derived from medial and lateral ganglionic eminences, dissociated to a single cell suspension and plated in medium supplemented with B27, fibroblast growth factor 2 (FGF2) and epidermal growth factor (EGF) (Vescovi et al 1993). The cells continue to proliferate in culture and form non-adherent spherical clusters of cells which are able to generate the major cell types of the CNS. They provide a powerful tool to analyze differentiation and lineages.

 The neurosphere culture system is sensitive to small deviations in the culturing methods. Variations in cell density for instance alter the microenvironment in the cultures, affecting proliferation capacity and positional cues (Hack et al. 2004). Concentrations of the factors in the media and dissociation of the spheres before differentiation influence neurosphere composition and properties of the cells.

One must be aware of those factors capable of causing subtle or pronounced changes in the cultures when comparing data generated with different protocols in different groups. The neurosphere culture does not completely reflect the situation of the progenitor cells *in vivo*. It could be shown that telencephalic transcription factors are downregulated upon treatment with growth factors EGF and FGF2 (Hack et al. 2004).

1.3   Chromatin Modification

1.3.1   General aspects of chromatin modification

The modification of chromatin is a central aspect of the regulation of gene transcription in eukaryotic cells. DNA is wound around histone cores in the nucleus and can assume different grades of compaction. Epigenetic modifications influence condensation patterns of the chromatin and thereby change accessibility of the DNA for transcription factors. There is increasing evidence that genes involved in brain development are not only regulated via transcription factors but are subject to regulation on an epigenetic level (Jenuwein and Allis 2001).

Robin Holliday defined epigenetics as "the study of the mechanisms of temporal and spatial control of gene activity during the development of complex organisms" (Holliday 1990), which includes everything but the DNA sequence itself that can influence the development of an organism. Later on, other definitions were proposed; a recent one was put forward during a 2008 Cold Spring Harbour meeting. It defines epigenetics as a "stably heritable phenotype resulting from changes in a chromosome without alterations in the DNA sequence" (Berger et al 2009). Epigenetic modifications do not change the DNA sequence, but can modify activity of certain genes, either by modifications to the DNA or to nucleosomal proteins. These processes are summarized as chromatin remodeling. Epigenetic changes are preserved when cells divide; in the case of gene inactivation they can be even transferred to the next generation (Chandler 2007).

Eukaryotic DNA is packaged with the help of histones, small basic proteins. The basic unit of packaging is called nucleosome. It consists of a disc-like structure containing 2 copies of each core histone H2A, H2B, H3 and H4 and 147 bp of DNA wrapped around the histone core almost two times (Figure 1.5). Histones consist of a globular domain and a charged NH2-terminus protruding from the nucleosome. Linker histones H1 and H5 bind to the nucleosomes and the linker DNA (20-80 nucleotides) between the nucleosomes. The structure formed by DNA wrapped around histone cores interspersed with linkers, resembling beads on a string, constitutes the 10 nm fiber. Further

compaction arranges the nucleosomes in a helical way in close contact forming the 30 nm fiber.

The binding of DNA and histones is achieved through ionic bonds between basic residues in the histones and the acidic sugar-phosphate backbone of the DNA (Luger et al 1997).
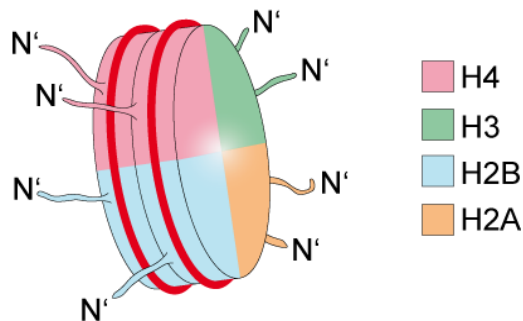
Figure 1.5. Nucleosome consisting of two copies of each core histone H4, H3, H2B and H2A and 147 bp of DNA wrapped around this core. The N-termini of the histones are the most important sites for histone modifications.

Chromatin remodeling is accomplished through two major mechanisms. Firstly, DNA is methylated, mostly at CpG sites, converting cytosine to 5-methylcytosine. Highly methylated areas of the genome were found to be less transcribed. Methylation is also involved in genetic imprinting where alleles are silenced in the germline and genes are therefore expressed only from the non-imprinted allele received from one parent.

The second mechanism of chromatin remodeling is actually an array of different posttranslational modifications to the histone proteins. The best known modifications include acetylation, methylation, ubiquitylation, phosphorylation and sumoylation (Figure 1.6). Histone modifications can be found throughout the protein sequence, however the N-termini of the histones are most frequently modified.
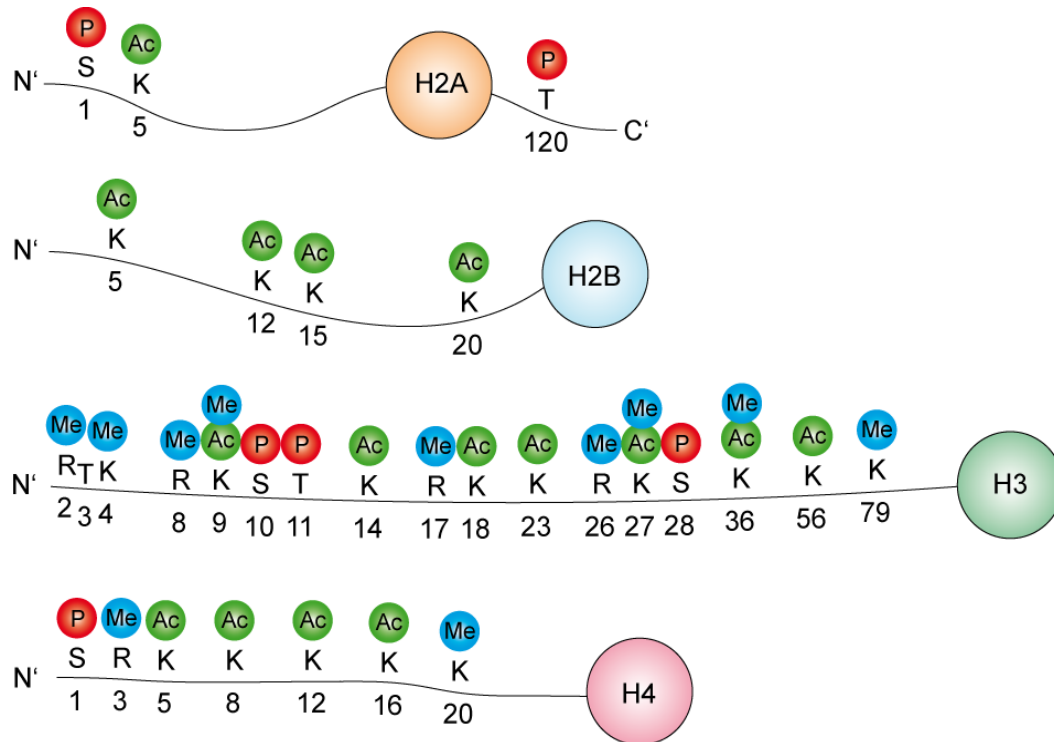
Figure 1.6. Specific sites of histone modifications in the amino-termini of core histones. Histone tails can be subjected to a large number of posttranslational modifications. Acetylation, methylation and phosphorylation are probably the most commonly known ones.

It was proposed by Jenuwein and Allis (2001) that different combinations of chromatin modifications constitute a code extending the amount of information stored in the genetic sequence and providing a mechanism important for gene regulation, DNA repair, mitosis and meiosis and on a larger scale for the regulation of cell fate and development.

Acetylation and deacetylation occur on lysine residues in the N-terminal tails of histones. Histone acetyltransferases (HATs) add acetyl groups to the ε–amino groups of lysine moieties, histone deacetylases (HDACs) remove these residues (Figure 1.7). Both processes are highly regulated.
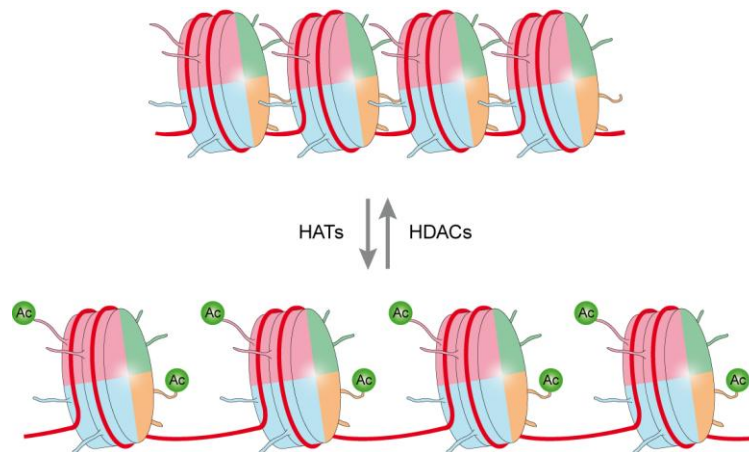
Figure 1.7. Histone acetylation and deacetylation alters the structure of the chromatin.
Addition of acetyl groups to the histone tails decreases the binding affinity between histones and DNA

The acetyl-group is derived from Acetyl-Coenzyme A and is transferred to Coenzyme A (Figure 1.8). Already in 1964, Allfrey et al. found histone acetylation to be related to transcription (Allfrey et al 1964). Specific sites of acetylation are associated with transcriptional activation or silencing. One example is acetylation of lysines 9 and 14 (K9 and K14) in histone H3 which is correlated with transcriptional activity.
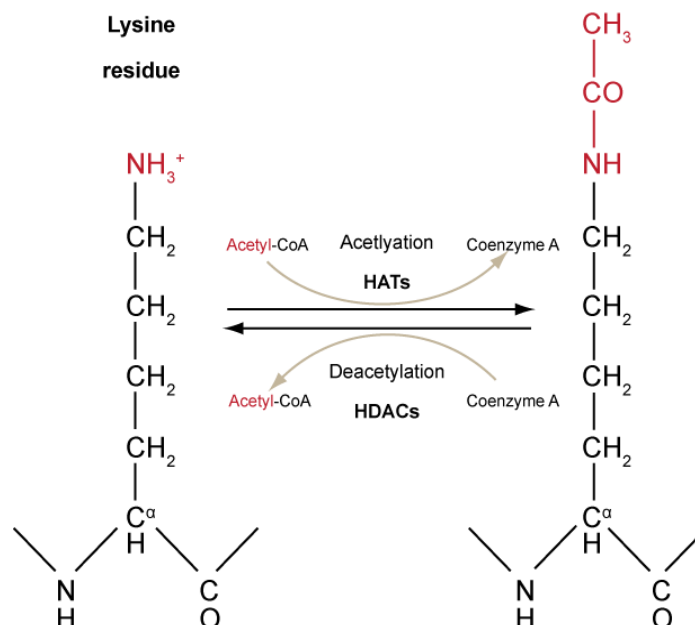
Figure 1.8. Acetylation of lysine residues in histone tails is carried out by histone acetyltransferases (HATs) using acetyl-CoA as the donor of the acetyl moiety. Acetyl groups are removed by histone deacetylases (HDACs).
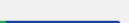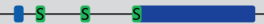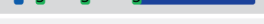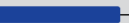
Lysine has a positively charged nitrogen atom at the end of the residue, which facilitates binding with the negatively charged phosphates in the backbone of DNA. Acetylation replaces the positive charge with a neutral amide moiety, which loosens the DNA from the histone core (Grunstein 1997, McGhee & Felsenfeld 1980). It was believed that acetylation therefore always opens the tightly packed chromatin structure and facilitates transcription (Cheung et al 2000), enabling transcription factors to bind more easily to the DNA (cis), but this was found not always to be the case (Berger 2007). Acetylation can also create a new binding site for chromatin modifying enzymes which can themselves act on the state of the chromatin (trans).

Along the same lines, hypoacetylation of histones was found to correlate closely with gene silencing (Lee & Workman 2007).

There are both nuclear and cytoplasmic HATs. The cytoplasmic enzymes acetylate histones before nuclear import and assembly of chromatin. Nuclear HATs acetylate histones after the assembly of chromatin and thereby influence chromatin-based processes such as gene transcription.

1.3.2   Classes of mammalian histone deacetylases

Histone deacetylases are a large family of enzymes present in both prokaryotes and eukaryotes. In mammals 11 HDAC genes with a highly conserved deacetylase domain are found and categorized as the classical HDACs. Those are grouped in four classes, class I, class IIa, class IIb and class IV (Figure 1.9). Another family, the Sir2 (silent information regulator)-like family of NAD^+-dependent deacetylases or in brief sirtuins, are also referred to as class III HDACs. They differ in their structure and mechanism of deacetylation from the classical HDACs. Also, the classical HDACs differ in their structure, subcellular localization and expression pattern as well as their enzymatic function and activity. HDACs deacetylate their substrate by activating a water molecule via a divalent zinc ion coupled to a histidine-aspartate charge-relay system (Finnin et al 1999), whereas sirtuins use a different, NAD^+-dependent mechanism.

	Time of lethality	Phenotype
Class I HDAC1–[SS]—482	E10.5	Proliferation defects
HDAC2–[SS]—488	P1	Cardiac malformation
HDAC3–[S]–428	E9.5	Gastrulation defects
HDAC8–[S]—377	P1	Craniofacial defects
Class IIa HDAC4 —[S]—[S]—[S]—1084	P7-P14	Chondrocyte differentiation defect in growth plate
HDAC5—[S]—[S]—[S]—1122	Viable	Exacerbated cardiac hypertrophy after stress
HDAC7—[SS]—[S]—[S]—912	E11	Endothelial dysfunction
HDAC9—[S]—[S]—[S]—1069	Viable	Exacerbated cardiac hypertrophy after stress
Class IIb HDAC6 —[ZnF]—1215	Viable	Increased tubulin acetylation
HDAC10—[Leucine rich]—669	ND	-
Class IV HDAC11–347	ND	-

Figure 1.9. Mammalian classes of HDACs. There are four classes of classic HDACs in mammals that can be distinguished by their sequence and domain structure. Modified from (Haberland et al 2009).

1.3.2.1   Class I HDACs

Class I consists of HDAC1, -2, -3 and -8. These HDACs localize to the nucleus where HDAC1, -2 and -3 were found to be parts of large transcriptional repressor complexes. HDAC1 and -2 for instance are part of the Co-REST complex which inactivates the expression of neuronal genes in non-neuronal tissues (Huang et al 1999). HDAC1 also associates with the methylCpG-binding protein MeCP2, providing a functional link between DNA methylation and histone modification (Tucker 2001). Class I HDACs are ubiquitously expressed in many tissues.

1.3.2.2   Class IIa HDACs

HDAC class IIa consists of HDAC4, -5, -7 and -9. These enzymes have a large N-terminal domain with 3-4 binding sites for 14-3-3 proteins which regulates the shuttling between nucleus and cytoplasm. Binding of 14-3-3 proteins can, depending on their phosphorylation state, either stimulate nuclear export or cytoplasmatic retention. CaM-kinases (McKinsey et al 2000) as well as several other kinases regulate phosphorylation of the 14-3-3 binding sites and thereby influence the subcellular localization.

1.3.2.3   Class IIb HDACs

This class consists of HDAC6 and -10. HDAC6 has two deacetylase domains and a C-terminal zinc finger domain. It has an important function in the cytoplasm deacetylating α-tubulin and Hsp90 (Hubbert et al 2002, Kovacs et al 2005), which regulates cell motility and adhesion as well as exhibits chaperone function. The function of HDAC10 is not well understood.

1.3.2.4   Class IV HDACs

Class IV consists of only one enzyme, namely HDAC11. Its expression patterns and function are not yet understood.

1.3.3   Functions of histone deacetylases

Histone deacetylases do not bind DNA directly. They associate with transcriptional activators and repressors and are part of large multiprotein complexes regulating transcription (Grunstein 1997, Heinzel et al 1997, Shahbazian & Grunstein 2007). The specificity of their activity largely depends on interaction partners in individual cells and tissues. Deacetylation of histones in promoters is generally associated with the formation of heterochromatin and transcriptional inactivation, yet some genes were found to be activated by HDACs (Nusinzon & Horvath 2005).

Apart from histones, also other proteins in the cytoplasm can be deacetylated by HDACs. Inhibition of histone deacetylases has been shown to significantly affect the acetylation of various tissue-specific or ubiquitous non-histone proteins such as p53 (Gu & Roeder 1997, Juan et al 2000), c-Myb (Tomita et al 2000), PCNA (Naryzhny & Lee 2004) and α-tubulin (Hubbert et al 2002).

Class IIa HDACs have a very limited deacetylase activity on histones, which might hint to a more important function on other, cytoplasmic, substrates (Lahm et al 2007).

Specific acetylation sites could be found such as lysine 16 of histone H3, which has been found to be important for the regulation of chromatin structure (Shogren-Knaak et

al 2006). In humans, the loss of H3 lysine 16 acetylation is a hallmark of certain types of cancer.

HDACs of both class I and II have been recently associated with control of neuro- and astrogliogenesis. Class I HDACs are believed to act as the main deacetlyases in the brain. Class II HDACs bind to class I HDACs and thereby modulate their activity.

In the brain, HDACs have been shown to be involved in many postnatal functions and dysfunctions including the consolidation of memory in the hippocampus (Vecsey et al. 2007; Miller et al. 2008), epileptic seizures, and depression (Miller et al 2008, Phiel et al 2001, Tsankova et al 2006, Vecsey et al 2007). During the development of the nervous system, HDACs have been shown to play an important role in neurogenesis in motor and retinal neurons in zebrafish (Cunliffe 2004, Yamaguchi et al 2005) and in the generation and maturation of oligodendrocytes in the vertebrate brain (Cunliffe & Casaccia-Bonnefil 2006, Marin-Husstege et al 2002, Shen et al 2005).

So far, there is little evidence for the role of HDACs in neurogenesis and astrogliogenesis in the developing vertebrate brain. Vega et al. found that Hdac4 null mice sometimes show exencephaly (Vega et al 2004b), but no evidence for abnormal brain development was found in other gene knockouts of classic HDACs. HDAC1 and 2 were found to be important for Schwann cell development and myelination. HDAC regulated deacetylation of the p65 subunit of NF-κB activates positive regulators of Schwann cell development, while at the same time antagonizing inhibitors of their differentiation (Chen et al 2011).

This raises the question of functional redundancy because of the large number of HDAC family members being expressed in the developing brain (Shen et al 2005). However, studies hint to a rather specific cellular expression pattern and function of individual HDACs (MacDonald & Roskams 2008).

1.3.4   Class IIa HDAC transgenic mice

In contrast to the ubiquitously expressed class I HDACs, histone deacetylases of class IIa exhibit more restricted expression patterns. The *in vivo*-apporach of this study is

focused on HDAC4 and HDAC5, which were found to be expressed in human brain in comparatively high levels (Grozinger et al 1999).

Class II HDACs are comparatively larger than class I HDAC proteins. They do not only consist of the deacetylase domain, but have large aminoterminal domains containing binding sites for myocyte enhancer factor 2 (MEF2), a transcription factor and the chaperone protein 14-3-3. Several kinases, for instance calcium/calmodulin-dependent protein kinase (CaMK) and protein kinase D (PKD), can phosphporylate class II HDACs and enable them thereby to bind to 14-3-3, which is followed by nuclear export (McKinsey et al 2000, Passier et al 2000, Vega et al 2004a). The phosphorylation of class II HDACs and their shuttling between cytoplasm and nucleus appears to be a link between cell signaling and gene transcription. MEF2 can be rendered from being a transcriptional repressor to an activator by dissociating from an HDAC and thereby exposing the binding site for the HAT p300 (Lu et al 2000).

1.3.4.1 HDAC4 transgenic mice

HDAC4 was shown to be expressed in the brain and growth plates of the skeleton (Vega et al 2004b). In this study we examined HDAC4 knockout mice generated by Vega et al (Vega et al 2004b). In these mice, HDAC4 expression is abolished because a *LacZ*-cassette is knocked into the exon 6 of the HDAC4 gene (see Figure 3.4), resulting in a deletion of the MEF2 binding domain, the nuclear localization sequence and the complete deacetylase domain. The authors examined skeletogenesis in the mutants and found HDAC4 to be crucial for chondrocyte hypertrophy during skeletogenensis. HDAC4 was shown to negatively regulate the activity of the Runx2 transcription factor and thus influence the Indian hedgehog (Ihh) pathway. Hdac4 null mice did not survive to weaning. They were found to be comparatively smaller than wildtype littermates and displayed severe skeletal abnormalities, as premature ossification of the skeleton led to growth retardation (Figure 1.10). The postnatal phenotype of the brain of the HDAC4 mutant mice included a 40% reduction in brain size compared to wildtype. Both hemispheres as well as the cerebellum were reduced in size as seen in Figure 1.11 (Majdzadeh et al 2008).

It is not clear whether the observed reduction in brain size is a result of the smaller size of the skull due to premature ossification. In order to investigate this, we created a mouse line deficient in HDAC4 selectively in neural progenitor cells thus circumventing the spatial restriction imposed by the skull morphology of the Hdac4 null mouse.
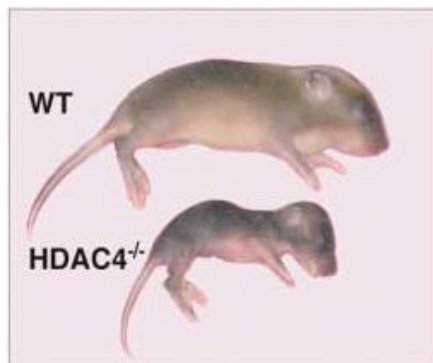
Figure 1.10. Hdac4 null mice have a drastically reduced body size compared to wildtype littermates. They die within 2 weeks after birth (Vega et al 2004b)

In 2008 Majdzadeh et al. were able to demonstrate that HDAC4 activity can be protective for cerebellar granule neurons in neurotoxic conditions such as low potassium concentrations or 6-hydroxydopamine, which otherwise led to apoptosis. This has been ascribed the inhibition of the cell cycle progression through repression of cyclin-dependent kinase 1 (CDK1) activity (Majdzadeh et al 2008).
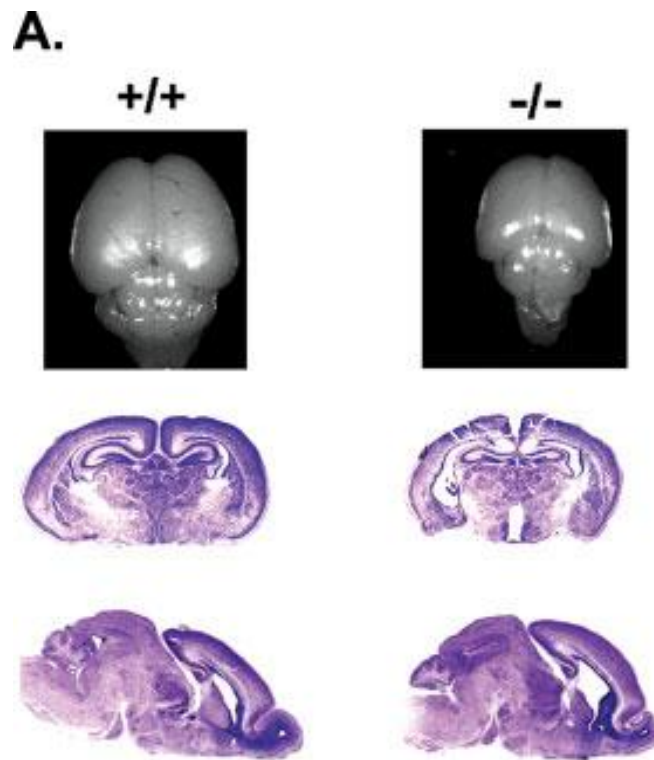
Figure 1.11. Brain phenotype of HDAC -/- mice. Brains of HDAC4 null mice are up to 40% smaller than the ones of wildtype littermates. The lower panel shows cresyl violet-stained coronal and sagittal sections of wildtype and mutant brain at P0. HDAC4 mutants have larger ventricles. The cortex, cerebellum, and olfactory bulb are slightly reduced in size

1.3.4.2 HDAC4 conditional knockout mice

While conventional full knockout of HDAC4 results in perinatal death, conditional knockout models allow for functional studies in specific tissues of post-natal animals. In this study, we used conditional knockout mice for HDAC4 in order to study the effect of the absence of HDAC4 solely on the CNS, isolated from secondary effects which might derive from the abnormally sized and shaped skeleton and skull of HDAC4 null mice. The mouse line was generated by Potthoff and colleagues (Potthoff et al 2007). For their studies, Potthoff et al have generated a conditional knockout of HDAC4 in the skeletal musculature of the mouse. This was achieved by mating mice expressing Crerecombinase under the control of the myogenin promoter/MEF2 enhancer (Li et al. 2005) with mice carrying an HDAC4 allele containing a floxed sixth exon, which if excised results in a frame shift rendering the protein dysfunctional.

We mated this mouse line bearing the HDAC4 allele containing the loxP sites together with a transgenic animal harboring a constitutively expressed Crerecombinase controlled by the nestin promoter (Tronche et al 1999). This enabled us to selectively knock out HDAC4 in the whole developing nervous system, more specifically: in neural progenitor cells and their progeny (see Figure 3.3).

1.3.4.3 HDAC5 mutant mice

HDAC5 and HDAC9 are highly enriched in muscle, heart and CNS (Chang 2004) as well as of HDAC9 (Zhang et al 2002), which like several other HDACs interact with the MEF2 transcription factor, results in a hypermyotrophic response upon cardiac stress, proving these proteins to be crucial for heart development.

Although HDAC5 shows a very high sequence homology with HDAC4, whose complete knockout leads to perinatal death, HDAC5 null mice are viable and fertile (Chang 2004). As HDAC5 is strongly expressed in the brain, it is not surprising that knockout leads to neurological abnormalities such as a hypersensitivity to chronic stress (Renthal et al 2007) and memory impairment (Agis-Balboa et al 2013).

In this study we employed mice generated by Chang and colleagues, in which HDAC5 is knocked out by inserting a *LacZ* expression cassette into the gene (Figure 3.5). X-Gal staining visualizes the expression of HDAC5 in the embryo, which can be detected in brain and spinal cord already at 10.5 dpc (Figure 1.12).

Figure 1.12. HDAC5 expression in embryos visualized by X-Gal staining. HDAC5 is highly expressed in the heart and CNS, expression in CNS can be detected already at E10.5

1.3.5   HDAC inhibitors

Apart from the use HDAC inhibitors serve in laboratory assays for the elucidation of HDAC function, they have long proven their therapeutical value for a wide range of ailments. Their most prominent are of use are the treatments of cancer (Drummond et al 2005) and epilepsy (Urdinguio et al 2009).

Recently, more and more clinical applications have emerged, such as treatment of psychological trauma or enhancers of cognitive functions (Graff & Tsai 2013) and medication of neurodegenerative disorders (Graff & Mansuy 2009).

HDAC inhibitors can be classified into six structurally distinct compound groups. They act by differential binding to the deacetylase domains of class I and II HDACs. The relatively weak HDACi group of the carboxylates includes the widely used sodium butyrate and valproic acid, which selectively inhibit class I HDACs.

Compounds of the hydroxamic acid type include trichostatin A (TSA) and subericbishydroxamic acid (SAHA). Benzamide-class inhibitors such as MS-275, which target class I HDACs (in particular HDACs 1 and 3) are usually weaker in their effect than hydroxamate or cyclic peptide HDACis.

Trapoxin B and HC-toxin, among others, are members of the epoxyketone-based HDACis. Their mechanism of action is not fully understood, but both the ketone as well as the epoxy-group are necessary for the compounds to effectively inhibit HDACs (Shute et al 1987).

Pure cyclic peptide HDACis such as apicidin act via the reversible binding of their macrocyclic peptide structure to the entrance of the catalytic pit (Miller et al 2003).

2   Aim of this study

In this project the role of HDACs in the generation of neurons and astrocytes in embryonic mouse brain was under investigation. It was shown that in differentiating neural progenitor cells many different HDACs are expressed (Shaked et al 2008). To investigate their function in neural development, pharmacological inhibitors of HDACs were applied.

Inhibition of class I and II HDACs with trichostatin A in cultures of *in vitro*-differentiating neural precursors from the examined brain regions leads to a considerable reduction in neurogenesis in the ganglionic eminences but to a slight increase in the cortex. While neurogenesis decreases in cultures from the GE, there is a concomitant increase in the production of immature astrocytes.

The aim of this project was to investigate which HDACs are responsible for this phenomenon and to dissect through which signaling pathway HDACs influence neuro- and gliogenesis.

Firstly, the expression of candidate genes which might be involved in controlling neurogenesis was examined through real-time RT-PCR. As the BMP2/4 signaling pathway had been implicated in the HDAC-mediated control of neurogenesis, genes encoding the corresponding growth factors, receptors, and downstream signaling proteins were examined. This was further complemented by a microarray analysis in collaboration with Dr. Catharina Scholl.

Secondly, in order to ascertain which HDAC family members are involved in this phenomenon, RNA interference was used to inhibit the expression of individual HDAC genes. shRNA against several class I and II HDACs was generated and expressed in neural precursor cultures via lentiviral vectors. 5 different shRNA oligos were generated against each HDAC, which were then tested for knockdown efficiency and potential cross-reaction with other, non-target HDACs.

Since recently generated knockout mouse models of individual HDAC genes have shown this family of enzymes to have highly specific roles in development and in adult

organisms, I also wanted to investigate the role of HDACs in neuro- and gliogenesis *in vivo*. The mutant mice provide a powerful tool for this experimental question. The class II family members HDAC4 and -5 show high expression levels in brain tissue, therefore we chose to investigate mutant animals deficient in these enzymes for brain development and morphology.

3 Materials and Methods

3.1 Materials

3.1.1 Basic Reagents

Acetone	Zentrallager INF 367 (Heidelberg, Germany)
Acrylamide/Bisacrylamide, 30% (w/v)	BioRad (München, Germany)
Agar	Merck (Darmstadt, Germany)
Agarose (elctrophoresis grade)	Roth (Karlsruhe, Germany)
Ampicillin	Sigma-Aldrich (St. Louis, USA)
Aquatex Mounting Medium	Merck (Darmstadt, Germany)
APS	Roth (Karlsruhe, Germany)
ß-Mercaptoethanol	Sigma-Aldrich (St. Louis, USA)
Boric acid	AppliChem (Darmstadt, Germany)
Bovine serum albumine (BSA)	Roth (Karlsruhe, Germany)
Bromphenol blue 4F057	Division Chroma (Münster, Germany)
CHAPS	Fluka (Buchs, Switzerland)
Citric acid	Sigma-Aldrich (St. Louis, USA)
Chloroform	Fluka (Buchs, Switzerland)
Coomasie R 250	Serva (Heidelberg, Germany)
DAB	Sigma-Aldrich (St. Louis, USA)
DMSO	Acros Organics (Geel, Belgium)
DNA Polymerase DreamTaq	Fermentas (Waltham, USA)
DNA Polymerase DreamTaq Mastermix	Fermentas (Waltham, USA)
DTT	AppliChem (Darmstadt, Germany)
EDTA	AppliChem (Darmstadt, Germany)
Entellan	Merck (Darmstadt, Germany)
Ethanol absolut puriss.	Sigma-Aldrich (St. Louis, USA)
Ethidium bromide	Fluka (Buchs, Switzerland)

Formaldehyde, 40% (w/v)   Carlo Erba Reagents (Arese, Italy)

Glacial acetic acid   Sigma-Aldrich (St. Louis, USA)

Glutaraldehyde (25% solution)   Merck (Darmstadt, Germany)

Glycerol   Sigma-Aldrich (St. Louis, USA)

Glycine   Sigma-Aldrich (St. Louis, USA)

ImmEdge Pen   Vector Laboratories (Burlingame, USA)

Kanamycin   Sigma-Aldrich (St. Louis, USA)

Methanol   Merck (Darmstadt, Germany)

Methylene blue   Merck (Darmstadt, Germany)

Milk powder   Roth (Karlsruhe, Germany)

MOPS   Sigma-Aldrich (St. Louis, USA)

Nitric acid   Mallinckrodt Baker B.V. (Deventer,
                                       Netherlands)

NP-40   Fluka (Buchs, Switzerland)

Paraformaldehyde   Sigma-Aldrich (St. Louis, USA)

Phenol/Chloroform/Isoamylalcohol,   Roth (Karlsruhe, Germany)
pH 7.5-8.0

PMSF   Sigma-Aldrich (St. Louis, USA)

2-Propanol   AppliChem (Darmstadt, Germany)

Protease inhibitor tablets,   Roche (Penzberg, Germany)
Complete, EDTA-free

Proteinase K   Roth (Karlsruhe, Germany)

Oligo(dT)12 – 18 primer   Invitrogen (Carlsbad, USA)

Orange G   Sigma-Aldrich (St. Louis, USA)

Random hexamer primer   Applied Biosystems (Darmstadt,
                                       Germany)

Sodium chloride   Sigma-Aldrich (St. Louis, USA)

Sodium citrate dihydrate   Sigma-Aldrich (St. Louis, USA)

Sodium dodecyl sulfate (SDS)   Serva (Heidelberg, Germany)

Sodium dihydrogen phosphate   AppliChem (Darmstadt, Germany)
 $NaH_2PO_4*H_2O$

Disodium hydrogen phosphate   AppliChem (Darmstadt, Germany)

Na2HPO4*2H2O

Sodium tetraborate decahydrate	Sigma-Aldrich (St. Louis, USA)
Sucrose	Sigma-Aldrich (St. Louis, USA)
TEMED	Sigma-Aldrich (St. Louis, USA)
Tissue freezing medium	Jung (Nussloch, Germany)
Trichostatin A	Sigma-Aldrich (St. Louis, USA)
Tris	Roth (Karlsruhe, Germany)
Tris ultrapure	Applichem (Darmstadt, Germany)
Triton X-100	Merck (Darmstadt, Germany)
Trypan blue	Sigma-Aldrich (St. Louis, USA)
Tween-20	Roth (Karlsruhe, Germany)
Xylene cyanol	Sigma-Aldrich (St. Louis, USA)
Xylol	AppliChem (Darmstadt, Germany)

3.1.2   Cell culture Reagents

B27 Supplement	Invitrogen (Carlsbad, USA)
Boric Acid	J. T. Baker (Deventer, Netherlands)
Brefeldin A	Sigma-Aldrich (St. Louis, USA)
Cycloheximide	Sigma-Aldrich (St. Louis, USA)
DMEM	Gibco (Carlsbad, USA)
Dimethyl sulfoxide (DMSO)	Sigma-Aldrich (St. Louis, USA)
D-PBS	Invitrogen (Carlsbad, USA)
Foetal Bovine Serum	Invitrogen (Carlsbad, USA)
Ham's F12 Medium	Sigma-Aldrich (St. Louis, USA)
HBSS	Invitrogen (Carlsbad, USA)
Human FGF2	Roche or R&D Systems
Human recombinant EGF	Sigma-Aldrich (St. Louis, USA)
L-Glutamine 100X (200 mM)	Gibco (Calsbad, USA)
OptiMem	Invitrogen (Carlsbad, USA)
Papain 10 U/mg, lyophilized powder	Sigma-Aldrich (St. Louis, USA)
Penicillin-Streptomycin, 100X	Gibco (Carlsbad, USA)

Poly-DL-ornithine hydrobromide   Sigma-Aldrich (St. Louis, USA)

Polyethyleneimine   Sigma-Aldrich (St. Louis, USA)

Poly-L-lysine hydrobromide   Sigma-Aldrich (St. Louis, USA)

Saponin   Sigma-Aldrich (St. Louis, USA)

Trypsin-EDTA   Gibco (Carlsbad, USA)

Versene   Invitrogen (Carlsbad, USA)

3.1.3   Buffer, media and solutions

3.1.3.1   Cell culture

hFGF2	5 µg/ml in DMEM, 5% (v/v) FCS
hEGF	20 µg/ml in DMEM/F12
5x poly-DL-ornithine	500 mg/l in 150 mM H_3BO_3, pH 8.3 (use 100 mg/l diluted in D-PBS)
10x poly-L-lysine	10 mg/ml in H_2O, sterile-filtered, use 1mg/ml für FACS, otherwise 0.1 mg/ml, wash 3x with D-PBS
Trypsin-Papain	0.25% (w/v) trypsin-EDTA, 2.5 U/ml papain
2x Cryomedium	48.75% (v/v) DMEM, 31.25% (v/v) FCS, 20% (v/v) DMSO, filter-sterilize and keep at –20 °C
FCS	Inactivated for 1 h at 57 °C, stored at –20 °C
MEF-Medium	DMEM, 1 U/ml P/S, 2 mM glutamine, 10% (v/v) FCS
Neurosphere (NS) medium	50% (v/v) DMEM, 50% (v/v) Ham's F12
NS growth medium	NS medium, 1 U/ml P/S, 2 mM glutamine, 10 ng/ml hFGF2, 20 ng/ml hEGF, 2% (v/v) B27
NS differentiation medium w/ FGF2	NS medium, 1 U/ml P/S, 2 mM glutamine,

	10 ng/ml FGF2, 2% (v/v) B27, 1% (v/v) FCS
NS differentiation medium w/o FGF2	NS medium, 1 U/ml P/S, 2 mM glutamine, 2% (v/v) B27, 1% (v/v) FCS
Trichostatin A	Stock: 100 µg/ml in 8% ethanol, dilute in D-PBS, final concentration 10 nM or 50 nM

3.1.3.2 FACS Analysis

Papain	1x PBS, 10 U/ml papain, 10% (v/v) FCS
PF	1x PBS, 2% (v/v) FCS
PFS	1x PBS, 2% (v/v) FCS, 0.18% saponin
Trypsin-papain	0.25% (w/v) trypsin-EDTA, 2.5 U/ml papain

3.1.3.3 Microbiology

3.1.3.3.1 General Microbiology

LB medium	10 g NaCl, 10 g tryptone, 5 g yeast extract, H_2O (pH 7.5) ad 1 l; autoclave
LB agar	10 g NaCl (5 g for low-salt), 10 g tryptone, 5 g yeast extract, 15 g agar, H_2O ad 1 l (pH 7.5); autoclave

3.1.3.3.2 Plasmid Minipreparation

Resuspension solution 1	H_2O, 50 nM glucose, 25 mM Tris-Cl, 10 mM EDTA (pH 8.0); autoclave and store at 4 °C
Lysis solution 2	H_2O, 0.2 N NaOH, 1% (w/v) SDS
Neutralization solution 3	H_2O, 3 M KOAc, 5 M glacial acetic acid

3.1.3.3.3 Hogness Modified Freezing Medium for Glycerol Stocks 10x (HMFM)

Solution A	H_2O, 5 mM $MgSO_4$, 20 mM sodium citrate, 85 mM $(NH_4)_2SO_4$, 45% (v/v) glycerol; autoclave
Solution B	H_2O, 0.66 M KH_2PO_4, 1.3 M K_2HPO_4; autoclave
Final 10x HMFM	Mix solutions A and B in a 4:1 ratio

Hogness modified freezing medium was used for storage of cultures at -80 °C. A log phase culture (OD 660 nm 0.8) was centrifuged to harvest cells. After pouring off the medium, cells were resuspended in sterile HMFM and frozen down.

3.1.3.4 Molecular Biology

3.1.3.4.1 General Molecular Biology

Orange G buffer	H_2O, 0.6% (w/v) Orange G, 50% (v/v) glycerol
Lysis buffer (tail buffer)	H_2O, 0.1 M Tris-Cl (pH 8.5), 5mM EDTA (pH 8.0), 0.2% SDS, 0.2 M NaCl, 100 µg/ml Proteinase K
1x PBS	H_2O, 140 mM NaCl, 2.7 mM KCl, 10 mM Na_2HPO_4, 1.8 mM KH_2PO_4 (pH 7.3); adjust pH to 7.4
10x PBS	H_2O, 1.4 M NaCl, 27 mM KCl, 100 mM Na_2HPO_4, 18 mM KH_2PO_4; adjust pH to 7.4
RLN-Buffer	H_2O DEPC, 50 mM Tris pH 8.0, 140 mM NaCl, 1.5 mM $MgCl_2$, 0.5% NP-40; adjust pH to 8.0, autoclave for 30'
50x TAE	H_2O, 2 M Tris base, 50 mM EDTA (pH 8.0), 5.71% (v/v) glacial acetic acid
5x TBE	H_2O, 0.445 M Tris base, 0.451 M H3BO3, 10 mM EDTA (pH 8.0)

3.1.3.4.2 Denaturing RNA Gel

3.1.3.4.2.1 Buffers

5x Formaldehyde gel running buffer	0.1 M MOPS (pH 7), 40 mM sodium acetate, 5 mM EDTA (pH 8.0); filter-sterilize (0.2 µm)
Loading buffer	H_2O (DEPC), 50% (v/v) glycerol, 1 mM EDTA (pH 8.0), 0.25% (w/v) bromophenol blue, 0.25% (w/v) xylene cyanol FF

3.1.3.4.2.2 Denaturing RNA-Gel

Agarose / H_2O	1.68 g (2.24 g) for 1.5% (2%), H_2O ad 70 ml
37% (w/v) formaldehyde	20 ml
5x running buffer	22 ml
Ethidium bromide	3 µl

Boil agarose, let cool to 60 °C before adding remaining components

3.1.3.4.3 In situ Hybridization

3.1.3.4.3.1 Solutions

0.2% (w/v) Glycine in 1x PBS	prepare fresh on the day of the in situ hybridization
Proteinase K	20 µg/ml in 1x PBS, prepared fresh
PBST	1x PBS, 0.1% (v/v) Tween-20
NTM	H_2O Milli-Q, 0.1 M Tris-HCl (pH 9.5), 0.1 M NaCl, 0.05 M $MgCl_2$
10x PBS	H_2O, 1.37 M NaCl, 0.027M KCl, 0.015M KH_2PO_4, 0.065M Na_2HPO_4; pH: 7.2 – 7.4
20x SSC	H_2O, 3 M NaCl, 0.3 M trisodium citrate; adjust pH to 4.5
B-Block	1x PBS, 2% (w/v) Boehringer Block, 0.1% (v/v) Tween-20, 10% (v/v) NGS; dissolve Boehringer Block in Tween/PBS in

	water bath at 65 °C (or autoclave w/o Tween and add Tween
	afterwards), add serum after cooling; store at –20 °C
4% PFA	Heat 150 ml H_2O to 60 °C, add 8 g PFA with 1 ml 2 N NaOH
	and 20 ml 10x PBS, wait for solution to become clear, filter,
	adjust pH to 7.4, add H_2O ad 200 ml; store at –20 °C
4% PFA + 0.2% glutaraldehyde	0.2% glutaraldehyde in 4% (w/v) PFA/PBS; prepare fresh on the day of in situ hybridization

3.1.3.4.3.2 Hybridization Mix (HYBmix)

Formamide	5 ml
20x SSC (pH 4.5)	2.5 ml
Boehringer Block	100 mg
H_2O Milli-Q	2 ml

Dissolve above reagents in water bath at 65 °C, then add the following:

0.5 M EDTA (pH 8.0)	100 µl
10% (v/v) Tween 20	100 µl
10% (w/v) CHAPS	100 µl
50 mg/ml Heparin	4 µl
50 mg/ml tRNa	200 µl, denature for 5' at 95 °C before adding

3.1.3.5   Protein biochemistry

3.1.3.5.1 Protein extraction from tissues and cells

3.1.3.5.1.1 Protease inhibitors

Inhibitor	Function	Stock	Final concentration
PMSF	Serine protease inhibitor	0.1 M in 2-propanol	0.2 mM
Benzamidine	Reversible competitive inhibitor of trypsin,	0.5 M in H2O	5 mM

	trypsin-like and serine proteases		
ε-Aminocaproic acid	Lysine derivative, inhibits lysine-binding enzymes	1 M in H2O	1 mM
Roche Complete, Mini, EDTA-free Protease Inhibitor Cocktail Tablets	Inhibits serine and cysteine proteases	1 tablet in 2 ml of autoclaved H2O Milli-Q (7x)	1x

3.1.3.5.1.2 Buffers

Buffer H H_2O, 20 mM Tris-HCl (pH 7.4), 1 µg/ml leupeptin, 1 µg/ml aprotinin, 17 µg/ml PMSF; prepare fresh

5x Laemmli SDS buffer H_2O, 0.125 M Tris-HCl (pH 6.8), 5% (w/v) SDS

RIPA buffer H_2O, 50 mM Tris-HCl, 1 % (v/v) Triton X-100, 1 % (w/v) SDS, 150 mM NaCl, 1 mM EDTA, 1% (w/v) DOC, autoclave

2x SDS sample buffer H_2O, 100 mM Tris, 25% (v/v) glycerol, 2% (w/v) SDS, 0.01% (w/v) bromophenol blue; adjust pH to 6.8, add 10% (v/v) β-mercaptoethanol

2x Urea sample buffer H_2O Milli-Q, 20% (v/v) glycerol, 8 M urea, 20 mM DTT, 125 mM Tris-HCl (pH 6.8), 5% (w/v) SDS, 0.01% (w/v) bromophenol blue; heat 5' at 42 °C

3.1.3.5.2 Protein PAGE

3.1.3.5.2.1 Solutions

10% SDS buffer	H2O Milli-Q, 10% (w/v) SDS; heat and filter-sterilize
10x SDS running buffer	H2O, 250 mM Tris base, 1.92 M glycine, 1% (w/v) SDS
1 M Tris buffer pH 6.8	H2O, 1 M Tris, pH 6.8; filter-sterilize
1.5 M Tris buffer pH 8.8	H2O, 1.5 M Tris, pH 8.8; filter-sterilize

3.1.3.5.2.2 SDS-Polyacrylamide Gels

12% Separating gel (2 Biorad Mini-PROTEAN gels, 1.5 mm wide)	
8 ml	H_2O
6.6 ml	30% acrylamide / 0.8% bisacrylamide
5 ml	1.5 M Tris pH 8.8
200 µl	10% SDS
200 µl	10% APS
16 µl	TEMED

7.5% Separating gel (2 Biorad Mini-PROTEAN gels, 1.5 mm wide)	
9.6 ml	H_2O
5 ml	30% acrylamide / 0.8% bisacrylamide
5 ml	1.5 M Tris pH 8.8
200 µl	10% SDS
200 µl	10% APS
16 µl	TEMED

5% Stacking gel (2 Biorad Mini-PROTEAN gels, 1.5 mm wide)	
5.4 ml	H_2O
1.34 ml	30% acrylamide / 0.8% bisacrylamide
1 ml	1.5 M Tris pH 8.8
80 µl	10% SDS
80 µl	10% APS
16 µl	TEMED

The gel solutions were prepared and poured immediately. After pouring the separation gel was immediately covered with a thin layer of 2-propanol until it was completely polymerized. Then the 2-propanol was removed, the stacking gel poured on top and the comb inserted.

3.1.3.5.3 Western blot

3.1.3.5.3.1 Buffers

Blocking buffer	5 % milk powder in TBS-T
10x TBS	H_2O Milli-Q, 1.5 M NaCl, 1.18 % (w/v) Tris-base, 6.35 % (w/v) Tris-acid
TBS-T	0.05 % (v/v) Tween-20 in 1xTBS
10x TBS	H_2O, 1.5 M NaCl, 500 mM Tris base (pH 7.5)
TBS-T	1x TBS, 0.05% (v/v) Tween 20
Transfer Buffer	H_2O Milli-Q, 0.381 % (w/v) $Na_2B_4O_7*10H_2O$

3.1.3.6   Immunologic analyses

3.1.3.6.1 Sera

Bovine serum albumine (BSA)	Roth (Karlsruhe, Germany)
Native goat serum (NGS)	Sigma-Aldrich (St. Louis, USA)

3.1.3.6.2 Dyes

DAPI   Sigma-Aldrich (St. Louis, USA)

3.1.3.6.3 Solutions

Antibody buffer   1x PBS, 5% (v/v) NGS , 1% (w/v) BSA in PBS

Blocking buffer   1x PBS, 0.5% (v/v) NGS, 1% BSA, 0.5% (v/v) Triton X-100

Coverslip storing solution   1% (w/v) NaN_3 in 1x PBS

DAPI stock solution   0.5% (w/v) DAPI in DMF

DAPI working solution 0.0004% (w/v) DAPI stock in PBS

3.1.4   Antibodies

3.1.4.1   Antibodies for Western Blotting

Primary antibodies	Description	Dilution	Reference
α-Tubulin	Mouse, monoclonal IgG against α-tubulin of microtubules	1:20 000	Sigma-Aldrich Chemie GmbH, Steinheim
ß-Actin	Mouse; monoclonal IgG1, HRP-(horse radish peroxidase)-conjugated	1:200 000	Sigma-Aldrich Chemie GmbH, Steinheim
ß-Actin	Mouse; monoclonal antibody against N-terminal epitope of ß-actin	1:1000	Santa Cruz Biotechnol. Inc.
GFP	Rabbit; polyclonal antibody against GFP	1:1000	Clontech
GFP	Rabbit; polyclonal antibody	1:3000	Novus Biological

	against GFP		
HDAC2	Rabbit; polyclonal antibody against histone deacetylase 2	1:500	Zymed Laboratories Inc.
HDAC4	Rabbit; polyclonal IgG against amino acids 530-632 of HDAC4 of human origin	1:1000	Santa Cruz Biotechnol Inc.

Secondary antibodies	Description	Dilution	Reference
Goat α-rabbit	HRP-conjugated rabbit IgG antibody	1:5000	Jackson Immuno-Research Laboratories Inc.
Goat α-mouse	HRP-conjugated AffiniPure mouse IgG antibody	1:10 000	Jackson ImmunoResearch Laboratories Inc.

3.1.4.2 Antibodies for Immunohistochemistry

Primary antibodies	Description	Dilution	Reference
BLPB	Rabbit, polyclonal antibody against BLBP	1:1500	Chemicon
Brn-2	Goat polyclonal antibody against C-terminus of human Brn-2	1:250	Santa Cruz
Ctip	Rat, monoclonal IgG for Ctip2	1:500	Abcam
GFAP	Rabbit, IgG fraction of antiserum cow Glial Fibrillary Acidic Protein (GFAP); strong reaction	1:500	DAKO

	against mouse GFAP		
GFP	Rabbit, polyclonal antibody against GFP	1:1000	Ulrich Mueller, Cripps Research Inst., San Diego, CA
HDAC2	Rabbit, Polyclonal antibody against histone deacetylase 2	1:1000	Zymed Laboratories Inc.
KI-67	Rat anti-mouse Ki67 antigen	1:25 – 1:50	
Nestin	Mouse anti-rat, monoclonal antibody IgG1 labeling neural stem cells	1:1000	BD Bioscience
O4	Mouse monoclonal antibody against O4	1:400	Millipore
Pax6	Mouse, monoclonal IgG against Pax6	1:1000	Chemicon
Pax6	Rabbit polyclonal antibody against C-terminus of mouse Pax6	1:1000	Chemicon
PH3	Rabbit, polyclonal antibody against phospho-histone H3 (Ser10)	1:1000	Upstate/Millipore
RC2	Rat anti mouse IgM against RC2	1:1000	Developmental Studies Hybridoma, (Iowa, USA)
Reelin	Mouse monoclonal IgG1 against reelin	1:1000	Calbiochem
S100ß	Monoclonal antibody against S100ß	1:1000	Sigma
Sox2	Goat, antibody against mouse Sox 2	1:1000	Abcam
Tbr2	Rabbit, polyclonal antibody against Tbr2	1:3000	Chemicon/Millipore
TuJ1	Mouse, monoclonal antibody	1:500 – 1:1000	HISS Diagnostics

	IgG2a against neuronal β-tubulin III		GmbH/COVANCE
TuJ1	Mouse, monoclonal antibody IgG2a antibody against ß-tubulin III	1:1000	R&D systems

Secondary antibodies	Description	Dilution	Reference
Alexa Fluor 488 goat α-mouse IgG conjugate	Fluorescent α-mouse IgG (green)	1:1000	Invitrogen (Carlsbad, USA)
Alexa Fluor 488 goat α-rabbit conjugate	Fluorescent α-rabbit (green)	1:1000	Molecular Probes
Alexa Fluor 546, goat α-mouse conjugate	Fluorescent α-mouse IgG (red)	1:1000	Molecular Probes
Alexa Fluor 546 goat α-rabbit IgG conjugate	Fluorescent α-rabbit IgG (red)	1:1000	Invitrogen

3.1.5   Primers

All primers were purchased from Thermo Electron GmbH.

3.1.5.1   Genotyping

3.1.5.1.1 tau::EGFP

Wildtype

WT-F   5'-CTC AGC ATC CCA CCT GTA AC-3'

WT-R   5'-CCA GTT GTG TAT GTC CAC CC-3'

Product   187 bp

Mutant

KO-F   5'-CAG GCT TTG AAC CAG TAT GG-3'

KO-R   5'-TGA ACT TGT GGC CGT TTA CG-3'

Product   218 bp

3.1.5.1.2 Nestin::Cre

NesCre$^+$ 5'-GCC GAA ATT GCC AGG ATC AG-3'

NesCre$^-$ 5'-AGC CAC CAG CTT GCA TGA TC-3'

Product   500 bp

3.1.5.1.3 HDAC4

HDAC4-fwd   5'-ATC TGC CCA CCA GAG TAT GTG-3'

HDAC4-rev   5'-CTT GTT GAG AAC AAA CTC CTG CAG CT-3'

nLacZ-rev   5'-GAT TGA CCG TAA TGG GAT AGG TTA CG-3'

Product   wildtype   480 bp

                floxed   620 bp

                LacZ   810 bp

3.1.5.1.4 HDAC5

gt-HD5-fwd   5'-CAA GGC CTT GTG CAT GCT GGG CTG G-3'

gt-HD5-rev   5'-CTG CTC CCG TAG CGC AGG GTC CAT G-3'

gt-HD5-lacZ-rev   5' GCC AGT TTG AGG GGA CGA CGA CAG TAT CG-3'

Product   wildtype   300 bp

                  mutant   500 bp

3.1.5.2   PCR to control cDNA-synthesis

3.1.5.2.1 Gapdh-PCR

A PCR for the housekeeping gene Gapdh was run to test the quality of cDNA after *in vitro* translation.

G3PDH F   5´-AAC ACA GTC CAT GCC ATC AC-3´

G3PDH R   5´-TCC ACC ACC CTG TTG CTG TA-3´

3.1.6   TaqMan Gene Expression Assays (Applied Biosystems)

3.1.6.1   Endogenous controls

Name	Assay number	Gene	Species	Amplicon length	
Gapdh	Mm99999915_g1	glyceraldehyde-3-phosphate dehydrogenase	mouse	107	Inventoried
Hprt1	Mm00446968_m1	hypoxanthine guanine phosphoribosyl transferase 1	mouse	65	Inventoried

3.1.6.2   Genes of interest

Name	Assay number	Gene	Species	Amplicon length	
Bmpr1a	Mm00477650_m1	bone morphogenetic protein receptor, type 1A	mouse	64	Inventoried
Bmpr1b	Mm00432117_m1	bone morphogenetic protein receptor, type 1B	mouse	84	Inventoried

Bmpr2	Mm00432134_m1	bone morphogenic protein receptor, type II (serine/threonine kinase)	mouse	81	Inventoried
Bmp2	Mm01340178_m1	bone morphogenetic protein 2	mouse	58	Inventoried
Bmp4	Mm00432087_m1	bone morphogenetic protein 4	mouse	61	Inventoried
Hdac1	Mm01351188_m1	histone deacetylase 1	mouse	121	Made to Order
Hdac2	Mm00515108_m1	histone deacetylase 2	mouse	62	Inventoried
Hdac3	Mm00515916_m1	histone deacetylase 3	mouse	71	Inventoried
Hdac4	Mm01299557_m1	histone deacetylase 4	mouse	110	Inventoried
Hdac5	Mm00515917_m1	histone deacetylase 5	mouse	82	Inventoried
Hdac7a	Mm00469520_m1	histone deacetylase 7A	mouse	65	Inventoried
Hdac8	Mm01224986_m1	histone deacetylase 8	mouse	57	Made to Order
Ngn1	Mm00440466_s1	neurogenin 1	mouse	82	Inventoried
Ngn2	Mm00437603_g1	neurogenin 2	mouse	64	Inventoried
Smad1	Mm00484721_m1	MAD homolog 1 (Drosophila)	mouse	63	Inventoried
Smad7	Mm00484741_m1	MAD homolog 7 (Drosophila)	mouse	138	Inventoried

| Stat1 | Mm00439518_m1 | signal transducer and activator of transcription 1 | mouse | 144 | Inventoried |
| Stat3 | Mm00456961_m1 | signal transducer and activator of transcription 3 | mouse | 93 | Inventoried |

3.1.7   Enzymes

3.1.7.1   Polymerases and Ligase

DreamTaq DNA-Polymerase	Fermentas (Waltham, USA)
SuperScript II Reverse Transcriptase	Invitrogen (Carlsbad, USA)
SP6 RNA-Polymerase	Fermentas (Waltham, USA)
T3 RNA-Polymerase	Fermentas (Waltham, USA)
T7 RNA-Polymerase	Fermentas (Waltham, USA)
T4 DNA-Ligase	NEB (Ipswich, USA)

3.1.7.2   Restriction Enzymes

All restriction enzymes were were obtained from Fermentas or NEB.

3.1.8   Antibiotics

Antibiotic	Dilution
Ampicillin	1:1000 from stock (150 mg/ml in H_2O)
Kanamycin	1:1000 from stock (30 mg/ml in H_2O)

3.1.9   Cells

3.1.9.1   Bacteria

DH5α competent *E. coli*   Invitrogen (Carlsbad, USA)

XL-1 blue competent *E. coli*   Stratagene (La Jolla, USA)

TOP10 competent *E. coli*   Invitrogen (Carlsbad, USA)

3.1.9.2   Permanent cell lines

HEK293T   ATCC

3.1.10   Plasmids

Plasmid	Insert	Reference
pBluescript II KS (+/-)	Ampicillin resistance gene	Genbank
pLKO.1-puro	shRNA against HDACs puromycin resistance gene	Sigma-Aldrich Chemie GmbH (Steinheim, Germany)
pLentiLox 3.6	EGFP, ampicillin resistance gene	Didier Trono, unpublished
N1-EGFP	EGFP	Clontech (Mountain View, USA)
AAV hRluc	Synthetic Renilla luciferase, ampicillin resistance	David Lau
pBREx4-luc	BMP responsive elements, four copies	Hata et al. (2000)

3.1.11 Mission™ shRNA sequences

HDAC	Oligo#	TRCN	shRNA sequence
HDAC1	Oligo 1	TRCN0000039399	CCGGGCTTGGGTAATAGCAGCCATTCTCG AGAATGGCTGCTATTACCCAAGCTTTTTG
	Oligo 2	TRCN0000039400	CCGGCCGGTATTTGATGGCTTGTTTCTCGA GAAACAAGCCATCAAATACCGGTTTTTG
	Oligo 3	TRCN0000039401	CCGGCCCTACAATGACTACTTTGAACTCG AGTTCAAAGTAGTCATTGTAGGGTTTTTG
	Oligo 4	TRCN0000039402	CCGGGCCAGTCATGTCCAAAGTAATCTCG AGATTACTTTGGACATGACTGGCTTTTTG
	Oligo 5	TRCN0000039403	CCGGGCGTTCTATTCGCCCAGATAACTCG AGTTATCTGGGCGAATAGAACGCTTTTTG
HDAC2	Oligo 1	TRCN0000039398	CCGGCGATCAATAAGACCAGATAATCTCG AGATTATCTGGTCTTATTGATCGTTTTTG
	Oligo 2	TRCN0000039396	CCGGCCTGTGAAATTAAACCGGCAACTCG AGTTGCCGGTTTAATTTCACAGCTTTTTG
	Oligo 3	TRCN0000039395	CCGGCCCAATGAGTTGCCATATAATCCGA GATTATATGGCA ACTCATTGGGTTTTTG
	Oligo 4	TRCN0000039397	CCGGCGAGCATCAGACAAACGGATACTCG AGTATCCGTTTGTCTGATGCTCGTTTTTG
HDAC4	**Oligo 1**	TRCN0000039249	CCGGCCTCAGCAAGATAATCTCCAACTCG AGTTGGAGATTATCTTGCTGAGGTTTTTG
	Oligo 2	TRCN0000039250	CCGGCATGGGTTTCTGCTACTTTAACTCGA GTTAAAGTAGCAGAAACCCATCTTTTTG
	Oligo 3	TRCN0000039251	CCGGGTTCTACATCAGAGACCCAATCTCG AGATTGGGTCTCTGATGTAGAACTTTTTG
	Oligo 4	TRCN0000039252	CCGGGAGGCACAGTTGCATGAACATCTCG AGATGTTCATGCAACTGTGCCTCTTTTTG
	Oligo 5	TRCN0000039253	CCGGACTCTCTGATTGAGGCGCAAACTCG

			AGTTTGCGCCTCAATCAGAGAGTTTTTTG
HDAC5	Oligo 1	TRCN0000039384	CCGGCTGGGCAAGATCCTTACCAAACTCG AGTTTGGTAAGGATCTTGCCCAGTTTTTG
	Oligo 2	TRCN0000039385	CCGGCCAAACCAGTTCAGCCTCTATCTCG AGATAGAGGCTGAACTGGTTTGGTTTTTG
	Oligo 3	TRCN0000039386	CCGGGCTCAAGAATGGATTTGCTATCTCG AGATAGCAAATCCATTCTTGAGCTTTTTG
	Oligo 4	TRCN0000039387	CCGGGCACCAGTGTATGTGCGGAAACTCG AGTTTCCGCACATACACTGGTGCTTTTTG
	Oligo 5	TRCN0000039388	CCGGCCAGGAATTCCTGTTGTCCAACTCG AGTTGGACAACAGGAATTCCTGGTTTTTG
SHC002			CCGGCAACAAGATGAAGAGCACCAACTC GAGTTGGTGCTCTTCATCTTGTTGTTTTTG

3.1.12 DNA and Protein standards

25 bp DNA ladder	Promega (Madison, USA)
50 bp DNA ladder	Promega (Madison, USA)
GeneRuler^{TM}100 bp DNA Ladder, ready-to-use	Fermentas (Waltham, USA)
1 kb DNA Ladder	NEB (Ipswich, USA)
peqGOLD Prestained Protein-Marker III	peqLab (Erlangen, Germany)
Spectra Multicolor Broad Range Protein Ladder	Fermentas (Waltham, USA)

3.1.13 Kits

Applied Biosystems (Darmstadt, Germany)	TaqMan® Universal PCR Master Mix, No AmpErase® UNG
Amaxa Biosystems (Gaithersburg, USA)	Rat Neuron Nucleofactor Kit
BioRad (München, Germany)	Bradford-Assay
GE Healthcare Amersham™ (Little	ECL™ Plus Western Blotting Detection

Chalfont, UK)	System
Invitrogen (Carlsbad, USA)	SuperScript® II First-Strand Synthesis System
	TOPO TA Cloning Kit for subcloning
	Zero Blunt TOPO PCR cloning Kit
Genomed (Löhne, Germany)	NoEndo Jetstar Endotoxin-Free Maxi Kit
Macherey and Nagel (Düren, Germany)	Nucleospin Extract II QIAEX II
Promega (Fitchburg, USA)	Dual Luciferase Assay System
Qiagen (Hilden, Germany)	RNeasy Mini-Kit
	QIAquick Gel Extraction Kit
Roth (Karlsruhe, Germany)	Gel Drying Frames
Sigma-Aldrich (St. Louis, USA)	GenElute HP Plasmid Midiprep Kit
	GenElute Plasmid Maxiprep Kit
Thermo Scientific (Waltham, USA)	BCA Protein Assay Kit

3.1.14 Instruments

AGFA-Gevaert (Mortsel, Belgium)	Curix 60 Developing Machine
Amaxa Biosystems/Lonza (Basel Switzerland)	Nucleofector I
Amersham Bioscences (Amersham, UK)	Ultrospec 3100 pro UV/Visible Spectrophotometer with DPU-414 thermal printer
Applied Biosystems (Foster City, USA)	ABI Prism 7000 Sequence Detection System
Beckman Coulter (Brea, USA)	Avanti J-25 Centrifuge
	Avanti J-26 Centrifuge
	Optima LE-80K Ultracentrifuge
	SW32 Ti Ultracentrifuge Rotor
	JA-10 Ultracentrifuge Rotor
Becton Dickinson (Franklin Lakes, USA)	FACSCalibur

Bender & Hobein (Zurich, Switzerland)	Vortex Genie 2 G-560E Mixer
Biometra (Goettingen, Germany)	TPersonal Thermal Cycler,
Bio-Rad (Hercules, USA)	GS-800 Calibrated Densitometer
	Icycler 582BR Thermocycler
	Mini-PROTEAN II Electrophoresis Gel System
	Mini Trans-Blot Electrophoretic Transfer Cell
	PowerPac 200 Power Supply
	Trans-Blot SD Electrophoretic Transfer Cell
Carl Roth (Karlsruhe, Germany)	IR Microcentrifuge
CAT Ingenieurbüro M. Zipperer (Staufen, Germany)	ST5 Shaker
Dr. Goos-Suprema (Heidelberg, Germany)	X-Ray Casette
Edmund Bühler (Hechingen, Germany)	TH 15 heating cover
	KS-15 control shaker
Eppendorf (Hamburg, Germany)	Microcentrifuge 5415 D
	Thermomixer compact
GFL Gesellschaft für Labortechnik (Burgwedel, Germany)	Water Bath Type 1008
	Hybridisation Incubator 7601
Heidolph Instruments (Schwabach, Germany)	MR 2002 Magnetic Stirrer
Hettich (Tuttlingen, Germany)	Mikro 20 Tabletop Centrifuge
	Mikro 200R Tabletop Centrifuge
Heraeus (Hanau, Germany)	HERAcell 150 Incubator
	HERAsafe HS 9-18 Safety Cabinet
	UT 12P Heating and Drying Oven
Herolab (Wiesloch, Germany)	Gel Documentation System
	ICU-1
	UVT-20 SL UV Transilluminator with

	Panasonic Video Monitor WV-CM 1020
Hirschmann Laborgeräte (Eberstadt, Germany)	Pipetus Pipette Filler
Holten (Allerød, Denmark)	LaminAir Safety Cabinet Model 1.2
Incucell Medcenter (München, Germany)	Incubator for Microbiological Cultures
Integra Biosciences (Fernwald, Germany)	Fedegari FVA3 Autoclave
Kern und Sohn (Balingen, Germany)	Precision Balance 440-33N
Leica Microsystems (Wetzlar, Germany)	DM LB Light Microscope
	DFC320 Microscope Camera
	BioMed Microscope
	CM3050 S Cryosat
	Rotary Microtome Leica RM 2235
	S6E Dissecting Microscope with
	Fiber Optic Illuminator KL 1500 LCD
membraPure (Bodenheim, Germany)	Astacus Water Purification System
Memmert (Schwabach, Germany)	Waterbath
Mettler-Toledo (Greifensee, Switzerland)	SevenEasy pH-Meter
Nikon (Tokyo, Japan)	Eclipse 90i upright automated microscope
	DS-QiMc black and white CCD camera
	Nikon DS Ri1 color CCD camera
	Plan Apo 4x NA 0.2 objective
	Plan Apo 10x NA 0.45 objective
	Plan Apo 20x NA 0.75 objective
	Plan Apo 40x NA 0.95 objective
Olympus Germany (Hamburg, Germany)	BX61WI Fluorescence Microscope
	CKX41 Fluorescence microscope
Paul Marienfeld & Co. (Lauda-Königshofen, Germany)	Neubauer Counting Chamber
Sartorius (Göttingen, Germany)	Potter S Homogeniser

Schott (Mainz, Germany)	KL 1500 LCD Light Source
Sigma Laborzentrifugen (Osterode am Harz, Germany)	2-5 Tabletop Centrifuge
Starlab (Hamburg, Germany)	RM Multi-1 Programmable Rotator-Mixer
Tecan (Männedorf, Switzerland)	Sunrise^{TM} microplate reader
Techne (Staffordshire, UK)	Hybridiser HB-1D Incubator
Visitron Systems (Puchheim, Germany)	SpoRT CCD Camera
Zeiss (Oberkochen, Germany)	Axiovert 200 M Microscope
	FluoArc Light Source
	Plan NeoFLUAR 40x/1.3 Oil Objective
	Plan Apochromat 63x/1.4 Oil Objective
	Plan FLUAR 100x/1.45 Oil Objective

3.1.15 Software

4D (San Jose, USA)	4D Client
Applied Biosystems (Darmstadt, Germany)	ABI Prism 7000
Adobe Systems (San Jose, USA)	Adobe Acrobat
	Adobe Photoshop
	Adobe Illustrator
Biorad (München, Germany)	Quantity One 1-D Analysis Software
Wayne Rasband (NIH)	ImageJ
Microsoft (Redmond, USA)	MS Office 2007
Soft Imaging Systems GmbH (Münster, Germany)	AnalysisSIS
Tecan (Männedorf, Switzerland)	Magellan Data Analysis Software
Visitron Systems (Puchheim, Germany)	Metamorph Software (Version 6.2r6)

3.1.16 Disposables

Autoclave bags CPP clear	Nerbe Plus (Winsen/Luhe, Germany)

Bacteriological petri dishes, 10 cm	Zentrallager (INF 367, Heidelberg, Germany)
Cell scraper 1.9 cm long	Covance (Princeton, USA)
Cell scraper	Greiner Bio-One GmbH (Kremsmünster, Austria)
Cell strainer 100 μm	Millipore (Billerica, USA)
Conical tubes, 15 ml and 50 ml	Greiner Bio-One GmbH (Kremsmünster, Austria)
Cryo vials, CryoS, PP, with screw cap	Greiner Bio-One GmbH (Kremsmünster, Austria)
Embedding Medium Aqua Poly Mount	Polysciences Europe GmbH (Eppelheim, Germany)
Embedding molds Peel-A-Way truncated / T12	Polysciences Europe GmbH (Eppelheim, Germany)
FACS tubes Polystylene Round Bottom Tubes 5 ml	BD Falcon (San José, USA)
Filter pipette tips (10 μl, 20 μl, 200 μl and 1000 μl)	Sarstedt (Nümbrecht, Germany) or Starlab (Hamburg, Germany)
Glass cover slips 13 mm, 15 mm	Marienfeld (Lauda-Königshofen, Germany)
Gloves Nitril S	VWR (Radnor, USA)
Gloves Peha-soft S	Hartmann (Heidenheim,Germany)
Hyperfilm ECL	GE Healthcare/Amersham™ (Little Chalfont, UK)
Injection needles (21 G x 1 ½ " Nr. 2, 25 G x 1" Nr. 18, 24 G, 30 G x ½")	BD Microlance (San José, USA)
Kimwipes	Kimberly Clark (Roswell, USA)
Microscope glass slides Superfrost	Roth (Karlsruhe, Germany)
Microtome Blades 819 Low Profile	Leica Microsystems (Wetzlar, Germany)
Microtome blades S35	Feather (Osaka, Japan)
Parafilm	Pechiney (Akron, USA)
Pasteur Capillary Pipettes (150 mm/	Wilhelm Ulbrich (Bamberg, Germany)

230 mm)

PCR tubes with attached lids	Kisker (Steinfurt, Germany)
Pipette tips (10 μl, 20 μl, 200 μl and 1000 μl)	Greiner Bio-One GmbH (Kremsmünster, Austria)
Plastic cuvettes 1 ml	Sarstedt (Nümbrecht, Germany)
PVDF-Membrane	Millipore (Billerica, USA)
Real Time RT-PCR MicroAmp Optical 96well reaction plate	Applied Biosystems (Darmstadt, Germany)
Real Time RT-PCR Optical adhesive films	Applied Biosystems (Darmstadt, Germany)
Reaction tubes (1.5 ml, 2.0 ml)	Greiner bio-one (Kremsmünster, Austria)
Safe-Lock reaction tubes (1.5 ml, 2.0 ml)	Eppendorf (Hamburg, Germany)
Sterile filter (Steritop-GP 0.45 μm 150 ml 45 mm width)	Millipore (Billerica, USA)
Syringes (1 ml)	BD Plastipak (Franklin Lakes, USA)
Syringe driven filter unit 0.22 µm / 0.45 µm	Millipore (Billerica, USA)
Tissue culture Flasks (25 cm^2, 50 cm^2)	Nalgene Nunc (Penfield, USA)
Tissue culture petri dishes 3.5 cm	Greiner Bio-One (Kremsmünster, Austria)
Tissue culture petri dishes 6 cm	Nalgene Nunc (Penfield, USA)
Tissue culture petri dishes 10 cm	Greiner Bio-One (Kremsmünster, Austria)
Tissue culture petri dishes 15 cm	BD Falcon (Franklin Lakes, USA)
Tissue culture pipettes (2 ml, 5 ml, 10 ml)	Greiner Bio-One (Kremsmünster, Austria)
Ultracentrifuge tubes „Polyallomer Röhrchen, 38,5 ml, PA, dünnwandig"	Beranek (Weinheim, Germany)
Whatman paper	Schleicher und Schuell Bioscience (GE Healthcare, Little Chalfont, UK)

3.2   Methods

3.2.1   Cell culture

3.2.1.1   Permanent cell lines

3.2.1.1.1 Culture and passaging of HEK293 and HEK293T cells

HEK293 and HEK 293T cells were grown in either 10- or 15 cm cell culture petri dishes. The cells were grown to exponential growth at 70 – 80% confluency. The cells were passaged three times a week as follows: cells were rinsed very carefully with D-PBS and incubated with 0.5 ml (10 cm dishes) or 1.5 ml (15 cm dishes) Trypsin/EDTA for 1 minute at 37 °C. They were resuspended in fresh medium and centrifuged for 5 min at 800 x g. After centrifugation, the medium was aspirated, the cells resuspended in fresh culture medium and plated out in dilutions of 1:5 or 1:10 in fresh culture dishes.

For the production of lentivirus, cells were counted and 19 million cells plated on a 15 cm culture dish coated with 0.001% poly-L-lysine. Those were then grown for another day before being transfected.

3.2.1.2   Primary cultures

3.2.1.2.1 Neurosphere cultures

Culture medium was supplemented just before preparation and warmed to 37 °C in an incubator. The mice employed for neurosphere cultures were of the inbred background C57BL/6. Neurospheres were prepared from E15.5 embryonic brain tissue as described (Gritti et al 2001, Reynolds & Weiss 1996). The pregnant female was sacrificed, the embryos removed from the uterus and decapitated. The dissection was carried out in petri dishes with PBS.

The heads were opened using fine forceps and the brains removed. The hemispheres were separated carefully and the meninges removed. From the hemispheres either the lateral and medial ganglionic eminences or for cortical cultures, respectively, a part of the frontal cortex, were dissected out. The tissue was collected in PBS during the dissection and cooled on ice.

The tissue was then triturated with a fire-polished Pasteur pipette in order to obtain a single cell solution. The cells were counted and plated out in culture flasks in a density of 100 000 cells/ml in NS growth medium (striatal cells) or 150 000 cells/ml (cortical cells). The neurospheres were incubated in suspension at 37 °C, 5% CO_2 for one week. After 5 days they were fed with an equal volume of NS growth medium. The cells were plated out on polyornithine-coated culture dishes or cover slips for differentiation after 7 days in culture. Cryosections of neurospheres stained with developmental markers after 7 das in culture can be found in the Appendix.

3.2.1.2.2 Hippocampal cultures

Primary hippocampal cultures were obtained from Stefanie Schumacher.

3.2.1.3 Differentiation of neurosphere-derived cells

Differentiation medium containing FGF2 was prepared freshly and warmed to 37 °C in an incubator. Neurospheres were collected in 50 ml conical tubes. Upon centrifugation for 4 min at 100 x g, the medium was removed and a small amount of fresh differentiation medium added to the cells, 2 – 5 ml depending on the amount of neurospheres collected. The neurospheres were then triturated with a fire-polished Pasteur pipette and the single-cell suspension plated out on polyornithine-coated (200 mg/ml) petri dishes in differentiation medium without EGF and with 1% fetal calf serum (FCS, Invitrogen), a medium that supports the differentiation of both neurons and astrocytes.

For virus infections the cells are plated out on petri dishes coated with poly-L-Lysine in the following densities:

Plating density of striatal cells

Cell culture vessel	Regular cultures	
12 well plate, per well	200 000	300 000 – 400 000
6 cm petri dish	1 million	1.5 – 2 million
10 cm petri dish (for RNA or protein isolation)	3 millon	4 – 5 million

For FACS Analysis, the cells were plated out on dishes coated with 1 mg/ml poly-L-lysine. For lentivirus infection cells were plated out on coverslips coated with polyornithine (washed 2x with PBS) and 1 µg/ml Laminin (2 h, washed 3x with PBS).

2.5 days after plating, the medium was changed to differentiation medium without FGF2 and EGF, but containing 1% FCS.

During the differentiation protocol cells were either infected with lentivirus or adeno-associated virus or treated pharmacologically to examine the effects of HDAC inhibition. Thereupon they were lysed for either RNA or protein analysis, fixed for immunostainings or examined with FACS Analysis.
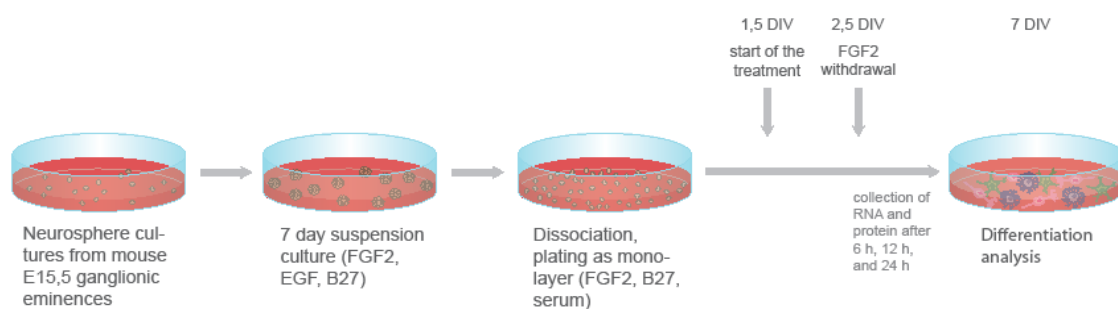
Figure 3.1. Scheme of the neurosphere culture and differentiation protocol

3.2.1.4   Amaxa nucleofection and Dual-Luciferase Reporter Assay

150 000 cells were used for one well of a 24-well plate. The cells were counted and aliqouted. They were spun down and the medium aspirated. Afterwards the cells were resuspended in Amaxa nucleofection medium.

Plasmids containing firefly luciferase and *Renilla* luciferase as a reporter (BREx4-luc) are added, everything pipetted into the Amaxa nucleofection cuvette which is then placed into the nucleofection device and transfected according to manufacturer's specifications (programme A-33). Afterwards, the cells are immediately resuspended in pre-warmed medium and plated in 24 well plates. They were treated with 10 nm, 25 nm or 50 nM TSA or 10 ng/ml BMP2 for different durations and after the incubation they were lysed with passive lysis buffer and the lysates stored at –80 °C.

3.2.1.4.1 Measurement

In the Dual-Luciferase Reporter Assay, the activities of firefly (*Photinus pyralis*) and Renilla (*Renilla reniformis*) luciferases are measured as reporters sequentially from a single sample. First, the firefly luciferase reporter is measured by adding Luciferase Assay Reagent II (LAR II) to generate the luminescent signal. After measuring the evoked luminescence, the reaction is quenched, and simultaneously the Renilla luciferase reaction initiated by adding Stop & Glo® Reagent. The Renilla luciferase signal decays slowly over the course of the measurement. The Dual-Luciferase Reporter Assay is constructed in a way that both reporters yield linear readouts.

The BRE(2243/2191)x4-luc construct was generated by cloning four copies of the BRE sequence upstream of the E1b TATA box in the pE1b-luc vector (Hata et al 2000).

The lysates were removed from –80 °C and allowed to adjust to room temperature. 200 µl of lysate were transferred from each well to a 96-well microtitre plate. In the software Glomax 2.4 the delay was set to 10 sec and integration time to 10 sec. 2

measurements were made with a delay of 5 sec to determine the decay of the fluorescence signal.

75 µl Luciferase II solution were added to each well and lysates and mixed. Then the firefly luciferase fluorescence is measured. For Renilla fluorescence integration time was set to 3 sec. Stop & Glo® solution was supplemented with 50x Renilla substrate to a final concentration of 1x. 75 µl of this mixture were added to each well and mixed briefly. The Renilla fluorescence was measured.

The average fluorescence value of all empty wells was considered as a blank and subtracted from each firefly fluorescence value. The lowest fluorescence value of the Renilla measurement was used to normalize all values (Renilla fluorescence/lowest Renilla fluorescence value). All firefly luciferase values were normalized with the Renilla fluorescence from the respective well. An average of all wells with the same sample was calculated and all averages normalized to control.

3.2.1.5 Pharmacological treatments

The following pharmacological reagents were added in different experiments: trichostatin A (Sigma, Calbiochem) 10 nM, 25 nM, or 50 nM or human recombinant bone morphogenetic protein 2 (BMP2) (1 ng/ml; prepared and provided by Dr. Peter Hortschansky, Jena).

3.2.1.6 Fixation

Cells were rinsed with 1x PBS, then fixed with 4% PFA in PBS for 10 minutes at 4 °C and rinsed again 3 times with 1x PBS. They were then either stored in PBS at 4 °C or immediately processed for immunofluorescence stainings.

3.2.2   FACS Analysis

Neurospheres were grown in suspension culture as described above for 7 days. Tissue culture petri dishes were freshly coated with poly-L-lysine (1 mg/ml in water) for either 2 h or overnight at 37 °C in the incubator.

Neurospheres were dissociated with a fire-polished Pasteur pipette and plated out in a density of 3.5×10^6 cells on the poly-L-lysine coated 6-cm cell culture dishes. They were cultured according to the standard differentiation protocol described above.

At DIV 7 cells were dissociated from the plates. First, the medium was discarded, the cells were then washed with 1x PBS and incubated with 1 ml Versene for 1 min at 37°C. After this, Versene was removed and 1 ml of a trypsin-papain-mixture [0.25% Trypsin; 2.5 U/ml papain] added for 6 min at 37 °C.

The cells were then dissociated by gently tapping the culture dish and repeated trituration by pipetting. The cell suspension was diluted in 1x PBS with 10% FCS, transferred to a fresh tube and centrifuged for 2 min at 4000 rpm. After discarding the supernatant, the cells were fixed in 4% PFA in 1x PBS for 20 min at 4 °C, then washed 3 times in 1x PBS with 2% FCS (PF) by centrifugation for 2 min at 4000 rpm and subsequent resuspension in PF. Eventually the cells were resuspended in PF with 0.18% saponin (PFS).

The cell suspension was divided according to the different antibody stainings and controls.

3.2.2.1 Antibody stainings – Neurogenesis

To assess the extent of neurogenesis in the cultures, stainings with TuJ1 antibody were carried out in order to label and subsequently quantify newborn neurons. Primary TuJ1 antibody was prediluted in PFS and applied to the cells at a concentration of 1:1000 for 30 min at 4 °C (100 µl per sample). The cells were washed three times with PFS, each time centrifuged for 2 min at 4000 rpm and resuspended in PFS. They were incubated with secondary antibodies conjugated with Alexa546 at a dilution of 1:1000 in PFS for 30 min at 4 °C. Afterwards, the cells were washed with PFS twice, once with PF and resuspended 200 µl of in PF.

The stained cells were then analyzed using a Becton Dickinson FACSCalibur flow cytometer.

3.2.3   Molecular biology

3.2.3.1   Transformation of bacteria

Chemically competent E. coli cells were stored in aliquots at −80 °C. For each transformation one vial of competent cells was gently thawed on ice. 50 µl of the cell suspension was mixed with 0.5 µl of DNA and incubated on ice for 30 min. Following a heat shock of 30 s in a 42 °C water bath, 450 µl of LB-medium without antibiotics was immediately added to the cells. The bacteria were incubated on a bacterial shaker at 37 °C and 180 rpm for 45 min. 50 − 100 µl of the bacteria suspension were plated on agar plates containing the appropriate antibiotic for selection.

3.2.3.2   Minipreparation of plasmid DNA

Plasmid DNA was isolated from bacteria in an alkaline lysis essentially as described by Birnboim and Doly and Ish.Horowicz and Burke (Birnboim & Doly 1979, Ish-Horowicz & Burke 1981). Solutions 1 and 3 were stored at 4 °C and put on ice before starting the protocol. From an agar plate a single colony was picked with an autoclaved pipette tip and incubated in 5 ml of LB-medium containing the appropriate selection antibiotic. The culture was incubated overnight in a bacterial shaker at 37 °C. 4 ml of the culture were centrifuged for 1 min at 12 000 x g and 4 °C to pellet the bacteria and remove the medium. The bacterial pellet was thoroughly resuspended in 100 µl solution 1 by pipetting up and down and vortexing. To lyse the cells, 200 µl lysis solution 2 were added. The tubes were closed firmly, rapidly inverted five times and placed on ice. 150 µl ice-cold solution 3 was added to neutralize the lysis buffer. Each tube was vortexed gently for 10 s and incubated on ice for 3 − 5 s. Afterwards, the samples were centrifuged at 12 000 x g and 4 °C. Supernatants were transferred into new tubes and the volume measured for subsequent DNA extraction.

3.2.3.3 Plasmid isolate purification

3.2.3.3.1 Phenol-chloroform extraction

In order to purify the DNA sample, phenol-chloroform extraction was perfomed. An equal volume of phenol-chloroform was added to the supernatant and the sample vortexed. The sample was then centrifuged for 2 min at 12 000 x g and 4 °C and the supernatant transferred into a new tube.

3.2.3.3.2 DNA ethanol precipitation

In order to precipitate the DNA upon phenol-chloroform extraction, ethanol precipitation was performed. Two volumes of 100% ethanol were added to the supernatant and vortexed briefly. After 2 min at room temperature, the solution was centrifuged for 5 min at 12 000 x g and 4 °C. The supernatant was removed, the pellet washed once with 1 ml 70% ethanol, centrifuged 5 min at 12 000 x g and 4 °C. The supernatant was removed again, the DNA pellet dried for approximately 10 min and resuspended in 50 µl Tris-HCl, pH 8.0. The Plasmid-DNA was stored at –20 °C.

Alternatively, plasmid minipreparations were carried out with the QIAgen QIAprep Spin Miniprep Kit according to manufacturer's instructions.

3.2.3.4 Plasmid midipreparation

Plasmid midipreparations were carried out with Sigma GenElute Plasmid Midiprep Kit according to manufacturer's instructions.

3.2.3.5 Plasmid maxipreparation

To amplify plasmid DNA on a larger scale, an overday culture was prepared. From an agar plate one bacterial colony was picked and incubated in 5 ml LB-medium in a bacterial shaker at 37 °C. In the evening, 2 ml of this culture were used to inoculate 500

ml of LB-medium containing the appropriate selection antibiotic which was incubated overnight in a bacterial shaker at 37 °C and 250 rpm.

The plasmids were then isolated using the GenElute Plasmid Maxiprep Kit (Sigma) according to manufacturer's specifications. The plasmid DNA was eluted in the elution buffer provided and then precipitated to increase the purity of the preparation.

The plasmid eluate was supplemented with 1/10 of its volume of 3 M sodium acetate (pH 5.3) and a volume of ethanol twice as large as the volume of the eluate was added and everything mixed. To precipitate, the mixture was incubated for 30 min at –80 °C, then centrifuged for 10 min at 4 °C and 13 000 rpm, the DNA pellet washed with 70% ethanol and again centrifuged for 10 min at 4 °C and 13 000 rpm. The pellet was air-dried and subsequently resuspended in 200 µl 10 mM Tris (pH 8.0). After determining concentration and purity by measuring the $OD_{260/280}$ the plasmid DNA was stored at –20 °C.

3.2.3.6 Plasmid maxipreparation for lentivirus production

For lentivirus production plasmid DNA was prepared using the NoEndo Jetstar Endotoxin Free Maxi Kit, Genomed (Löhne, Germany) according to manufacturer's instructions. Overday and overnight cultures were set up as described above. Plasmid DNA was eluted using the buffer provided, concentration and purity determined measuring the $OD_{260/280}$ and DNA stored at –20 °C.

3.2.3.7 Agarose gel electrophoresis

To analyze DNA samples on an agarose gel, the samples were supplemented with a 10x Orange G loading dye to a final concentration of 1x. The samples were then loaded on an agarose gel (1 – 2% agarose in TAE (w/v) with ethidiumbromide at a concentration of 7 µl per 120 ml Gel) and electrophoresis carried out at 100 V – 130 V. After separation the DNA was visualized on a UV table and the bands photographed for documentation.

3.2.3.8   Gel extraction

For the extraction of DNA from the agarose gels, the QIAquick Gel Extraction Kit was used. The bands were visualized on a UV table, cut out of the gel with a scalpel, weighed and then processed with the kit according to manufacturer's instructions.

3.2.3.9   Restriction digest

Restriction enzymes and buffers were used both from NEB and Fermentas. The buffer compositions and restriction times were adapted to manufacturer's suggestions. For double digestion reactions, optimal conditions were determined according to manufacturer's specifications.

3.2.3.10 RNA isolation

3.2.3.10.1   RNA isolation using Trizol

Cells were grown in a monolayer in 6 cm petri dishes. The cells were lysed within the dishes by adding 1 ml of Trizol to a 3.5 cm petri dish (1 ml/10 cm^2). The lysate was pipetted up and down two or three times and was then either further processed immediately or stored at –80 °C.

The lysate was incubated 5 min at RT to ensure dissociation of nucleoprotein complexes. 200 µl Chloroform were added per 1 ml of Trizol, the tube shaken for 15 sec and incubated at RT for 2 – 3 min. The lysate was centrifuged for 15 min at 4 °C and 12 000 x g which resulted in a colourless upper aqeous phase containing the RNA, an interphase and a lower red phenol-chloroform phase.

To precipitate the RNA, the upper phase was transferred to a fresh tube, 500 µl isopropyl alcohol per ml of Trizol reagent were added and incubated for 10 min at RT. The mixture was then centrifuged for 10 min at 4 °C and 12 000 x g, the supernatant removed and the RNA pellet washed with at least 1 ml 75% ethanol per ml of Trizol reagent used. The mixture was vortexed and centrifuged for 5 min at 4 °C and 7500 x g.

The RNA pellet was air-dried for 5 – 10 min, resuspended in RNAse-free water and incubated for 10 min at 55 °C.

3.2.3.10.2   RNA isolation with QIAgen RNA Mini-Kit

RNA from tissues and cell cultures was isolated using the QIAGEN RNeasy Mini Kit according to the manufacturer's instructions. RNA was eluted with 30 µl of water. To further increase the concentration, the eluate was used to elute remaining RNA from the membrane a second time. The concentration was determined by UV spectrophotometry at 260 nm. The RNA was stored at –80 °C.

3.2.3.10.3   RNA isolation from embryonic brain tissue

RNA was isolated from E13.5 or E15.5 brain tissue. The brains were dissected in PBS and the tissue collected in Eppedorf tubes cooled in a mixture of liquid nitrogen and dry ice. 600 µl RLT buffer were applied to each sample. With a rotor-stator-homogenizer the tissue is homogenized immediately upon adding the lysis buffer for two minutes at a medium speed. Afterwards the RNA is isolated using the QIAquick RNA isolation Kit according to manufacturer's specifications.

3.2.3.11   cDNA work

3.2.3.11.1   cDNA synthesis

Reverse transcription of RNA was carried out using the SuperScript® II Reverse Transcriptase from Invitrogen. The DNA polymerase synthesizes a complementary DNA strand from single-stranded RNA.

Reaction setup for 1 – 5 μg of total RNA

2 µg	RNA (volume 13 µl, diluted with Millipore water if necessary)
1 µl	random hexamer primers (100 µM, Fermentas)
1 µl	oligo(dT)$_{18}$ primer (0.5 mg/ml, Fermentas)
1 µl	dNTP-Mix

This mixture was incubated for 5 min at 65 °C on a Biorad iCycler thermocycler and subsequently put on ice. After collecting the liquid at the bottom of the tube by centrifugation, the following reagents were added:

5 µl	5x First Strand buffer (Invitrogen)
2.5 µl	0.1 M DTT
1.25 µl	Ribolock RNase Inhibitor (Fermentas, 40u/µl)

Everything was mixed carefully by pipetting up and down and incubated for 2 min at 42 °C. After this 1 µl Super Script II reverse transcriptase was added, the reaction mixed carefully and incubated for 1.5 h at 42 °C. The cDNA was diluted 1:5 for real time RT-PCR.

3.2.3.11.2   Gapdh-PCR to control cDNA quality

To control for the quality of the cDNA, a PCR reaction with primers for Gapdh was performed. As Gapdh is a housekeeping gene, equal amounts of its PCR product (expected size 500 bp) were expected in each cDNA preparation.

Mastermix for 1 sample

H_2O	15.3 µl
10x PCR buffer	2.0 µl
50 mM $MgCl_2$	0.8 µl
10 mM dNTPs	0.4 µl
GAPDH 3' primer	0.4 µl
GAPDH 5' primer	0.4 µl
Taq polymerase	0.2 µl
Total	19.5 µl

To the mastermix, 0.5 µl DNA were added per sample. The PCR reaction was performed according to the following programme on a Biometra PCR Cycler TPersonal.

Temperature	Time	n cycles
94 °C	5 min	1
94 °C	30 s	
60 °C	30 s	32
72 °C	30 s	
72 °C	5 min	1

The PCR products were separated on a 1.2% agarose gel at 100 V for about 30 min and visualized with ethidium bromide and UV light. When all samples showed the same amount of Gapdh PCR product, cDNA was used for quantitative real time RT-PCR.

Figure 3.2: Results of the Gapdh PCR after cDNA transcription. The expected size of the PCR product is at 500 bp. 100 bp molecular size marker. Gelelectrophoresis was carried out for 45 min on a 1.2% agarose gel.

3.2.3.11.3   Real Time RT-PCR

To perform quantitative real time RT-PCR, equal amounts of cDNA (1 – 5 µg) of each sample were diluted in water to a final volume of 13.5 µl. The reaction mix was prepared by mixing 15 µl TagMan Master Mix per sample with 1.5 µl of the respective TaqMan Gene Expression Assay. This mixture was then pipetted into the relevant wells of a 96 well reaction plate and the DNA dilution added. Each sample was assayed in triplets. The plate was sealed with an adhesive cover and centrifuged for 2 min at 1500 rpm to remove bubbles from the reaction volumes and collect the liquid at the bottom of the tubes. Sterile-filtered water (Sigma) served as negative control.

Amplification was performed on an Applied Biosystems AbiPrism 7000 Cycler. The program used was the following:

50 °C	2 min
95 °C	10 s
95 °C	15 s
60 °C	1 min

A total of 50 cycles were run. Analysis of the data was carried out using the provided software. The data were analyzed using the ΔΔCt method which assumes a duplication of DNA during one cycle. For all analyzed genes, an auto-baseline was set in order to eliminate background noise. The threshold is determined as the region in which amplification progresses in a linear fashion. The cycle of threshold is also automatically determined.

3.2.3.12 Production and harvest of lentiviral particles

3.2.3.12.1   PEI-Transfection of HEK293T cells

Plasmids containing shRNAs to knock-down individual HDACs were purchased from Sigma Aldrich. shRNA sequences were generated by Sigma algorithms. To select infected cells, the Sigma plasmids contain a sequence for puromycin resistance. However, they did not contain a reporter sequence for a fluorescent protein. Therefore, for the production of lentiviral particles, the knock-down construct was cloned into a pLentiLox3.6 plasmid vector.

Plasmids for Lentivirus production were isolated using the GenoMed NoEndo Maxiprep Kit as described above. The HEK293T cells used to produce virus were cultured in low passage numbers and split the day before transfection. 19 million cells were plated on one 15 cm culture dish and grown until the next day to about 70 – 80% confluency.

Lentivirus production was based on three plasmids (Lois et al. 2002; Naldini et al. 1996): the transfer vector plasmid pLKO1.puro or pLL3.6 containing the gene of interest, the HIV-1 packaging vector ΔR8.9 and the VSVG envelope encoding vector.

Equimolar amounts of all three plasmids were transfected into HEK293T cells using PEI (polyethyleneimine, Sigma). 22 µg pΔR8.9, 15 µg pVSVG and 30 µg of the respective plasmid containing the shRNA sequence were used. The plasmids were pipetted into a vial containing 2.2 ml OptiMem medium, while the PEI was pipetted into a vial containing 2.4 ml OptiMem medium. The mixtures were incubated at room temperature for 5 min and then the DNA solution pipetted into the PEI solution. After incubation of 1 h at RT, DNA and PEI have formed complexes which are able to penetrate the cells and to deliver DNA to the cells. Prior to transfection 10 ml medium were removed from the cells and kept at 37 °C. Then, the transfection mix was carefully and dropwise added to the cells. 4 h after transfection the medium was changed.

Transfection efficiency was estimated after 48 h visually by determining the rate of GFP-expressing cells in the cultures. Transfection efficiency was usually between 60 and 70%. After 48 to 72 h the medium was removed from the cells, pooled and subjected to low speed centrifugation for 5 min at 800 x g at RT to remove cell debris. The supernatant was sterile filtered through 0.45 µm filters and transferred to ultracentrifuge vials. It was then centrifuged at 25 300 rpm in an ultracentrifuge with a SW32Ti rotor at 4 °C for 90 min. The supernatant was carefully decanted and the pellet of viral particles resuspended in 200 µl PBS and layered on a sucrose cushion (1.5 ml 20% Sucrose in HBSS). It was then purified through the sucrose cushion by centrifugation in a SW50.1 rotor for 2 h at 21 000 rpm. The pellets were then resuspended in 200 µl HBSS, aliquoted into eppendorf tubes, deep frozen in liquid nitrogen and stored at –80 °C.

Transfection mixture for virus production, per 15 cm dish HEK293T cells

Plasmid	Amount per 15 cm dish
pCMV ΔR8.9	7.5 µg
pVSVG	5 µg
pLentilox3.6 (shRNA)	10 µg
PEI	75 µl
OptiMem	925 µl

3.2.3.12.2   *Infection of neurosphere-derived precursor cells to knock down HDACs*

Neurosphere cells were plated out in a monolayer without FGF2 and with serum and infected one day after plating or on the same day. One virus aliquot was gently thawed on ice. The virus was added to the medium of the cells, the plates were gently shaken to distribute the virus and incubated between 1 and 7 days before preparation of RNA lysates.

Volumes of lentivirus used for infection	12-well (per well)	6-cm petri dish
Striatal cells	1.5 µl	7 µl
Cortical cells	2 µl	10 µl

3.2.4   Biochemistry

3.2.4.1 Protein extracts

3.2.4.1.1 *Protein extracts from cells*

Cells were grown in cell culture petri dishes and subjected to treatment. To obtain lysates for immunoblotting, the medium was removed from the dishes and the cells were washed once with PBS. The plates were put on ice. For 3 million cells, 200 µl RIPA buffer complemented with the following protease inhibitors: 1 mM ε-aminocaproic acid (stock 1 M), 0.2 mM PMSF (stock 0.1 M in 2-propanol), 5 mM benzamidine (stock 0.5 M). The lysis buffer was applied to the cells and the cells scraped off in the buffer. The cell lysate was then transferred to a 1.5 ml reaction tube. To shear genomic DNA, the lysate was slowly passed through a 21 G needle 10 – 15 times and then centrifuged at 4 °C and 13 000 rpm to remove debris. The cleared lysate was then aliquoted into new reaction tubes and stored at –80 °C or subjected to SDS-PAGE and immunoblotting immediately.

3.2.4.1.2 *Protein lysates from embryonic brain tissue*

Brain tissue from brain and spinal cord tissue were prepared as follows. The tissue was dissected out of the embryos. From each embryo, the tail was removed for extraction of genomic DNA and genotyping. The brain or spinal cord was then weighed and according to the weight homogenizing buffer added.

To 1 mg of tissue, 20 µl of buffer were added. A glass homogenizer was inserted into a Potter, the tissue and homogenizing buffer put into the glass tube and homogenized for 2 min at 900 rpm. The homogenizer tube was kept in a beaker with ice throughout this procedure. The lysate was then transferred to a reaction tube on ice. The volume was measured and 5x Lämmli buffer added. The lysate was sheared subsequently with needles of decreasing diameter: 21G, 25G, and 30 G.

The lysates were incubated at 95 °C for 5 min, subsequently centrifuged at 13 000 rpm and 4 °C for 10 min, the cleared supernatant removed. 40 µl were frozen down for assessment of protein concentration and the lysate volume measured. They were eventually complemented with ß-mercaptoethanol to a final concentration of 5%.

3.2.4.2 Bradford-Assay

To determine protein concentrations of cell lysates, Bradford Protein Assay was applied. Protein standards were generated by dissolving BSA in water and adding RIPA according to the volume of the diluted protein samples . The measurement was carried out in a TECAN Sunrise Reader using Magellan Software.

3.2.4.3 BCA-Assay

The concentration of protein samples derived from embryonic tissue was determined in a BCA assay according to manufacturer's instructions.

3.2.4.4 Polyacrylamide-gel-based work

3.2.4.4.1 Polyacrylamide Gels

Acrylamide gels for the polyacrylamide gel electrophoresis (PAGE) and subsequent immunoblot analysis were prepared prior to electrophoresis according to the molecular weight of the protein of interest. For HDAC2 and BMP2 western blots, 12.5% acrylamide gels were poured. For HDAC4 western blot, 7.5% polyacrylamide gels were prepared.

Protein	Molecular weight	% Acrylamide
ß-Actin	42 kDa	12%
BMP2 precursor	60 kDa	12%
heterodimer	30 kDa	
monomer	18 kDa	
GFP		
HDAC2	56 kDa	12%
HDAC4	140 kDa	7.5%

Once the gels were fully polymerized, the electrophoresis was set up and the gel loaded immersed in electrophoresis buffer.

3.2.4.4.2 SDS-PAGE

Protein extracts were thawed on ice and complemented with 2x urea loading buffer. The samples were heated for 5 min at 42 °C and cooled to room temperature. 15 – 60 μg of protein per lane were separated on an acrylamide gel using the Bio-Rad Mini Protean III Gel System at a current of 35 mA.

3.2.4.4.3 Western Blot

After gel electrophoresis the separated proteins were transferred from the gel to a PVDF membrane. The membrane was activated in methanol for 15 s followed by 2 minutes in

double-distilled water and then kept in transfer buffer. The blot sandwich was assembled in a bowl filled with transfer buffer. The membrane was put onto three sheets of whatman paper with the water-repelling side facing away from the paper. The gel was carefully removed from the chamber and placed onto the membrane. This construction was covered by two more sheets of Whatman paper. The transfer was carried out using a Bio-Rad tank blot system, either for 3 h at 400 mA or overnight at 180 mA and 4 °C. Alternatively a semi-dry blot system was used for 1 – 1.5 h at 150 – 200 mA.

After blocking for 1 h in blocking buffer (5% milk/TBST) at RT on a rocker, the membrane was incubated with primary antibody diluted in blocking buffer for 1 h at RT or overnight at 4 °C. The membrane was washed 3 x 15 min with TBS-T and subsequently incubated with secondary antibody diluted in blocking buffer for 30 – 60 min at RT. Afterwards, it is again washed 3 x 15 min in TBS-T and once in TBS. For detection, ECL plus solution (GE) was applied to the membrane according to manufacturer's instructions. The membrane was then very shortly rinsed in TBS. Subsequently it was dried, put into a cassette, and Hyperfilm (GE) exposed to the signal. Development of the films was carried out using a Curix developing machine. As controls, housekeeping proteins like ß-actin or tubulin were detected in the samples using the described detection procedure a second time on the same membranes.

3.2.4.4.3.1 Quantification

For semi-quantitative analysis, films were scanned with a BioRad GS-800 Calibrated Densitometer and analyzed using QuantityOne software. Protein bands of interest were encircled and subsequently measured. Actin or tubulin bands were used as a reference for analysis.

3.2.5   Histological techniques

3.2.5.1   Fixation of cells on coverslips

Cells grown and treated on coverslips were fixed in order to be immunostained later on. The cells were washed once with pre-warmed D-PBS (37 °C). Subsequently 4 % PFA (RT) was added to the cells followed by incubation for 10 min at RT. The PFA was removed and the cells were washed three times with D-PBS at RT.

3.2.5.2   Fixation of embryonic brains for immunohistochemistry

13.5 or 15.5dpc timed-pregnant females were sacrificed, the embryos dissected from the mother and collected in cold 1x PBS. A tail sample was collected from the mother and from each embyo and processed in tail buffer.

The embryos were treated one by one to ensure that the genotyping results could be matched to the individual embryo samples later on. The embryo was decapitated and the heads placed in individual tubes with 10 ml 4% PFA and fixed overnight on a shaker at 4 °C. The next day, the heads were washed 2 times for 1 h in 1x PBS to remove residual PFA before embedding.

3.2.5.3   Embedding of embryos for cryosections

The heads were incubated in a series of sucrose solutions at increasing concentrations: 10%, 20% and 30% sucrose in 1x PBS. Each incubation was carried out on a shaker at 4 °C overnight. "Peel-Away" mounting moulds were labelled with the sample name and line, the date, the intended orientation of the head and filled with Jung tissue freezing medium and the heads placed carefully inside. After 30 min incubation at RT, the heads are carefully orientated as intended and the mould dipped into liquid nitrogen several times to keep the samples in position. Then the moulds are placed on dry ice to freeze through. The samples were stored in cryoboxes at –80 °C.

3.2.5.4　Cryosectioning

Cryosections were prepared on a Leica Cryostat. The chamber and sample temperatures had to be adapted according to the temperatures and conditions of the day the sections were prepared. Usually a chamber temperature of –21 °C and an object temperature of –19 °C was intended.

The sections were cut, collected on superfrost slides and examined with a microscope. For each slide a note was taken about in which region of the brain the sections were located, using an atlas of the developing mouse brain for comparison.

3.2.6　Immunological techniques and histochemistry

3.2.6.1　Immunofluorescence staining of fixed cells

Coverslips carrying the fixed cells were placed on a layer of parafilm into a humid chamber. The cells were incubated for 1 h with blocking buffer and subsequently with primary antibody diluted in antibody buffer, either for 1 h at RT or overnight at 4 °C. After incubation, the cover slips were washed in 1x PBS three times for 10 min and then incubated for 1 h at RT with the secondary antibody diluted in antibody buffer. If the nuclei were to be visualized the cover slips were then incubated for 10 min at RT with DAPI in PBS (0.0004% w/v) The cells were then washed again three times for 10 min in 1x PBS, the coverslips then dipped briefly into Millipore water and mounted with Aqua-Poly/Mount on a previously cleaned glass slide. The mounted cells were kept at 4 °C until they were examined by fluorescence microscopy.

3.2.6.2　Immunofluorescence staining of cryosections

Slides with cryosections were removed from –80 °C and allowed to adjust to RT. The sections were encircled with Roti-Liquid Barrier marker to contain the buffers on the sections. After the Roti-Liquid barrier marker was dried the sections were rehydrated in 1x PBS for 15 min at RT. Excessive 1x PBS was carefully removed using Kimwipes. 200 μl of blocking buffer was added onto each slide and incubated for 1 hour at RT in a

wet chamber. The blocking buffer was subsequently removed and 200 μl of antibody buffer with the appropriate primary antibodies were added to the slides. The sections were incubated with the primary antibody in a wet chamber at 4 °C overnight. The next day the primary antibody was removed and the sections were washed 4 x 10 min with 1x PBS at RT in glass cuvettes. Then the appropriate secondary antibodies diluted in antibody buffer were added to the slides and incubated in a wet chamber in darkness for one hour at RT. Afterwards, the secondary antibodies were removed and the sections were washed 1 x with DAPI in 1x PBS for 10 min at RT and 3 x in 1x PBS for 10 min at RT. The sections were briefly dipped in MilliQ H_2O which was then removed using a Kimwipe. The sections were mounted with coverslips using Aqua-Poly/Mount and stored at 4 °C in the dark.

3.2.6.3 ß-Galactosidase staining

ß-Galactosidase was used as a reporter gene in transgenic mice deficient for HDAC4 and HDAC5. HDAC4$^{-/-}$ mice were generated by knock-in of a nuclear-localized *LacZ* cassette into exon 6 of HDAC4 such that *LacZ* was in-frame with amino acid 162 (Rick B. Vega 2004). In HDAC5-deficient mice expression of the enzyme takes place in cells with a perturbation of the endogenous HDAC-expression. ß-Galactosidase staining can therefore be used to assess the tissue distribution of HDAC5 expression.

The pregnant female was sacrificed and E13.5 or E15.5 embryos removed from the uterus. The embryos were incubated in ß-galactosidase fixation solution for 60 minutes at 4 °C. They were washed three times for 20 min in wash buffer and three times for 20 min in 1x PBS. The embryos were then incubated in 15% sucrose in PBS at 4 °C overnight. Then they were incubated in 30% sucrose overnight at 4 °C and eventually embedded in Jung tissue freezing medium and stored at –80 °C.

From the embedded embryos 10 μm sections were prepared using a Leica CM1850 cryostat and collected on slides. The slides were stored at –80 °C.

Before staining the sections on glass slides were encircled with clear nail polish. The sections were then encircled re-fixed in 0.2% glutaraldehyde in PBS for 10 min at 4 °C

and washed three times for 5 min in wash buffer and subsequently incubated with ß-galactosidase staining solution at 37 °C overnight. The next day they were washed for 10 min with PBS. A part of the stained sections on each slide was counterstained with nuclear fast red by incubating the two separate brain slices in a 1:4 dilution of Nuclear Fast Red for 1 min. The sections were then incubated in dilutions of ethanol of increasing concentrations: 50% ethanol for 5 min, 70% ethanol for 5 min, 80% ethanol for 5 min, 90% ethanol for 5 min and pure ethanol for 5 min. They were incubated in xylol for 5 min in a fume hood and eventually mounted in Entellan.

3.2.7   Mouse strains and genotyping

3.2.7.1   Mouse Strains

All animal experiments were carried out according to the guidelines of the University of Heidelberg and the State of Baden-Württemberg.

The mouse lines were kept in the animal facility of the University of Heidelberg (IBF). They were exposed to light between 6:00 AM to 6:00 PM. For the administration of the colonies the software 4D Client (TierBase) was used.

To obtain timed-pregnant females, one male and two female mice were set up per cage on a certain day and the females controlled each day for the rest of the week for a vaginal plug. Once a plug was detected, the animals were separated. E0.5 was assumed to be at noon of the day when the vaginal plug was detected.

3.2.7.1.1 C57BL/6 mice

C57BL/6 is a substrain of C57BL which was created by Clarence Cook Little in 1921 at the Bussey Institute for Research in Applied Biology. The subline C57BL/6 became the inbred strain which is most extensively used for creating transgenic lines today (Bult et al 2008). In 2002, the genome of the substrain C57BL/6J was sequenced (Waterston et al 2002).

3.2.7.1.2 HDAC4 conditional knock-out mice

In order to allow for a conditional knock-out of HDAC4 in specific tissues, Potthoff et al inserted two loxP sites into the HDAC4 gene, which are flanking exon 6. This insertion leads to an out-of-frame mutation of the HDAC4 open reading frame (Potthoff et al 2007).
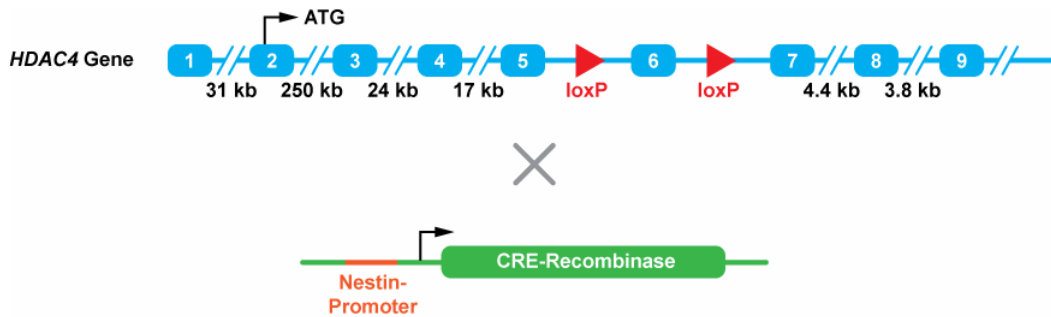
Figure 3.3. Targeting of Cre-REcombinase to the HDAC4 Gene (modified from (Potthoff et al 2007))

3.2.7.1.3 HDAC4 LacZ knock-in mice

HDAC4 *LacZ* knock-in mice were generated by Vega et al via gene targeting. Genomic sequences between exons 5 and 6 and between 6 and 7 were cloned into a targeting vector encoding nuclear *LacZ* and a neomycin resistance cassette. The vector was linearized and electroporated into ES cells. This insertion led to in-frame knock-in of those elements into exon 6 by homologous recombination. Generation of chimeric mice from successfully targeted ES clones and subsequent breeding of the offspring to obtain germline transmission were carried out using C57BL/6/129 mixed background mice (Vega et al 2004b).

HDAC4 *LacZ* knock-in mice were mated to C57BL/6 mice to enable for screening of HDAC4 expression in the embryonic brain.
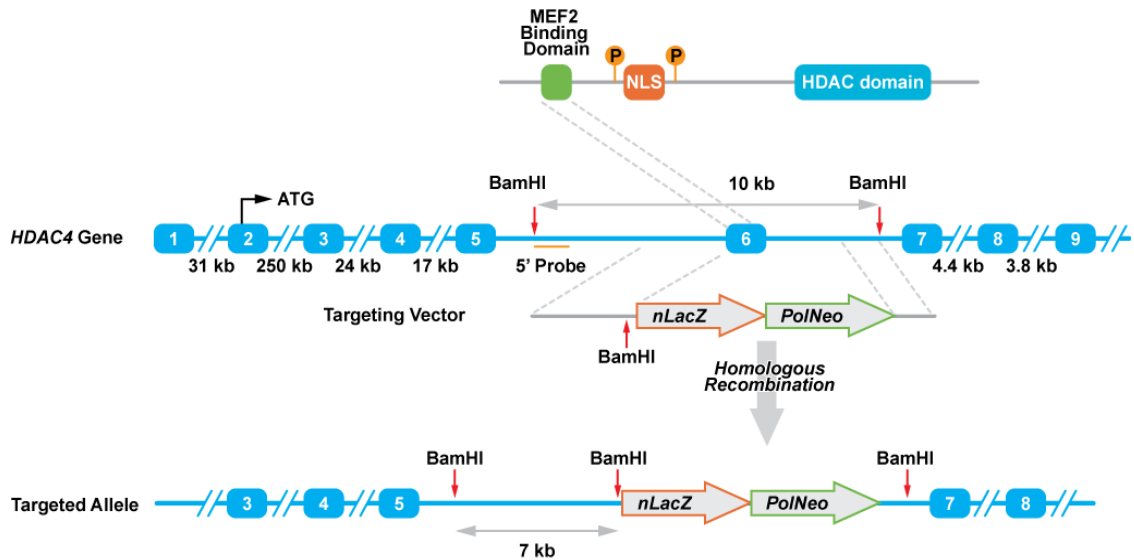
Figure 3.4. Gene targeting of the HDAC4 locus (modified from (Vega et al 2004b))

3.2.7.1.4 HDAC5 LacZ knock-in mice

HDAC5 *LacZ* knock-in mice were generated by Cheng et al. similarly to the HDAC4 *LacZ* knock-in strain by gene targeting. The HDAC5 targeting construct was generated with the pN-Z-TK2 vector, containing a nuclear *LacZ* cassette and a neomycin resistance gene. The *LacZ* cDNA and neomycin resistance cassette controlled by a PGK promoter were fused in-frame with the 5' region of exon 3, placing the ß-galactosidase reporter gene under the control of the endogenous HDAC5 promoter. The targeting vector was linearized and electroporated into mouse D3 embryonic stem (ES) cells. Correctly targeted ES cell clones were identified by Southern blotting and injected into 3.5-day mouse C57BL/6 blastocystst to generate chimeric males. Those were then bred to C57BL/6 females to achieve germ line transmission of the mutant allele.
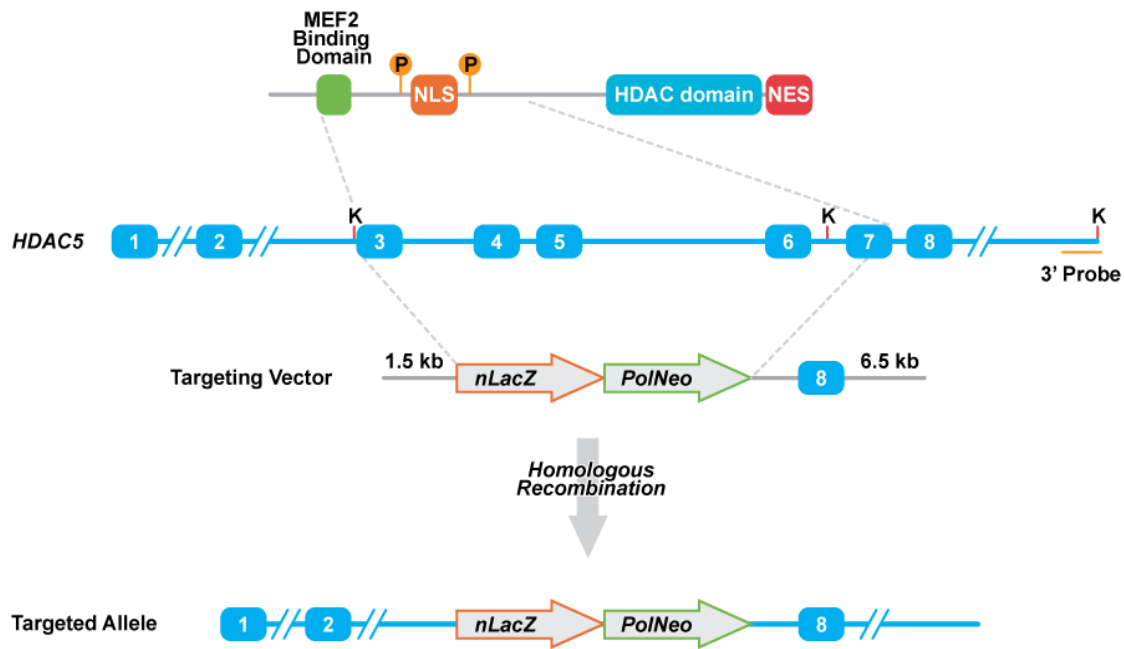
Figure 3.5. Gene targeting of the HDAC5 locus (modified from Chang et al. 2004)

3.2.7.1.5 Nes::cre mice

Tronche et al. generated this line expressing the cre-recombinase via injection of the nestin::cre DNA construct into oocytes from strain mouse BL6/SJF2 (Tronche et al 1999). Nestin is an intermediate filament protein expressed in neural stem cells of the developing central nervous system (Chang 2004). Although its expression is claimed to be restricted to the central nervous system, it has also been detected in the peripheral nervous system (PNS) (Tucker et al 2001). The targeting vector encoded for cre under the control of the nestin promoter. Downstream of the polyadenylation signal (human growth hormone polyadenylation signal) (Tronche et al 1999) the vector also contained a nervous system-specific enhancer present in the second intron of the rat nestin gene (Zimmerman et al 1994).

HDAC4 conditional mice were mated to Nes::Cre mice in order to achieve conditional knock-out of HDAC4 in the developing central nervous system.

3.2.7.2 Genotyping

In order to genotype transgenic animals, DNA was extracted from tail tissue of embryos, newborn or adult mice according to a modified protocol of Laird et al. (1991). Tails were digested overnight with 500 µl lysis buffer supplemented with 5 µl proteinase K each at 55 °C in a hybridization oven in a rotating glass tube. After digestion DNA was precipitated by adding 500 µl 2-propanol to each sample, the mixture vortexed and incubated at −80 °C for 30 minutes. Afterwards, the samples were centrifuged for 15 minutes at 13 000 rpm and 4 °C. The supernatant was discarded; the DNA pellet was washed with 300 µl of 70% ethanol and centrifuged for another 10 min at 13 000 rpm and 4 °C. Ethanol was removed and the pellets were allowed to dry. The dried pellets were redissolved in 70 µl of TE buffer overnight at 55 °C.

Genotypes of transgenic animals were determined by polymerase chain reaction (PCR). All genotyping experiments were carried out with both negative and positive controls. In negative controls water was added instead of DNA to exclude unspecific amplification. As a positive control, a sample from a either heterozygous or homozygous mutant animal was used.

3.2.7.2.1 HDAC4 conditional knock-out mice and HDAC4 LacZ knock-in mice

The expected PCR product for wildtype animals was 480 bp, the one for the floxed allele 620 bp and the product for the *LacZ* knock-in allele 810 bp.

The reaction mix for the PCR reaction was as follows

Reagent	HDAC4 cond. knock-out	HDAC4 *LacZ* knock-in
	Volume [µl]	Volume [µl]
10 mM HDAC4 fw	0.4	
10 mM HDAC4 rev	0.4	1.5 (primer mix*)
10 mM HDAC4 *LacZ* rev	-	
10 mM dNTPs	0.4	0.4

50 mM MgCl2	0.8	0.8
1 x reaction buffer	2.0	2.0
dd H2O	15.7	15.0
Taq polymerase	0.1	0.1
DNA	0.5	0.5

* The primer mix consisted of HDAC4 fw, HDAC4 rev and HDAC4 *LacZ* rev in a ratio of 2:1:1.

The PCR reaction was carried out in either a Biometra Tpersonal cycler or a BioRad iCycler. The programme used was the following:

94 °C	2 min	
96 °C	15 sec	
58 °C	30 sec	35 cycles
72 °C	2 min	
72 °C	10 min	

3.2.7.2.2 NesCre mice

To test for the presence of the cre allele in animals, a PCR reaction was carried out. The expected PCR product was 500 bp long, if there was no cre allele, there would not be any product. This set-up does not allow discriminating in cre positive animals, whether there are one or two copies present. The reaction mix is as follows:

Reagent	Volume [µl]
10 mM Nes::Cre fw	0.4
10 mM Nes::Cre rev	0.4
10 mM dNTPs	0.4
50 mM MgCl$_2$	0.8
10x reaction buffer	2.0
dd H$_2$O	15.7
Taq polymerase	0.1
DNA	0.5

The PCR was carried out in a Biometra Tpersonal cycler according to the following programme:

95 °C	5 min	
95 °C	30 sec	
60 °C	30 sec	40 cycles
72 °C	37 sec	
72 °C	5 min	

3.2.7.2.3 HDAC5 LacZ knock-in mice

The expected size for the PCR product of a wildtype allele is 300 bp, the size of the *LacZ* knock-in allele 500 bp.

Reagent	Volume [µl]
10 mM gt-HDAC5-fw	
10 mM gt-HDAC5-rev	1.5 (primer mix*)
10 mM gt-HDAC5-*LacZ*-rev	
10 mM dNTPs	0.4
50 mM MgCl$_2$	0.8
10x reaction buffer	2.0
dd H$_2$O	15.0
Taq polymerase	0.1
DNA	0.5

* The primer mix consisted of HDAC4 fw, HDAC4 rev and HDAC4 *LacZ* rev in a ratio of 2:1:1.

The PCR reaction was carried out in a BioRad iCycler according to the following programme:

95 °C	4 min	
95 °C	30 sec	
62 °C	30 sec	35 cycles
72 °C	45 sec	
72 °C	5 min	

The PCR product was either applied on an agarose gel or stored at −20 °C until electrophoresis. The product is separated via agarose gelelectrophoresis in an 1.5% agarose gel. Each sample is supplemented with 10x Orange G marker. 10 µl of PCR product and Orange G are applied to each lane of the gel. Electrophoresis is run at 120 V. After the run, the gel is stained in ethidium bromide for 15 min and eventually photographed on an UV transilluminator.

3.2.8   In situ Hybridization

3.2.8.1   Preparation of tissue samples

3.2.8.1.1 Fixation

The pregnant female was sacrificed, the embryos dissected out of the uterus and decapitated. The heads were collected in cold 1 x PBS and then fixed overnight on a rocker in 4% PFA at 4 °C, pH 7.4. The PFA was filtered after preparation and adjustment of pH. Fixed tissue was either processed further for embedding or stored for a short period of time at 1% PFA at 4 °C.

The heads were dehydrated in a series of ethanol solutions with ascending concentrations and subsequently acetone. In order to be penetrated completely, tissues should not exceed 5 mm in length. The heads were placed in ethanol solutions and incubated on a laboratory rocker at room temperature. Afterwards, they were incubated

in acetone and eventually in liquid paraffin in and incubation oven. The incubation protocol is as follows:

repetitions	time	solution	temperature
3	30 min	1x PBS	RT
3	1 h	50% ethanol	RT
2	1 h	70% ethanol	RT
1	over night	70% ethanol	4 °C
2	30 min	80% ethanol	RT
2	30 min	90% ethanol	RT
2	30 min	96% ethanol	RT
2	30 min	absolute ethanol	RT
1	1 h	aboslute ethanol	RT
1	1 h	ethanol:acetone (1:1)	RT
2	1 h	acetone	RT
1	over night	paraffin	65 °C
2	2 h	paraffin	65 °C

The paraffin was melted in the incubation oven at 65 °C before use. Also the embedding moulds were pre-heated in the oven prior to embedding. They were then placed on a heater and about half of each mould filled with liquid paraffin. The heads were placed in the moulds, oriented as desired for coronal sectioning and afterwards the heater turned off and the paraffin allowed to cool down and harden. The blocks with the heads were removed from the moulds, labelled with laboratory tape and kept in Ziploc bags at room temperature until sectioning.

3.2.8.1.2 Paraffin sectioning

The embedded embryo heads were cut with a Leica microtome and Feather blades to 10 – 12 μm thick paraffin sections. The sections are collected with a small water bath just behind the blade, transferred with a paintbrush to another water bath at 50 – 52°C. The sections flattened on the surface of the warm water and were immediately picked up and mounted on a superfrost ultra plus microscopy glass slide. The sections were dried

overnight at 37 °C and subsequently stored at 4 °C until in situ hybridization is carried out on them.

3.2.8.2   Generation of in situ probes

For in situ probes for HDAC4 and HDAC5 we used sequences that had been published within the Allen brain atlas.

3.2.8.2.1 HDAC4

Length: 598

GC Percent: 56.6890

Reverse Primer Tag: SP6

Forward Primer: CCTCTGCCAGAAAAGGTTCTAC

Reverse Primer: CAACTTGATTCAGCAACTCTGC

Sequence:

```
CCTCTGCCAGAAAAGGTTCTACATCAGAGACCCAATGCCAATGCTGTCCACTCC
ATGGAGAAAGTGATGGACATCCACAGCAAGTACTGGCGCTGCCTGCAGCGTCT
GTCCTCCACGGTGGGGCACTCTCTGATTGAGGCGCAAAAGTGTGAGAAGGAAG
AAGCTGAGACAGTCACCGCCATGGCCTCGCTGTCTGTAGGCGTCAAACCTGCTG
AGAAGAGATCTGAGGAGGAGCCCATGGAGGAGGAACCACCACTGTAGCCCGA
AGCTGCTGTTCTCTCCTTTGTTTGTCTGTCTTGAAGCTCAGCCAAGAAACTTACC
CGTATCACTCCTGCGTCCTGCCTTGGTGCTCTCTTGAGTACAAAGGGACAGCAG
GCGTGCAGCAGCAACGGGAAGCCTTTCTGCCGCCCTGGACCACAGGTCTGGAG
ACGCACACGGAACACCGGGTGTGGCAGATCACATGGAACACAGGACAGCGCG
CAACACACGGGCACACAGACATGTGGAAGCCAAGCACACGCTGGTGGCTCCCC
CTCCCCCTGGGAAGCCTCGAAGGAAGAAGCTTGTGGCAACTTGGGCAGAGTTG
CTGAATCAAGTT
```

3.2.8.2.2 HDAC5

Length: 684

GC Percent: 62.8655

Reverse Primer Tag: SP6

Forward Primer: CTATACGTCTCCTTCTCTGCCC

Reverse Primer: CTCCTCCTCCTCCTCTTCTAGG

Sequence:

```
CTATACGTCTCCTTCTCTGCCCAACATCTCCCTAGGGCTGCAGGCCACTGTCACT
GTCACCAACTCGCACCTCACCGCCTCCCCGAAGCTGTCAACACAGCAGGAGGC
TGAGAGGCAGGCCCTTCAGTCCCTGCGGCAGGGCGGCACACTGACCGGCAAGT
TCATGAGCACATCCTCCATCCCTGGCTGCCTGTTGGGAGTGGCACTGGAGGGTG
ACACAAGCCCCCACGGGCACGCTTCCCTGCTGCAGCACGTTTGCTCCTGGACAG
GCCGGCAACAGAGCACGCTCATAGCAGTGCCGCTTCATGGGCAGTCCCCACTG
GTGACGGGTGAACGTGTGGCCACCAGCATGAGGACGGTGGGTAAGCTCCCGAG
GCACCGACCTCTGAGCCGCACTCAGTCCTCCCCGCTGCCGCAGAGTCCCCAGGC
CCTGCAGCAGCTGGTCATGCAGCAGCAGCACCAGCAGTTCCTGGAGAAGCAGA
AGCAGCAGCAGATGCAGCTGGGCAAGATCCTTACCAAAACTGGGGAGCTGTCA
AGGCAGCCCACCACTCACCCGGAGGAGACAGAAGAGGAGCTGACGGAGCAGC
AGGAGGCCTTGCTGGGAGAGGGGGCCCTGACCATTCCCCGGGAAGGCTCTACA
GAAAGTGAGAGCACCCAGGAAGACCTAGAAGAGGAGGAGGAGGA
```

The plasmids containing the desired sequence are linearized using appropriate restriction enzymes according to the following reaction setup: 20 µg plasmid DNA, 1 µl restriction enzyme, 3 µl 10 x restriction buffer, dd H_2O ad 30 µl. The reaction mixture was incubated for 2 h at 37 °C or RT, depending on the reaction temperature of the enzyme. Linearization was controlled by gel electrophoresis, 1 – 2 µl of the reaction mix was loaded on a 0.75 or 1% agarose gel together with one lane of the original circular plasmid.

In case that the plasmid was not completely linearized yet, another volume of enzyme was added and the mix incubated again at the appropriate temperature.

After linearization the plasmid was purified using the Nucleospin Extract II Kit according to manufacturer´s instructions. The concentration of the purified plasmid was measured by spectrophotometry and the DNA stored at –20 °C.

3.2.8.2.3 Probe synthesis

To synthesize the probe the following reaction was set up:

Reagent	volume [µl]
5x transcription buffer	2
10x DIG nucleaotide mix	1
linearized plasmid [1 μg/μl]	1
RiboLock RNase Inhibitor	0.25
T3, T7 or Sp6 RNA polymerase	1
dd H$_2$O	4.75

The RNA synthesis reaction was incubated overnight in a water bath at 37 °C. Subsequently, to precipitate the probe, 5 µl of 10 M Ammonium acetate and 40 µl ethanol were added and the reaction mix incubated at -80°C for one hour. It was then centrifuged for 45 min at 4 °C and 13 000 rpm in a benchtop centrifuge. After removing the supernatant, the probe pellet was washed with 300 µl 70% ethanol and centrifuged for 10 min at 13 000 rpm and 4 °C: The supernatant was removed and the pellet air dried. Afterwards, the probe was dissolved in 30 µl of hybridization mix and stored at – 20 °C. To control for the probe synthesis, 2 µl of the probe were analyzed via electrophoresis in a 2% agarose gel in TBE buffer.

3.2.8.3 Denaturing RNA gel

The gel chamber was cleaned with water before using. It was filled with water which was left in the chamber for about 20 minutes. The Gel comb was incubated with 0.5 NaOH and also the gel tray cleaned with 0.5 N NaOH.

The gel was prepared as follows 2.2 M formaldehyde and 1.5% or 2.0% agarose in formaldehyde gel running buffer. Ethidiumbromide (0.5 µg/ml) was added to the gel.

As controls total-RNA from heads was used, in which 18 S and 28 S RNA are readily visible. Those samples were obtained from Marc Willaredt.

3.2.8.3.1 Sample preparation

2 µl in situ probes are supplemented as follows to be analyzed in a gel:

RNA (probe)	2.25 µl
5x formaldehyde gel-running buffer	1.0 µl
Formaldehyde	1.75 µl
Formamide	5 µl

RNA, 5x formaldehyde gel running buffer, formaldehyde, and formamide were mixed, incubated 15 min at 65 °C and then chilled on ice. The samples were briefly centrifuged to collect the liquid and supplemented with 1 µl sterile, DEPC treated formaldehyde gel-loading buffer.

Before loading the samples the gel was run without any sample for 5 minutes at 5 V/cm. To prevent the samples from floating up out of the gel pockets, the gel was loaded without buffer and the 1 x formaldehyde gel running buffer only filled into the gel chamber exactly until the upper edge of the gel.

The gel was run at 60 V (3 V/cm) for 4.5 h. Every hour, the buffer from the two gel chamber reservoirs was collected, mixed and returned to the gel apparatus.

After running the entire gel was fluorescing strongly in UV-light. To decrease the background fluorescence, the gel was washed in DEPC treated water for 2.5 h up to overnight. After the washing the background was sufficiently decreased and the bands clearly visible.

3.2.8.3.2 Hybridization protocol

Paraffin sections of embryo heads were allowed to adjust to RT. At first, paraffin was removed and the sections re-hydrated. The sections were therefore incubated in the following solutions:

Repetitions	Time	Solution	Temperature
3	7 min	100% xylene	RT
1	2 min	ethanol:xylene (1:1)	RT
1	1 min	Absolute ethanol	RT
1	1 min	96% ethanol	RT
1	1 min	90% ethanol	RT
1	1 min	70% ethanol	RT
1	1 min	50% ethanol	RT
2	5 min	1x PBS	RT
1	5 min	20 µg/ml proteinase K in PBS	RT
1	5 min	0.2% glycine in PBS	RT
2	5 min	1x PBS	RT
1	20 min	4% PFA/0.2% glutaraldehyde in PBS	RT
2	5	1x PBS	RT

After the last wash as much liquid as possible was removed from the sections. The slide was dried a little with a laboratory tissue around the sections. The sections were encircled with a barrier pen (ImmEdge, Vector Laboratories). The microscope slides were placed on metal slide supports in a moist chamber with 50% formamide/ 2x SSC, pH 4.5. Hybridization mix was incubated for 5 min at 95 °C and subsequently 7.5 µl of hybmix were carefully pipetted on each section. The sections were prehybridized in the moist chamber for one hour at 70 °C. The in situ probes were diluted in hybmix to a final concentration of 1 ng/µl and incubated for 5 min at 95°C. After prehybridization hybmix was removed from the sections and 7.5 µl of probe diluted in hybmix added to the appropriate sections. Hybridization was carried out overnight in the moist chamber in the hybridization oven at 70°C. The chamber had to be sealed well to prevent drying of the sections.

After hybridization, slides underwent the following incubation or washing steps:

Repetitions	Time	Solution	Temperature
1	15	2x SSC, pH 4.5	RT
2	15	50% formamide/2 x SSC, pH 4.5	65 °C
3	10	1x PBST	RT

After washing with PBST liquid was removed as much as possible from the slides and they were placed on metal slide supports in a moist chamber with water. 100 µl B-block were pipetted onto each slide to cover the sections. Incubation was carried out in the moist chamber for one hour at RT. After removing B-Block, slides were incubated for two hours at 37 °C with anti-digoxygenin antibody diluted 1:1000 in B-Block. The sections were washed three times for 5 min with 1x PBST and then for 10 min with NTM on a shaker at RT. The slides were placed back on metal slide supports in a dark moist chamber. To start the colour development, 400 µl NBT/BCIP diluted 1:50 in NTM were added onto each slide. Incubation took place at RT and the progress of the colour reaction was controlled every half an hour using a microscope. Sense and antisense probes were developed the same amount of time. To stop the enzymatic reaction, slides were washed once with PBST and then post-fixed with 4% PFA for 10 – 20 min. After the fixation they were washed twice with 1x PBS for 5 min at RT. The sections were mounted with aquatex and stored at 4 °C.

The sections were examined with a Leica DM LB microscope and photographed with a Leica DFC320 microscope camera.

4   Results

4.1   Analysis of the role of class I and II HDACs in neuro- and gliogenesis in embryonic mouse brain *in vitro*

4.1.1   Class I and II HDACs are expressed in developing mouse brain - analysis through real time RT-PCR

Expression of HDACs in embryonic mouse brain was examined using real time RT-PCR on total RNA lysates of embryonic brain tissue at embryonic days E 13.5 and E 15.5.

4.1.1.1 HDAC1, -2, -3, -4, -5, 7a, and -8 are present in embryonic mouse brain at 13.5 dpc

In order to determine whether class I and II HDACs are expressed in the developing brain *in vivo*, quantitavtive real time RT-PCR analysis was performed on total RNA lysates from embryonic brain regions dissected at two different developmental ages. Cortex, developing basal ganglia and hippocampus were dissected from E13.5 and E15.5 brains as carefully as possible and RNA extracted from the samples. After reverse transcription, real time RT_PCR was performed with TaqMan Assays to detect individual HDACs.

The real time RT-PCR analysis confirmed expression of all examined HDACs at both 13.5 dpc and 15.5 dpc, however not all HDACs showed the same levels of expression. At 13.5 dpc the expression of HDAC1, -2, -3, -4, -5, -7a, and -8 was examined in cortex, striatum and hippocampus. HDAC2 showed the highest expression in all examined brain tissues, cortex striatum and hippocampus (Figure 4.1), HDAC3 the second highest. HDAC1 showed the lowest expression levels, HDAC4, -5, -7a and -8 intermediate levels, however all very similar to each other.
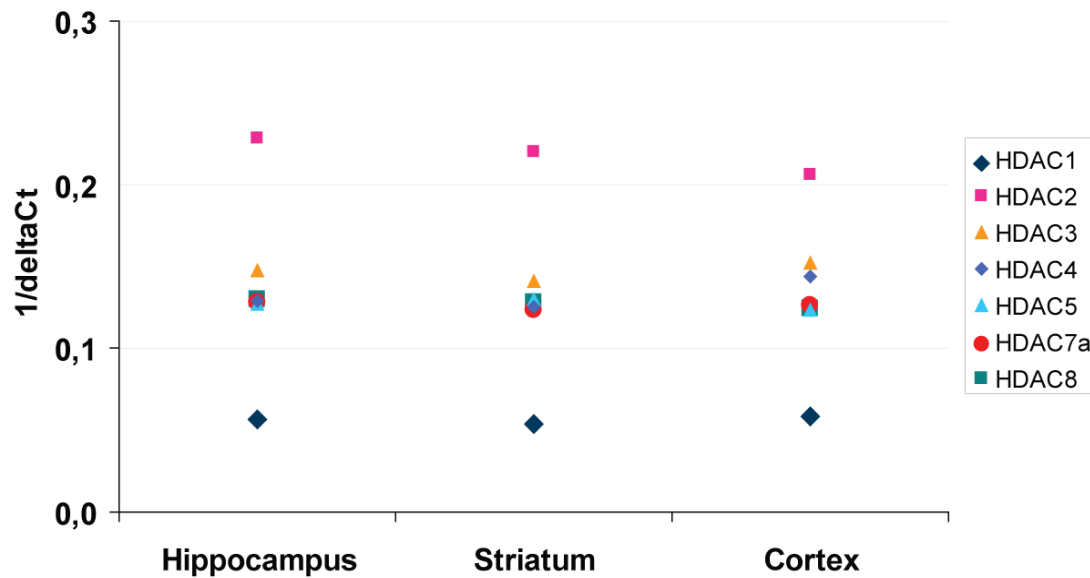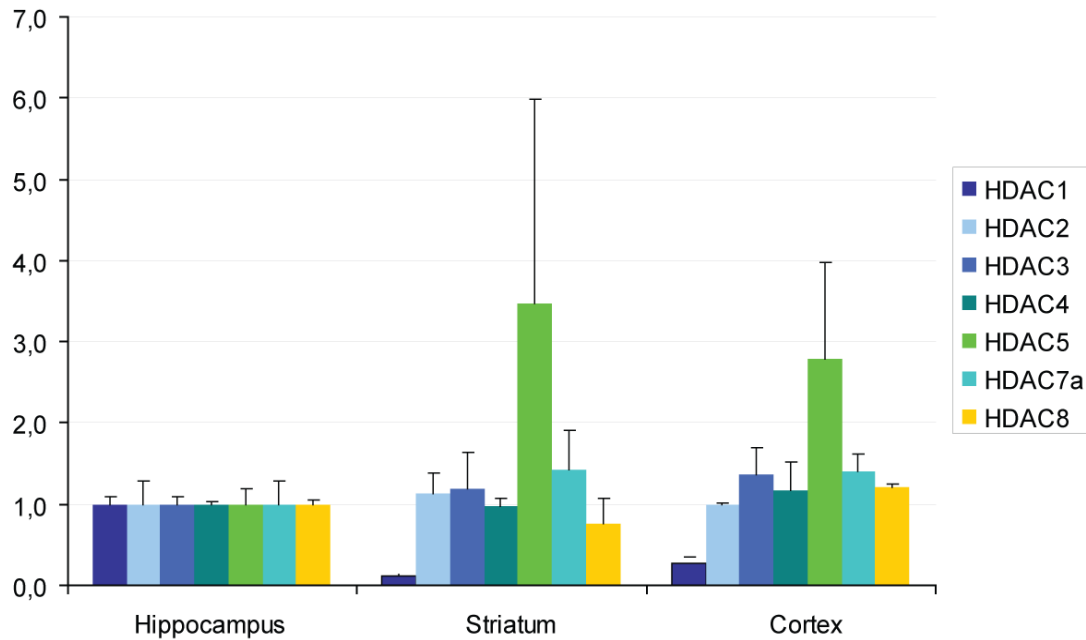
Figure 4.1. Expression levels of HDACs in embryonic brain tissue at E 13.5 determined
via real time RT-PCR using TaqMan Assays for HDAC1, -2, -3, -4, -5, -7 and -8

To compare expression levels not only compared within one brain area, but to compare respective expression levels between brain areas, relative expression of the individual HDACs is was normalized to the level in hippocampus as a standard.

Here HDAC1 was found to have a much higher expression in hippocampus compared to the other regions, which might hint to a specific role there.

On the other hand, expression of HDAC5 is more than 3-fold higher in striatum and almost 3-fold higher in cortex than in hippocampus. I am reluctant to conclude that HDAC5 expression levels are higher in these areas because the standard deviation is comparably high. Expression levels of all other HDACs are similar to each other in the different brain tissues (**Figure 4.2**).
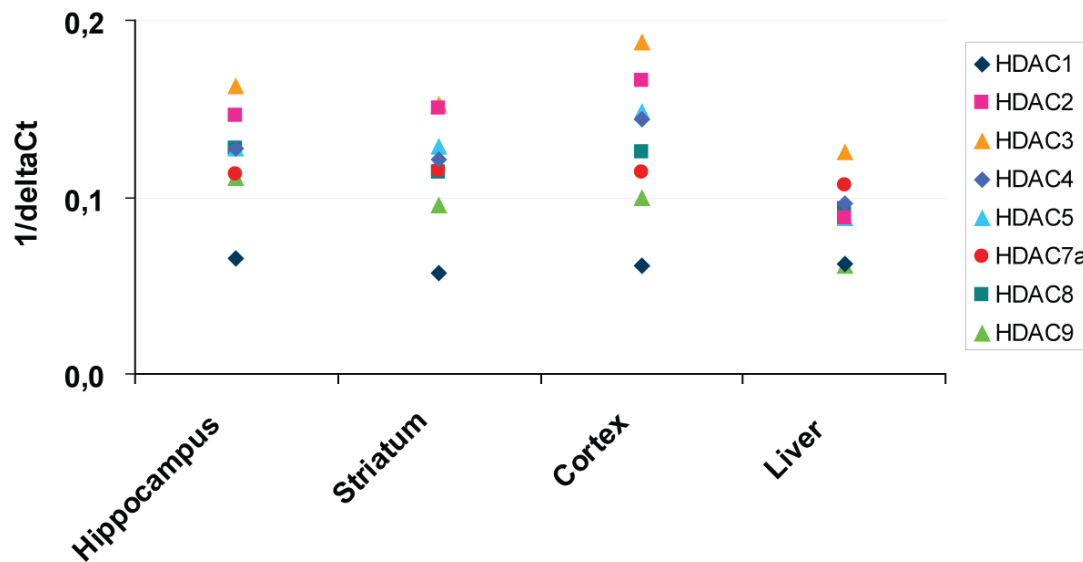
Figure 4.2. Relative expression of HDACs in embryonic brain tissue at E 13.5
normalized to hippocampus. Relative expression levels calculated with ΔΔCt method. SEM

4.1.1.2   HDAC1, -2, -3, -4, -5, 7a, -8, and -9 are present in embryonic mouse brain at 15.5 dpc.

The expression of HDAC1, -2, -3, -4, -5, 7a, -8 and -9 was also examined in 15.5 dpc in striatum, cortex, hippocampus and liver as a non-brain tissue for comparison. Differently to 13.5 dpc tissue, HDAC3 showed the highest expression in all tissues, except from striatum, where both HDAC2 and HDAC3 had highest expression levels.

HDAC2 had the second highest expression levels in brain, whereas HDAC7a was second highest in liver. Expression levels of HDAC 4 and 5 respectively were similar to each other and also similar in the different tissues (**Figure 4.3**).

Figure 4.3. Expression levels of HDACs in E 15.5 brain tissues determined by real-time RT-PCR using TaqMan Assays for HDAC1, -2, -3, -4, -5, -7 and -8

Looking at relative expression levels in cortex and striatum compared to those levels in hippocampus again, HDAC1- and HDAC2-expression were lower in striatum and cortex. This corresponds to the result of the E 13.5 tissue. HDAC5 expression was more than 2.5-fold higher in cortex than in hippocampus (**Figure 4.4**). Also this result corresponds to the results of the E 13.5 brain tissue analysis. A relatively high expression of HDAC5 in cortex could hint to a specific role of this HDAC in this area in development.

Taken together, all examined HDACs were expressed both at 13.5 and 15.5 dpc in all examined brain tissues. However, some prominent differences in expression levels could be observed. HDAC1 and -2 expression levels are relatively high in hippocampus compared to the other brain areas, whereas HDAC5 expression is high in those brain areas compared to hippocampus. These differences might hint to specific functions of different HDACs in the respective brain areas.
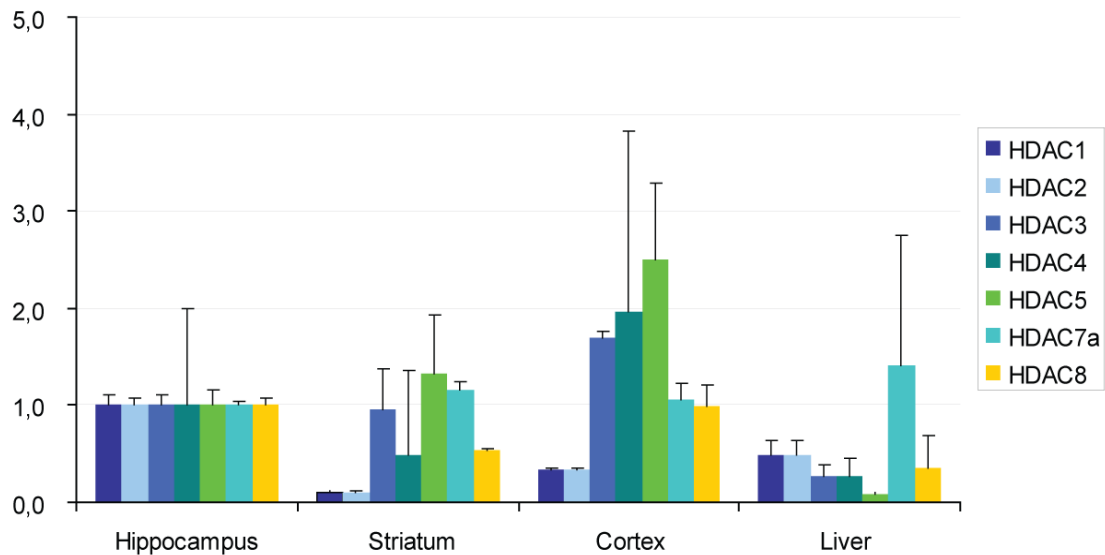
Figure 4.4. Relative expression of HDACs in embryonic brain tissue at E 15.5 normalized to hippocampus for comparison. Relative expression levels calculated with ΔΔCt method. SEM

4.1.2   *In vitro* analysis of influence of HDACs on embryonic neuro- and gliogenesis using the pharmacological inhibitor TSA

4.1.2.1   Pharmacological inhibition of all class I and II HDACs in neurosphere cultures

To test the influence of HDACs on neurogensis *in vitro*, we used neurosphere cultures to generate a uniform population of neural precursors from the medial and lateral ganglionic eminences of E15.5 dpc C57BL/6 mice (Reynolds & Weiss 1996). After 7 days in suspension culture, neurospheres were dissociated and plated out to differentiate according to standard protocol (Gritti et al 2001). TSA was applied to the cultures during different time windows; it was however always applied immediately prior to withdrawal of FGF2 at 2.5 DIV after plating. An addition of TSA in a time window of 3 h before withdrawal of FGF2 proved to be sufficient to inhibit neurogenesis in the cultures.

In order to analyze the signalling mechanisms involved in differentiation, RNA samples and protein lysates were prepared 6, 12, and 24 hours after treatment. RNA samples were examined by Real Time RT-PCR and Affymetrix GenChip 420 2.0. Protein samples were analyzed with western blot analysis.

4.1.2.1.1 HDAC promotes neurogensis in ganglionic eminences in vitro – HDAC inhibition decreases neurogenesis in GE

To assess the outcome of differentiation, neurosphere cultures were plated out for differentiation and cells fixed after 7 days *in vitro* and stained with appropriate antibodies. Staining with TuJ1 revealed that after 12 h of treatment with TSA or vehicle, neurogenesis was reduced to less than 50% in the TSA-cultures compared to controls (Figure 4.5). No change in astrogliogensis could be observed in this experiment.
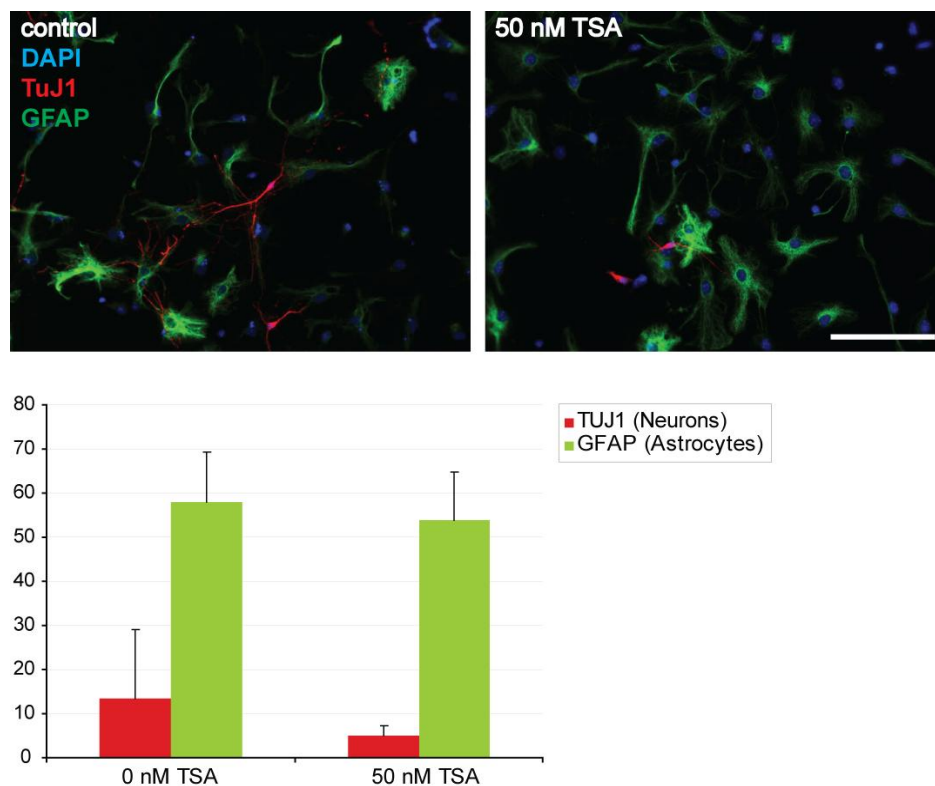

Figure 4.5. Decrease of neurogenesis in neurosphere-derived progenitor cultures upon treatment with TSA. Immunocytochemistry for neurons (TuJ1) and astrocytes (GFAP) in NS cultures differentiated for 7 days. Cells were treated with TSA or vehicle from DIV 1.5 to 2.5. Quantification of TuJ1 and GFAP positive cells in the cultures. Scalebar 100 µm

4.1.2.1.2 Establishing FACS analysis to quantify neurogenesis reliably and efficiently

As the method to quantify neurogenesis described above seemed to be tedious and prone to be biased by the individual round of immunostaining and counting, I intended to establish a more reliable method which would be less biased by the individual counting the cells in the microscopy images. FACS analysis seemed to be a very efficient and experimentally unbiased approach. After plating out neurosphere cultures to differentiate and treating the cells with TSA or vehicle as described, the cells were detached from the culture dishes, fixed and stained with TuJ1 antibody to determine the amount of newborn neurons in the cultures. The cultures were stained either with TuJ1 antibody and secondary antibody or with secondary antibody alone to determine the background fluorescence. The forward (FSC-H) and sideward scatter (SHC-H) plot shows counting events within the first gate that are considered to be actual cells and not debris. Counting events outside the gates are not taken into analysis. The plot displaying fluorescent channels shows two gates with cells. In R1, cells are not stained as they can also be found with secondary antibody only. In R2 the cells positive for TuJ1 are depicted. In the control cultures (0 nM TSA), the amount of TuJ1 stained cells is the largest; it decreases with increasing TSA concentration.

The FACS protocol confirmed the results of the conventional immunostainings and subsequent counting of stained cells on coverslips. Also with FACS, a dose dependent effect of TSA treatment on neurogenesis could be observed. Treatment with TSA led to a decrease in neurogenesis to almost 50% (Figure 4.7)

A
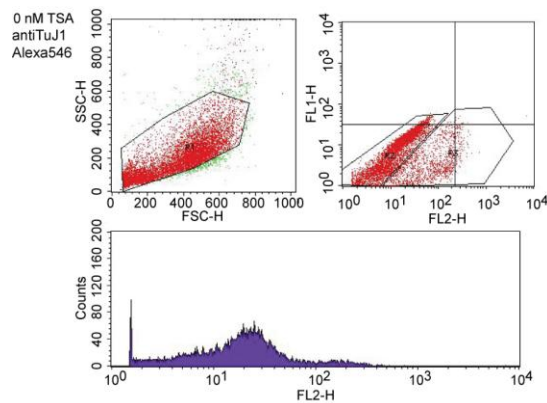
B
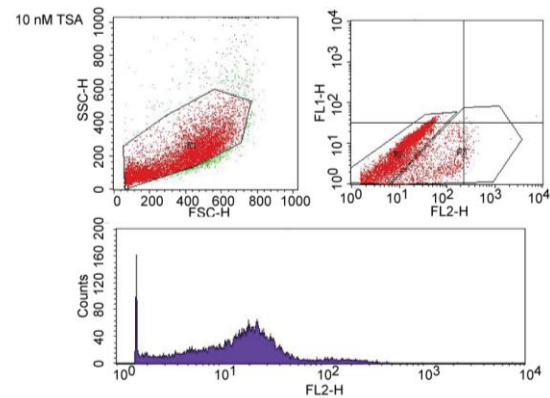
C
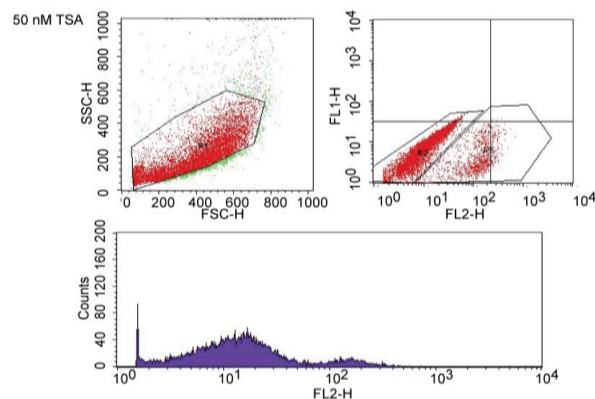
Figure 4.6. FACS analysis of neurosphere-derived cultures plated out to differentiate and treated with TSA (B: 10 nM C: 50nM) or vehicle (A: 0 nM) for 12 h between 1.5 DIV to 2.0 DIV. In the FSC and SSC plot, the gate R1 contains counting events considered to be cells. Those are further displayed in the fluorescence plot. R2 contains unstained cells, R3 cell positive for TuJ1 and considered to be newborn neurons.
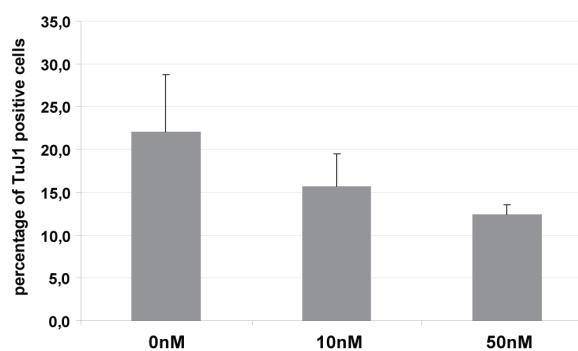
Figure 4.7. Quantification of neurogenesis determined through FACS analysis. Cultures were plated out to differentiate and treated with TSA or vehicle for 12 h between 1.5 DIV to 2.0 DIV. The percentage of TuJ1 positive cells is decreased by 50% upon treatment with 50 nM TSA. The effect is dose-dependent.

4.1.2.2   HDACs influence neurogenesis on a transcriptional level

To better understand by which mechanism HADCs influence the generation of neurons and glia in embryonic brain, we turned towards examining signalling pathways known to be involved in these processes. First, we investigated the expression of several genes involved in BMP2/4 signalling because BMPs had been shown to promote astroglial lineage commitment *in vitro* (Gross et al 1996) and *in vivo* (Bonaguidi et al 2005).

Since we expected HDACs to influence neuro- and gliogenesis on a transcriptional level, I performed Real Time RT-analysis to examine transcription of genes known to be involved in neuro- and astrogliogenic developmental programs. Neurospheres were prepared from E15.5 GE and cultured for 7 days. Subsequently, the cells were dissociated and plated out on polyornithine-coated coverslips. The cells were treated with TSA or vehicle in different time intervals, all of them ending at 2.5 dpc when FGF2 was removed from the cultures. Total RNA was collected and real time RT PCR carried out to examine transcription levels of potential target genes in TSA treated cells compared to controls.

Especially when TSA was applied for 12 h 2 days after plating out, several changes in transcription levels of potential target genes could be observed (Figure 4.8).

Upon inhibition of HDACs Bmp2 was transcriptionally upregulated, whereas Bmp4 showed a downregulation (Figure 4.8a). No change was observed in transcription levels of Bmp receptors 1a, 1b and 2 (Figure 4.8b). Interestingly, Smad7, a negative regulator of Bmp2/4 signaling was downregulated (Figure 4.8e), which together with the upregulation of Bmp2 hints to the idea that inhibition of HDACs by TSA releases an inhibition of BMP signalling.

Stat1 and Stat3, transcription factors known to promote astrogliogenesis, were upregulated 2- respectively 3-fold upon HDAC inhibition (Figure 4.8d).

Ngn1 is known to promote neurogenesis in cortex. Expression of Ngn1 in GE is upregulated up to 3fold upon treatment of the cultures with TSA. The increase seems to be dose-dependent. Ngn2 expression however does not change significantly upon

pharmacological inhibition of HDACs (Shaked et al 2008). The up- and downregulation of all genes examined happened in a dose-dependent manner.
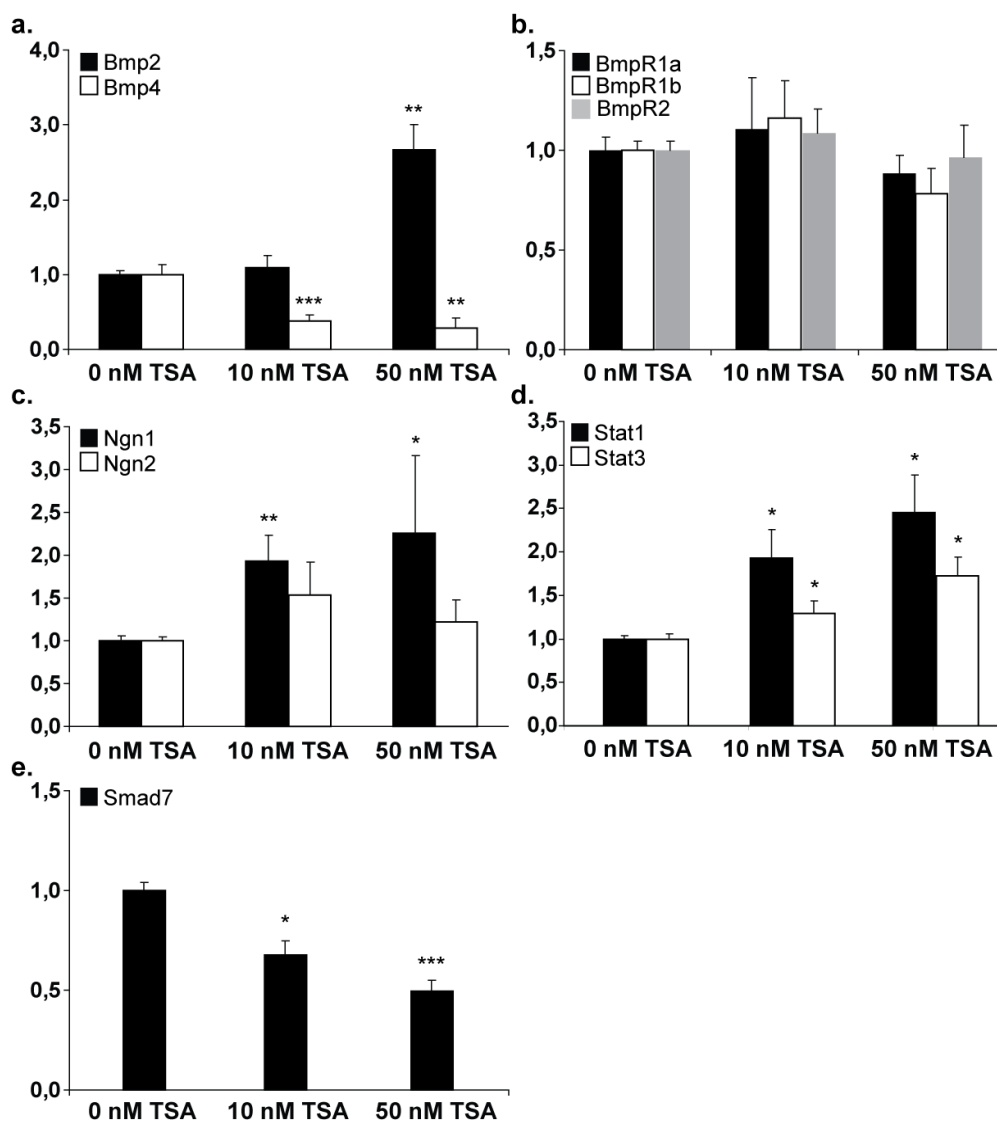
Figure 4.8. real time RT-PCR analysis of gene expression upon treatment of differentiating neurosphere cultures with TSA to inhibit all class I and II HDACs. Relative expression of a. Bmp2 and Bmp4, b. BmpR1a, BmpR1b, and BmpR2, c. Ngn1 and Ngn2, d. Stat 1 and Stat3, e. Smad7. All results were normalized to Gapdh expression. Values represent the mean (+/− SEM) of 3 individual experiments. * = p<0.05, ** = p<0.01, *** = p<0.001, Student's T-test.

In a second line of real time RT-PCR experiments we aimed to confirm the results obtained in the meantime with gene expression analysis through Affymetrix chips and also to look at the time course of gene expression upon HDAC inhibition in neurosphere cultures. In order to determine the influence of Bmp2 signalling on a transcriptional level, additional to TSA treatment, we also treated differentiating neurosphere cultures with 10 ng/ml BMP2.

We had previously observed that treatment of the differentiating neurosphere cultures with 10 ng/ml BMP2 (10 ng/ml) from DIV1.5 to DIV 2.5 led to an almost 50% increase in astrocytes in the cultures (Shaked et al 2008). When inhibitors of BMP2/4 signalling (Noggin and Alk3-ECD) were added to the cultures, they had no effect on neurogenesis. However, in the TSA treated cultures, these inhibitors restored normal levels of neuro- and astrogliogenesis (Shaked et al 2008).

RNA was isolated from the cells 6 h, 12 h and 24 h after the beginning of treatment at DIV 1.5. The observed dose-dependent increase of Bmp2 upon TSA-treatment corresponded to the previous experiments. The increase was transient; after 12 h the increase was less prominent and not detectable any more after 24 h. Bmp2 treatment did not change its own expression at all (**Figure 4.9**a). Bmp4 expression was decreased, especially after 6 hours of treatment in a dose-dependent manner, confirming the result of the previous experiments. Also adding Bmp2 to the cultures reduced the expression of Bmp4 (**Figure 4.9**b). Stat3 expression was upregulated in a dose-dependent manner at all three time points, with a slight increase from 6 h to 24 h. Treatment with Bmp2 increased Stat3 expression 6 h and 12 h as well. Smad7 was downregulated in a dose-dependent manner after TSA treatment. The downregulation was stronger at later time points than after 6 h. Treatment with Bmp2 however led to a strong upregulation of Smad7 expression, which would be expected.
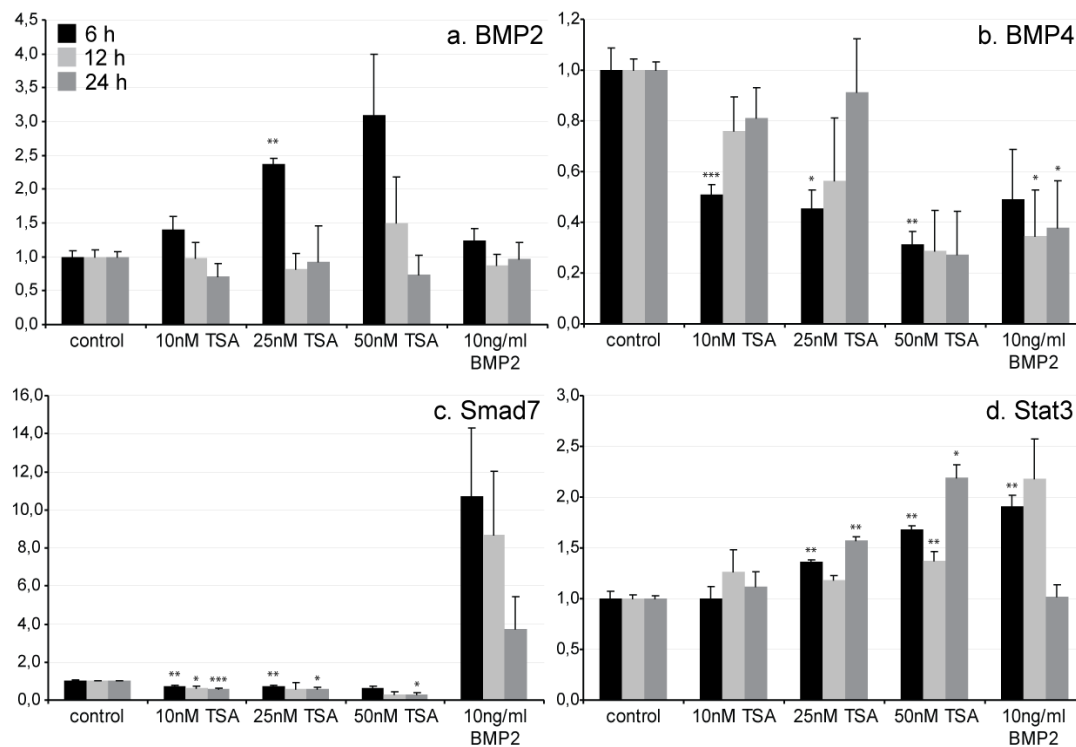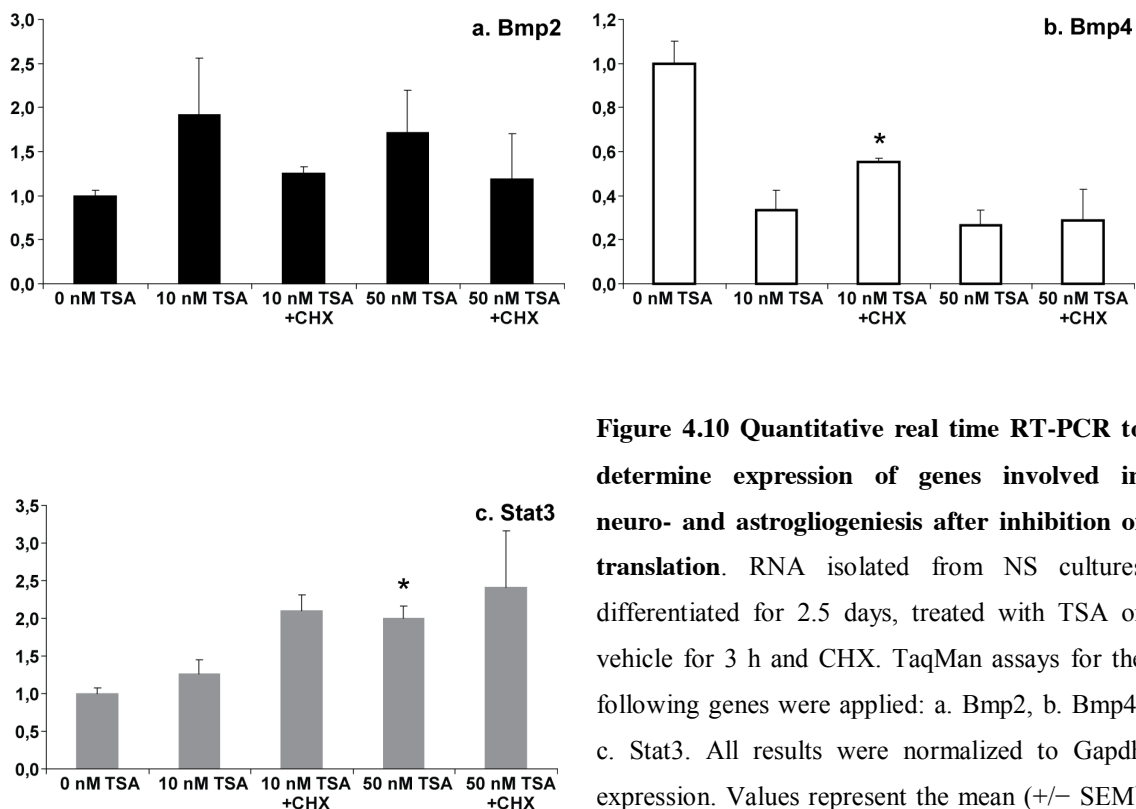
Figure 4.9. Quantitative real time RT-PCR to determine expression of genes involved in neuro- and astrogliogenic developmental programs. RNA isolated from NS cultures differentiated for 2.5 days, treated with TSA, BMP2 or vehicle for 6 h, 12 h or 24 h (DIV 1.5 − 2.0). TaqMan assays for the following genes were applied: a. Bmp2, b. Bmp4, c. Smad7 and d. Stat3. All results were normalized to Gapdh expression. Values represent the mean (+/− SEM) of 3 individual experiments (6 h and 24 h) or 2 individual experiments (12 h). * = p<0.05, ** = p<0.01, *** = p<0.001, Student's T-test.

4.1.2.3 Protein translation is necessary to upregulate BMP2 expression upon TSA treatment

In order to determine whether expression of BMP2 is directly or indirectly regulated by Stat3, the HDAC inhibition experiment was carried out with additional samples which were treated not only with TSA, but with cycloheximide (5 µg/ml). Cycloheximide (CHX) inhibits protein biosynthesis in eukaryotes. It blocks translational elongation by interfering with the translocation step of tRNA and mRNA in relation to the ribosome. The effect is reversible. CHX was added to the cultures 1 h before TSA treatment was started.

In the presence of both TSA and CHX for 3 hours, the upregulation of BMP2 expression did not take place as observed with only TSA treatment of the cultures. BMP2 expression is not upregulated in the presence of a translational inhibitor (Figure 4.10a). Moreover, the downregulation of Bmp4 expression did not occur as observed before without inhibition of translation (Figure 4.10b). We considered this finding as a hint that after treatment of the cultures with HDAC inhibitors a specific factor is expressed which then in turn upregulates BMP2 expression and the same applies for Bmp4 downregulation. One of the potential candidates to regulate the Bmp expression could be Stat3. The expression of Stat3 in striatal neurosphere cultures increases with HDAC inhibition through TSA treatment. When cultures were treated with CHX additionally, the increase in Stat3 expression was slightly lower than with TSA treatment only but still visible (Figure 4.10c). The expression of Stat3 does not seem to depend on the previous translation of other factors as it seems to be the case for BMP2.

Figure 4.10 Quantitative real time RT-PCR to determine expression of genes involved in neuro- and astrogliogeniesis after inhibition of translation. RNA isolated from NS cultures differentiated for 2.5 days, treated with TSA or vehicle for 3 h and CHX. TaqMan assays for the following genes were applied: a. Bmp2, b. Bmp4, c. Stat3. All results were normalized to Gapdh expression. Values represent the mean (+/− SEM) of 3 individual experiments. * = $p<0.05$, ** = $p<0.01$, *** = $p<0.001$, Student's T-test..

4.1.2.4   TSA and BMP2 treatment elicit similar responses of BMP2/ signaling in different time frames

The reporter assays with cells treated with TSA or BMP2 also confirmed our finding, that Bmp2/4 signaling is regulated in both treatment protocols, but following a different timely order. Bmp2 treatment elicits a response in BMP2/4 signalling already after few hours of treatment. The expression of firefly luciferase is driven by consecutively aligned BMP-responsive elements (BRE) which are binding motifs for Smads and therefore reporters for Bmp signalling. BMP2 treatment led to a strong increase in luciferase fluorescence intensity. TSA treatment, however, first led to a downregulation of BMP2/4 signaling and subsequently, after a longer time of treatment, to an upregulation. The effect of TSA on BMP2/4 signaling might be indirect. The directional change in the reaction should be investigated further.
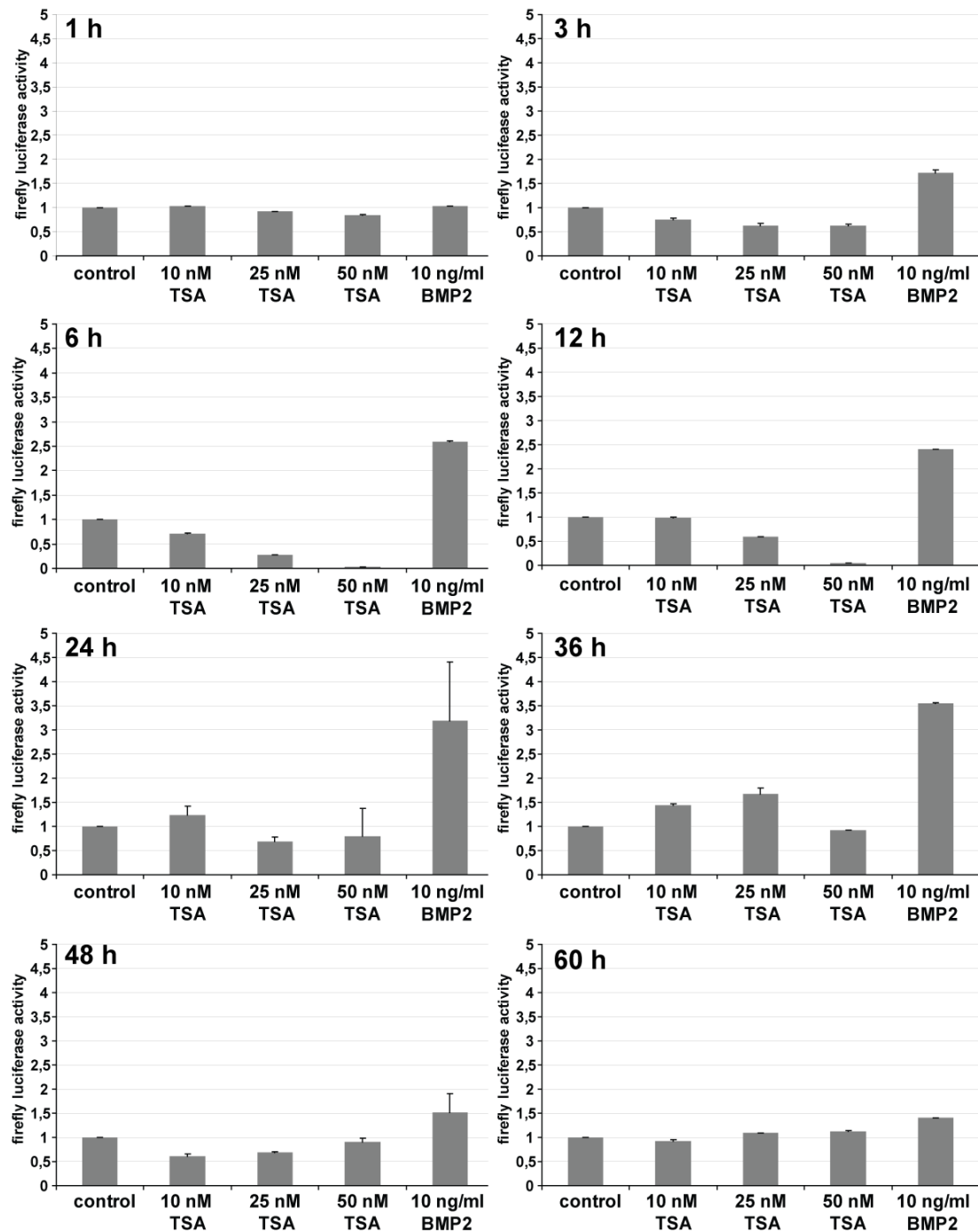
Figure 4.11. Time course of treatment intervals with TSA or BMP2 and subsequent luciferase assay to determine levels of BMP2/4 signaling in the cultures.

4.1.2.5   Microarray analysis of pathways potentially involved in HDAC influence on neurogenesis

Which pathways and genes are involved in TSA and BMP2-mediated regulation of neuro- and astrogliogenesis was addressed in a Microarray study with neurosphere-derived cultures treated with 10 nM or 50 nM TSA for 12 h before withdrawal of FGF2. RNA was collected 6h and 24 h after the end of the treatment window. Gene expressing profiling with Affymetrix GenChip 420 2.0 of samples after 6 h and 24 h. Genes were considered significantly regulated if their expression had changed more than 2-fold and exceeded a minimal difference of 100 comparing treated and mock-treated cells with a confidence greater than 90%. Since these experiments were carried out in collaboration and have been published previously (Scholl et al 2012), I don't want to present all results here and instead give a short overview.

220 genes were significantly different in expression in cells treated with BMP2 for 6 h, 573 in cells treated for 24 h. TSA treatment led to an expression change in 917 genes after 6h and in 982 genes after 24 h.

In order to identify an overlap of regulated genes within TSA and BMP2 treatments Venn analyses were carried out intersecting TSA 6 h and 24 h, BMP2 6 h and 24 h respectively. This analysis showed that a majority of regulated genes was unique to each treatment condition, only small numbers of genes occurred in the intersections. The largest intersection was found between TSA 6 h and 24 h; expression of more than half of the BMP2 6 h genes overlapped with the one of BMP2 24 h genes. More genes were in common between the two treatments after 24 h than after 6 h, but only eight genes were common to both treatments at all-time points: Gpr17 (G protein-coupled receptor 17), Lims2 (LIM and senescent cell antigen like domains 2), Bcas1 (breast carcinoma amplified sequence 1), Ptpre (protein tyrosine phosphatase, receptor type, E), Afap1l2 (actin filament associated protein 1-like 2), Dll3 (delta-like 3), G0s2 (G0/G1 switch gene 2), and Gpd1 (glycerol-3-phosphatase dehydrogenase1).

65 genes were regulated in three out of four experimental groups, most of them regulated in the same direction. Few genes showed opposed expression: Smad7, Papss2, Fam19a2, Cadps, Car8 and Efhd1.

Among the genes regulated by BMP2 6h and 24h and TSA 24h several genes involved in BMP2/4 signalling were detected (Bmp4, Smad7, Fst and Bambi)

Hierarchical clustering of the microarray data with the clustering option of dChip was carried out to illustrate the overall relationship between regulated genes. All genes regulated in at least one of the conditions were clustered using the same conditions mentioned above (twofold change, Euclidean distance 100).

The clustered genes were functionally annotated with the DAVID Database which allows classification of regulated genes according to their functional relevance. Each of the six sub-clusters was annotated separately; strong differences in the functional categories were detected.

Genes upregulated in TSA treated cells were annotated to the following groups: antigen processing, metabolism, cell membrane and cell adhesion. Genes downregulated upon TSA treatment belong to the functional groups chromosome organization, transcriptional processes, metabolism, and posttranslational processes.

Genes upregulated by BMP2 treatment were annotated in functional groups cell communication, cell membrane, extracellular matrix, and differentiation and development. Genes downregulated by BMP2 treatment belonged to the functional groups cell communication, signal transduction. Genes annotated to the functional groups extracellular matrix and cell adhesion were upregulated by both treatments, genes annotated to differentiation and development were downregulated by both treatments.

BMP2 and TSA treatment resulted in independent gene expression profiles, the downregulation of genes seems to reflect the similar phenotype seen after both treatments.

Only few primary target genes of TSA and BMP2 clustered together, but many genes involved in neural development were present: Mag (myelin-associated gly-protein), Mal (myelin and lymphocyte protein), Mog (myelin oligodendrocyte glycoprotein), Omg (oligodendrocyte myelin glycoprotein), Mbp (myelin basic protein), Mobp (myelin-

associated oligodendrocytic basic protein) were downregulated in one or both treatments

The functional annotation clustering did not reveal an enrichment of direct target genes of TSA or BMP2, therefore an additional DAVID analysis including genes regulated significantly after different times of treatment was carried out. After 6 h of BMP2 treatment genes annotated to developmental processes were regulated, after 24 h of BMP2 treatment groups like plasma membrane, cell adhesion, antigen-presenting, and developmental processes appeared in the annotation analysis. After 6 h of TSA treatment, genes could be annotated to the functional groups histone modification, chromatin organization, transcriptional regulation, cell cycle control. The functional groups of genes regulated after 24 h of TSA treatment were plasma membrane, cell adhesion, cell communication, as well as developmental processes. Thereby the treatments of TSA and BMP2 of 24 h showed the greatest similarity.

This suggests that genes regulated after 6 h directly reflected the well-established activity on gene regulation mediated by histone deacetylase inhibition, but that after 24 h already a secondary biological effect may have been observed.

The microarray data was further verified with mRNA expression and protein analysis.

Quantitative RT-PCR of selected genes was carried out. Gpr17, Bambi, Smad7 and Bmp4 were regulated in TSA and BMP2 treatments. All selected genes showed consistent expression patterns to the microarray. Stat3, Wnt5a and Wisp1 (both involved in Wnt signalling and upstream of BMP2 signalling) were found to be upregulated upon TSA treatment.

Western Blots were carried out, based on the upregulation of Stat3 expression and its well-established role in BMP2-triggered astrogliogenesis. Smad1/5/8 was phosphorylated in the BMP2 treated samples, but not in TSA treated ones. Stat3 was found to be phosphorylated upon TSA treatment, not in BMP2 treatment. TSA reduces phosphorylation of Gsk-3ß after TSA 24 h.

The stronger correlation in the 24 h gene expression data set between TSA- and BMP2-treated cultures reveals that even if the early gene expression response to the treatment

differs dramatically, similar downstream processes are induced, resulting in a comparable cell fate phenotype

4.1.3   RNA interference studies to dissect which HDAC family member(s) influence neuro- and astrogliogenesis

In order to ascertain which HDAC family members are involved in neuro- and astrogliogenesis, inhibition of the expression of individual HDAC genes using RNA interference was applied. Effective knockdown of the expression of HDACs 1, 2, 4 and 5 was observed at the mRNA level.

The consequences of these RNA interference experiments at the level of protein expression and effect upon neurogenesis were examined.

Five short hairpin RNA oligos had been generated against HDAC1, 2, 4 and 5 and were expressed from pLKO.1-puro-Vectors, as purchased from Sigma-Aldrich (Figure 4.12).

Figure 4.12. Mission shRNA-Vector pLKO.1-puro (Sigma-Aldrich) with shRNA insert. The vector contains a puromycin resistance sequence to select transfected or infected cells but no fluorescent reporter.

The shRNAs were expressed in neurosphere cultures prepared from embryonic GE via lentivirus infection. In the beginning, we used the pLKO.1-puro-Vectors to generate viral particles in HEK293T cells.

Since the pLKO1-puro vectors unfortunately lack a reporter protein being expressed together with the shRNA, to be able to determine infection rates at all, I cloned the shRNA oligos into a new vector containing *EGFP* as a fluorescent reporter protein.

As a first step, the different oligos were tested for knockdown of the respective target HDAC. Neurosphere cells prepared from embryonic mouse striatum taken at 15.5 dpc. were infected with Lentivirus containing the five different shRNA oligos. After different time periods, cells were lysed and RNA collected or protein. Gene knockdown was tested on the transcriptional level via real time RT PCR, on translational levels using western blot analysis and using immmunocytochemistry on infected cell cultures.

Moreover it was tested whether the oligos have an influence on other non-target HDACs to determine whether other HDAC genes than the specific target HDAC are influenced by the knockdown.

4.1.3.1 Analysis of shRNA knockdown of HDACs on the transcriptional level

4.1.3.1.1 SiRNA-knockdown of HDAC1

Neurosphere cultures were plated out to differentiate and infected with lentivirus expressing shRNA against HDAC1 or GFP as a transfection control. RNA was collected, reverse transcribed and subjected to quantitative real time RT-PCR. A TaqMan Assay specific for mouse HDAC1 was used for the quantification of the knockdown.

A knockdown of HDAC1 expression could be observed with oligo1, 2 and 5. Oligo 3 and 4 however led to an upregulation of HDAC1 expression, an effect contrary to the one intended. HDAC1 led to a decrease in expression of about 50%, oligo 5 of about 40% and oligo2 of about 35% (Figure 4.13).
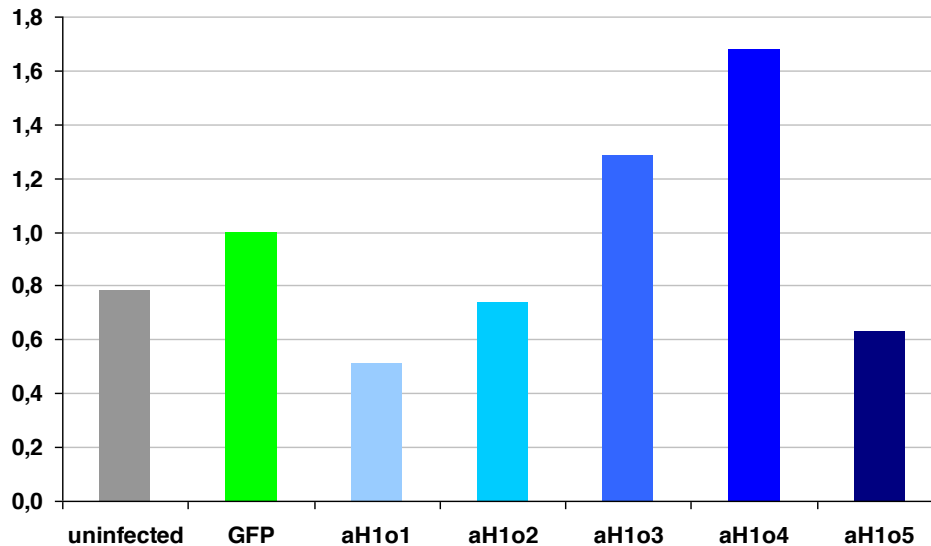
Figure 4.13. Relative expression of HDAC1&2 after siRNA-knockdown of HDAC1. GFP-infected cells as control. TaqMan assays for HDAC1 and Gapdh were applied. Relative expression was calculated through the ΔΔCt method. Results were normalized to Gapdh expression. n=1

To control for potential cross-reactions of the oligos with other HDACs, HDAC2 expression was also examined after siRNA knockdown of HDAC1 (Figure 4.14). Oligo1 led to a reduction in HDAC2 expression of about 20%, as well as oligo 5. Oligo 3 led to an increase in HDAC2 expression of about 20%, oligo 2 and 4 decrease HDAC2 expression with more than 40 percent. The shRNAs generated to knock down HDAC1 expression show cross reactions with at least one non-target HDAC. To determine specificity of the oligos, more experiments should be carried out.

Since oligo1 led to the largest knockdown of HDAC1 and has does not change HDAC2 expression as strongly as the other oligos, it would probably the oligo to choose for further experiments.
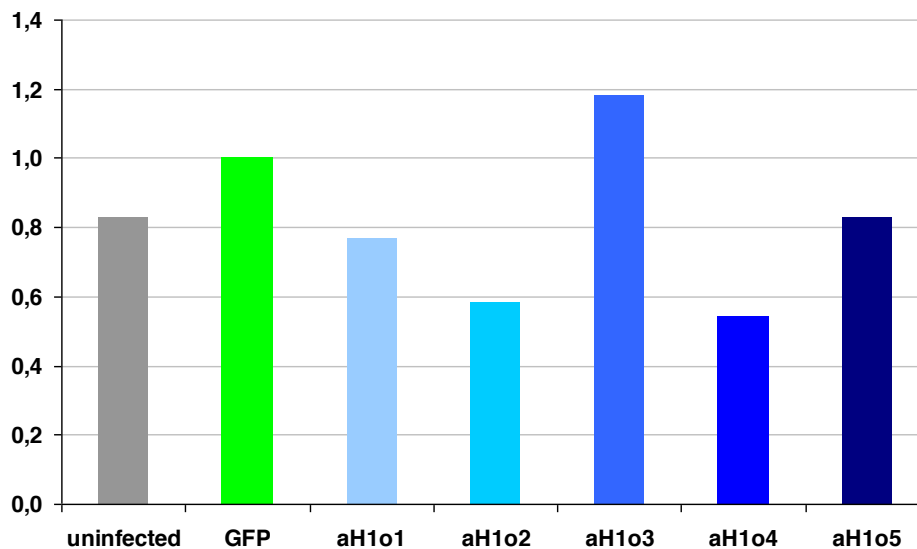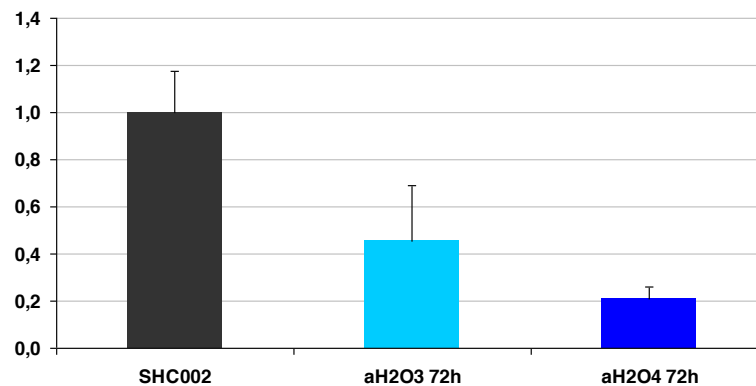
Figure 4.14. Relative expression of HDAC2 after siRNA-knockdown of HDAC1, GFP-infected cells as control. TaqMan assays for HDAC2 and Gapdh were applied. Relative expression was calculated through the ΔΔCt method. Results were normalized to Gapdh expression. n=1

4.1.3.1.2 SiRNA-knockdown of HDAC2

Neurosphere cultures were plated out to differentiate and infected with lentivirus expressing shRNA against HDAC2, GFP or a scambled sequence as control. Since the oligos against HDAC2 had already been tested previously, only 2 oligos were used for virus production. Since the virus is harvested in two rounds, virus from each harvesting day was used to infect cultures. RNA was collected, reverse transcribed and subjected to quantitative real time RT-PCR. A TaqMan Assay specific for mouse HDAC2 was used to quantify the degree of knockdown.

Knockdown of HDAC2 could be shown with both oligo 3 and 4, which had previously been selected from the initial 5 oligos generated against HDAC2. Lentivirus, harvested at two different time points after transfection of 293T cells were tested, virus collected after 48 h and 72 h respectively. The most effective knockdown could be seen with oligo 4 where virus was harvested 72 h after transfection. Oligo 3 led to a reduction in HDAC2 expression level of more than 50%, virus harvested after 72 h of about 50%. Oligo 4 reduces expression of HDAC2 to 20% (Figure 4.15).

However, the expression of HDAC2 seems to vary dramatically even in cultures which were not infected with any virus. I chose cells infected with SHC002 (a nonsense shRNA) as a control in real time RT-PCR, but the variation even in non-infected cultures should be kept in mind.

Figure 4.15. Relative expression of HDAC2 after siRNA-knockdown of HDAC2, SHC002-infected cells as control. TaqMan assays for HDAC2 and Gapdh were applied. Relative expression was calculated through the ΔΔCt method. Results were normalized to Gapdh expression. n=4

To exclude cross-reactions with other HDACs, relative expressions of HDAC1, 3, 4, 5, 7 and 8 were also determined after siRNA knockdown of HDAC2 in cell cultures.

HDAC1 expression seems to be influenced by HDAC2 knockdown. aHDAC2 oligo 3 causes down- or upregulation of HDAC1 expression, oligo 4 reduces HDAC1 expression to almost 50%. The variation within the experiments was however quite large, therefore drawing a consistent conclusion from these findings appears difficult (**Figure 4.16**).
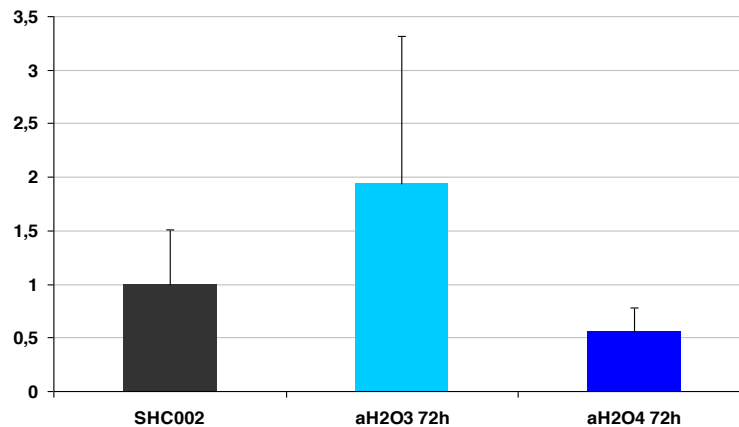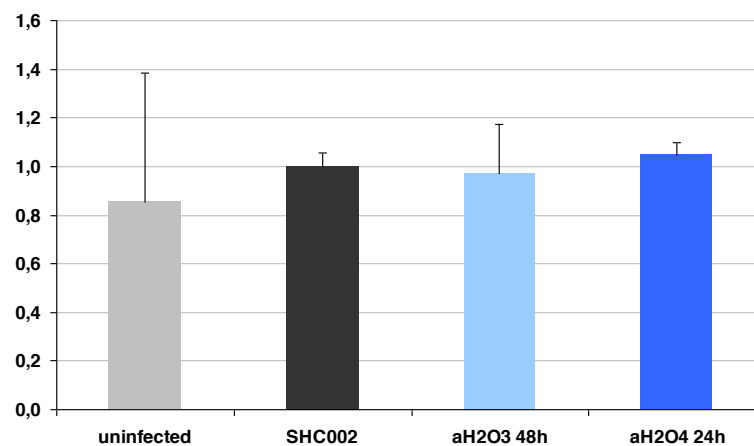
Figure 4.16. Relative expression of HDAC1 after siRNA-knockdown of HDAC2, SHC002-infected cells as control. TaqMan assays for HDAC1 and Gapdh were applied. Relative expression was calculated through the ΔΔCt method. Results were normalized to Gapdh expression. n=4

aHDAC2 oligo 3 and -4 both seem to elevate expression levels of HDAC3, oligo4 even more than doubled HDAC3 expression (Figure 4.17). Here it is difficult to draw a conclusion because the quantification was only performed once and should be repeated.
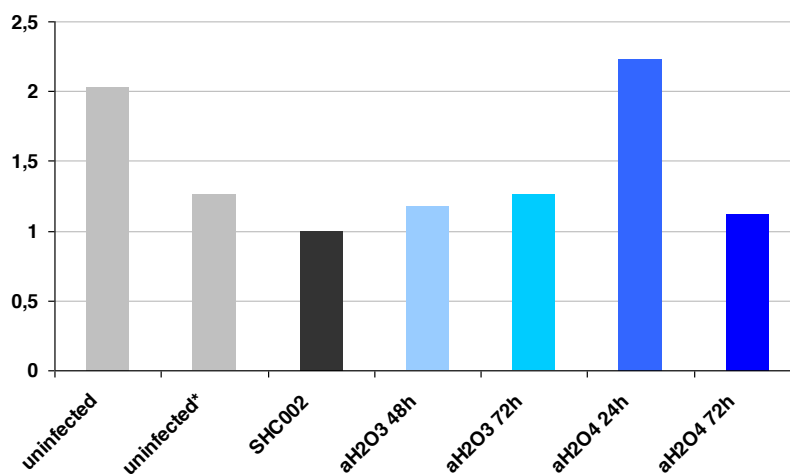
Figure 4.17. Relative expression of HDAC3 after siRNA-knockdown of HDAC2, SHC002-infected cells as control. TaqMan assays for HDAC3 and Gapdh were applied. Relative expression was calculated through the ΔΔCt method. Results were normalized to Gapdh expression. n=1

HDAC4 expression was also influenced by both oligos directed against HDAC2 in individual experiments. Summarizing different experiments, the change in HDAC4 expression was not detectable any more (Figure 4.18), which might even hint to the fact that if there were further experiments carried out concerning expression changes of other HDACs, the influences might show to be weaker as seen in these initial studies.
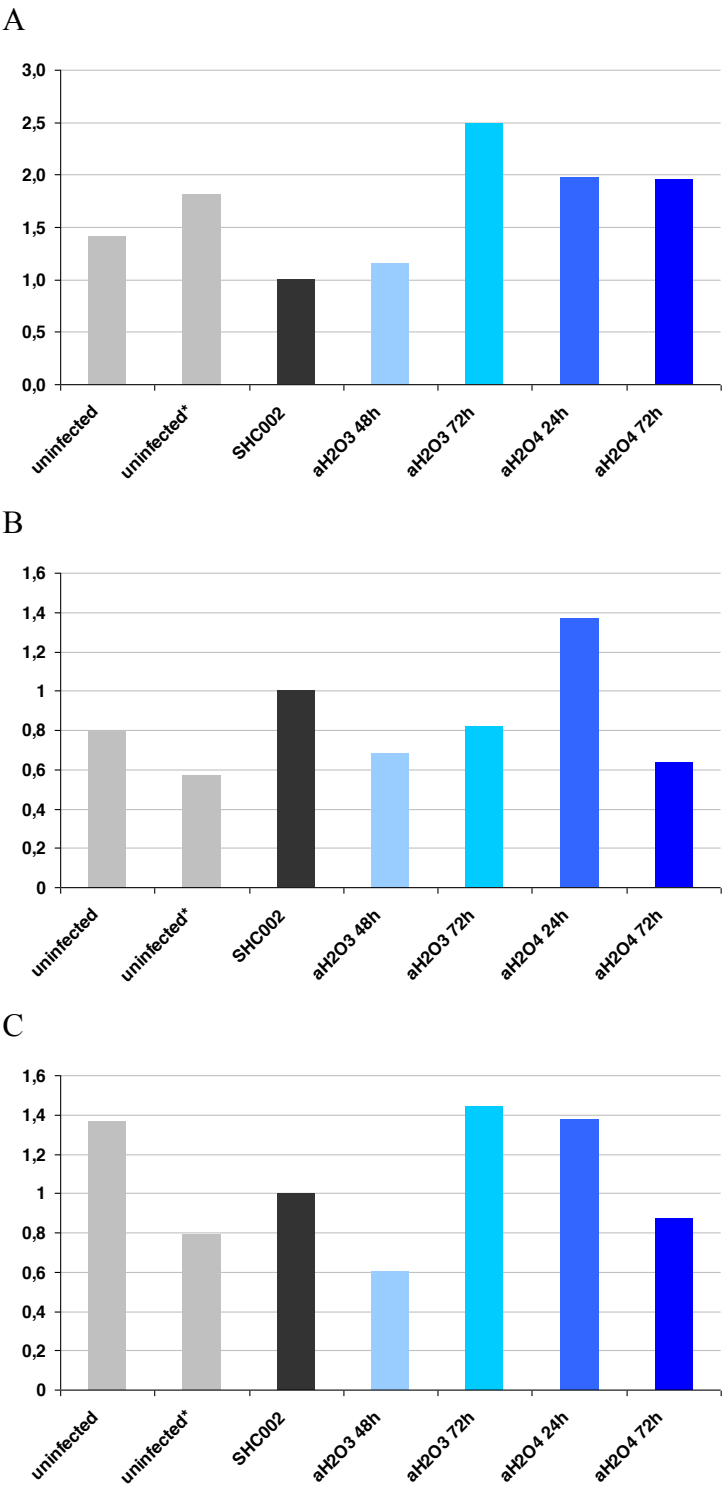

Figure 4.18. Relative expression of HDAC4 after shRNA-knockdown of HDAC2, SHC002-infected cells as control. TaqMan assays for HDAC4 and Gapdh were applied. Relative expression was calculated through the ΔΔCt method. Results were normalized to Gapdh expression. n= 2

Expression of HDAC5 was influenced upon knockdown of HDAC2, but should also be investigated further because it has only been quantified once (**Figure 4.19**a). The expression seemed to increase with both oligo 3 and 4. Again, since the variations between individual experiments were relatively high, these quantifications should be repeated to make a sound statement about cross-reactions.

The same holds true for HDAC7a and HDAC8, both showed changes in expression levels upon knockdown of HDAC2 in differentiating neurosphere cultures. Expression of HDAC7a seemed to be downregulated by aHDAC2 oligo 3 and upregulated by oligo 4 (**Figure 4.19**b). Considering the fact that also the detected expression levels in two independent non-virus infected cultures differed by about 25%, these quantifications have to be repeated.

HDAC8 expression was downregulated by aHDAC2 oligo 3 48 h and ahDAC2 oligo 4 72 h upregulated by aHDAC2 oligo 3 72h and aHDAC2 oligo 4 48 h (Figure 4.19c). Since the individual virus preparations are expected to be identical on both days; they were derived from the same plasmids being transfected into the same HEK293T cells, the changes cannot be explained by the shRNA knockdown of HDAC2 in the cultures. Perhaps, there are changes in expression level of an HDAC that are multiplied by the detection method which is very sensitive. The differences in expression levels in identical, untreated cultures would also support this thought. Also the procedure of infecting the cells might bring modifications along or have side effects that are difficult to control for.

A

B

C

Figure 4.19. Relative expression of (A) HDAC5, (B) HDAC7a, (C) HDAC8 after siRNA-knockdown of HDAC2, SHC002-infected cells as control, TaqMan assays for the different HDAC genes and Gapdh were applied. Relative expression was calculated through the ΔΔCt method. Results were normalized to Gapdh expression.n=1

4.1.3.1.3 SiRNA-knockdown of HDAC4

In an initial experiment, five oligos generated against HDAC4 were tested for their effect on HDAC4 expression. Oligo1 decreased HDAC4 expression to less than 50%, oligo 3 by 20% and oligo 4 by about 30%. Oligos 2 and 5 did not change HDAC4 expression. Oligo 1 was chosen to carry out further experiments because it showed the highest degree of knockdown for HDAC4. In three experiments, oligo 1 reduced HDAC4 expression by 30% (Figure 4.20).
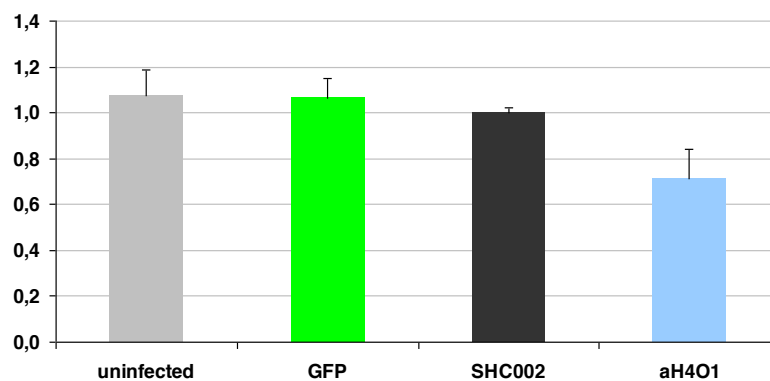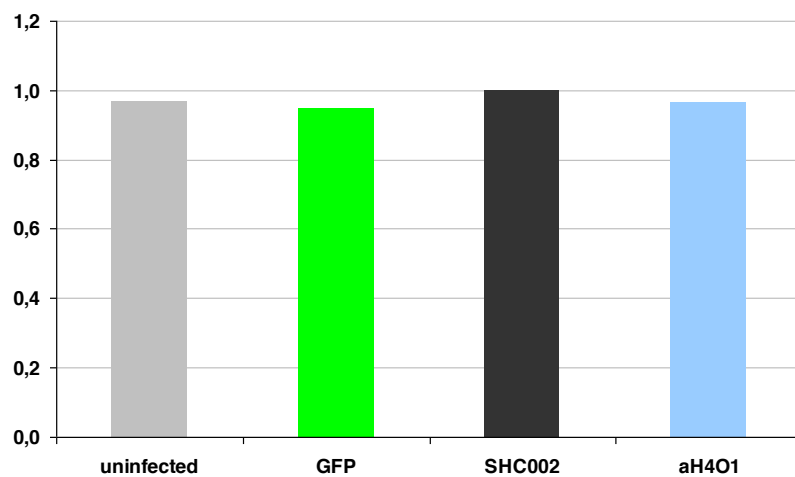

Figure 4.20. Relative expression of HDAC4 upon shRNA knockdown of HDAC4, SHC002-infected cells as control. TaqMan assays for HDAC4 and Gapdh were applied. Relative expression was calculated through the ΔΔCt method. Results were normalized to Gapdh expression. n=3

Again, to examine cross-reactions with other HDACs, expression of HDAC2 and 5 were examined upon shRNA knockdown of HDAC4. HDAC2 expression was not changed dramatically, but slightly reduced by about 10% (Figure 4.21).
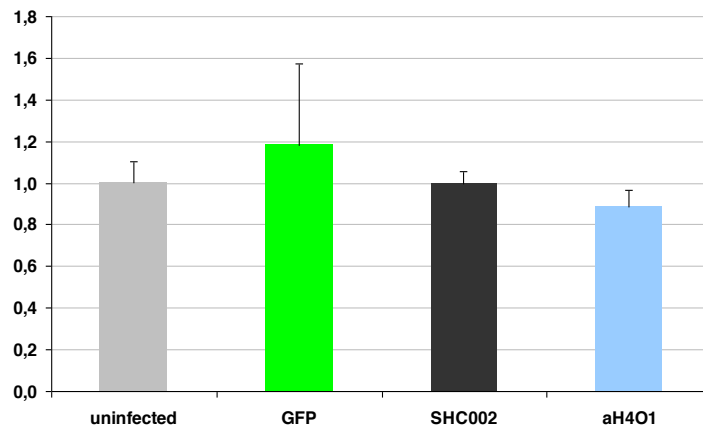
Figure 4.21. Relative expression of HDAC2 upon HDAC4 knockdown, SHC002-infected cells as control. TaqMan assays for HDAC2 and Gapdh were applied. Relative expression was calculated through the ΔΔCt method. Results were normalized to Gapdh expression. n=3

HDAC5 expression was not changed upon knockdown of HDAC4. aHDAC4oligo1 does not cross-react at least with HDAC2 and -5 and could therefore be used for further knockdown experiments (**Figure 4.22**).
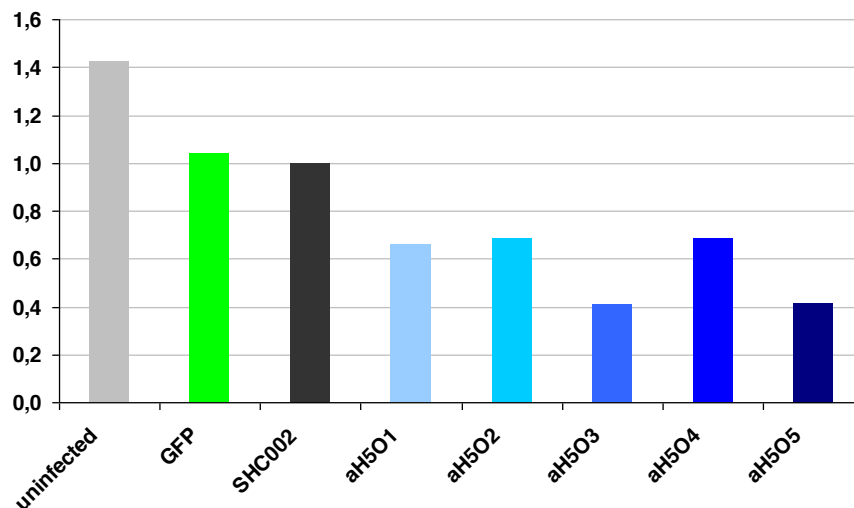

Figure 4.22. Relative expression of HDAC5 upon HDAC4 knockdown, SHC002-infected cells as control. TaqMan assays for HDAC5 and Gapdh were applied. Relative expression was calculated through the ΔΔCt method. Results were normalized to Gapdh expression. n=2

4.1.3.1.4 SiRNA-knockdown of HDAC5

All oligos generated against HDAC5 knocked down its expression, oligo1 by 20%, oligo2 to less than 20%, oligo3 to about 22%, oligo4 to almost 40% and oligo5 to less than 20%. Oligo4 does not show the strongest knockdown effect of all oligos, but was chosen for further experiments (Figure 4.23) because it was found to influence HDAC2 expression least of all oligos. HDAC2 expression upon HDAC5 knockdown was analyzed to investigate potential cross-reactions (Figure 4.24). However, also potential influences on other class II HDACs with a higher sequence similarity should also be examined.
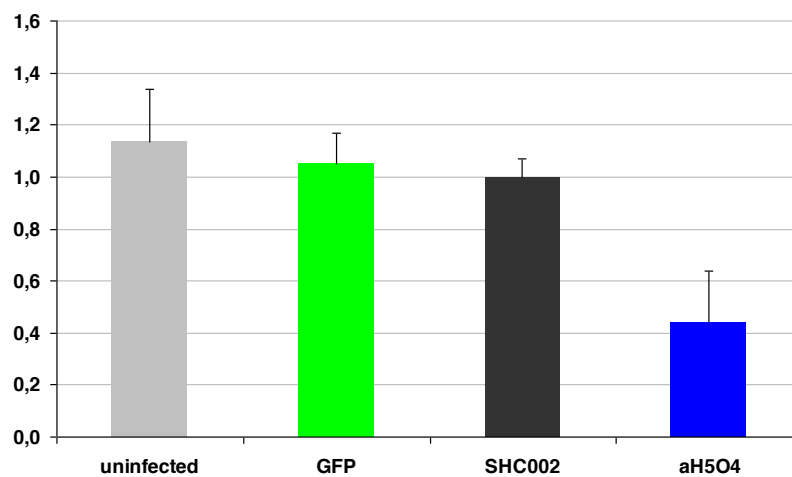
Figure 4.23. Relative expression of HDAC5 upon HDAC5 knockdown, SHC002-infected cells as control. TaqMan assays for HDAC5 and Gapdh were applied. Relative expression was calculated through the ΔΔCt method. Results were normalized to Gapdh expression. n=3

Figure 4.24. Relative expression of HDAC2 upon HDAC5 knockdown, SHC002-infected cells as control. TaqMan assays for HDAC2 and Gapdh were applied. Relative expression was calculated through the ΔΔCt method. Results were normalized to Gapdh expression. n=1

In general, many experiments were carried out only once and need to be repeated in order to draw sound conclusions. The lentivirus knockdown project was not continued so far because of the availablility of mouse models and the high variability between individual experiments.

### 4.1.3.2 Analysis of HDAC2 knockdown on the protein and the cellular level

We analyzed knockdown of HDAC2 because we knew HDAC2 to be ubiquitously expressed in brain, especially in GE and cortex, and since it was shown to play a role in several brain functions. It negatively regulates memory formation (Guan et al 2009) and can be found in higher levels in the brain and spinal cord of patients suffering from amyotrophic lateral sclerosis (ALS) (Janssen et al 2010).

4.1.3.2.1 Analysis of the knockdown of HDAC2 in cell cultures on protein level:
Western Blot analysis

Knockdown of HDAC2 was examined both in neurosphere cultures and in a permanent cell line (293T) to determine the efficiency of the shRNA oligos for knocking down HDAC2.

*4.1.3.2.1.1 Knockdown of endogenous HDAC2 in Neurospheres – analysis 4 days after*
infection

Lysates of the infected neurosphere cells were prepared 4 days after infection. The protein was separated in a PAGE and subsequently analyzed though western blotting. According to the quantification of the protein bands through the pixel intensity, HDAC2 protein levels were decreased in cultures infected with virus containing aHDAC2 oligo 3 in a dose-dependent manner. Compared to the control cultures infected with a scrambled shRNA virus, HDAC2 protein level was much higher in uninfected cultures (**Figure 4.25**). According to this result, knockdown of HDAC2 in neurosphere cultures leads to a reduction of protein levels to about 50%. This would support the idea that the infection rate of the cells on coverslips was too low to detect the change in immunostaining of the entire culture.
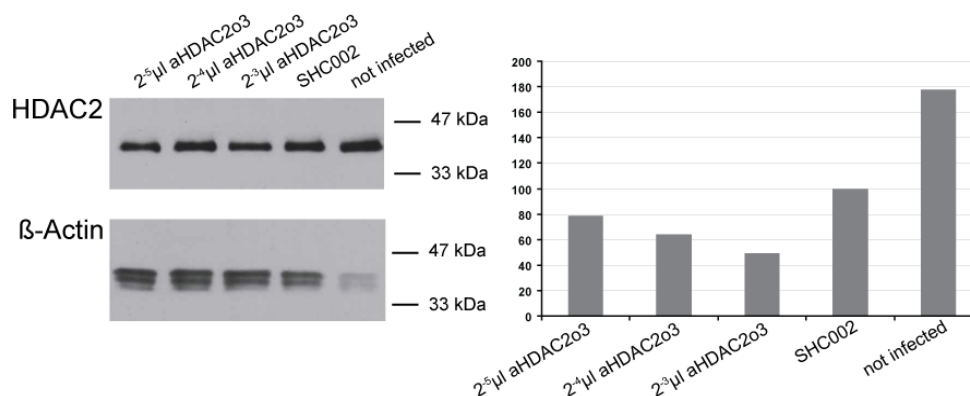
Figure 4.25. Western blot anaylsis of HDAC2 expression in lentivirus infected neurosphere cultures. A dose-dependet reduction of HDAC2 protein levels could be observed in cultures infected with aHDACs oligo 3 after 4 days of infection.

4.1.3.2.1.2 Knockdown of endogenous HDAC2 in Neurospheres – analysis 7 days after infection

After 7 days of infection, the same effect could be observed. A dose dependent decrease of HDAC2 protein levels upon infection with lentivirus containing shRNA against HDAC2. The downregulation was even more pronounced in the sample with the highest virus concentration than after 4 days of infection (**Figure 4.26**).
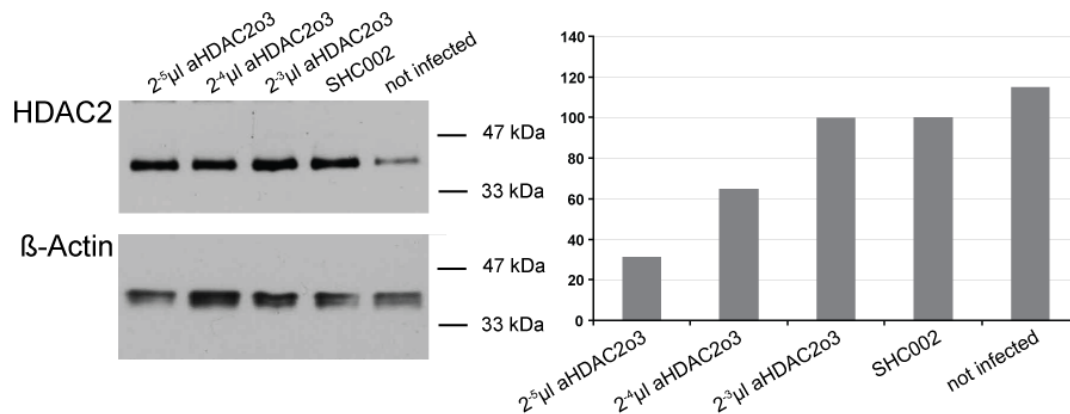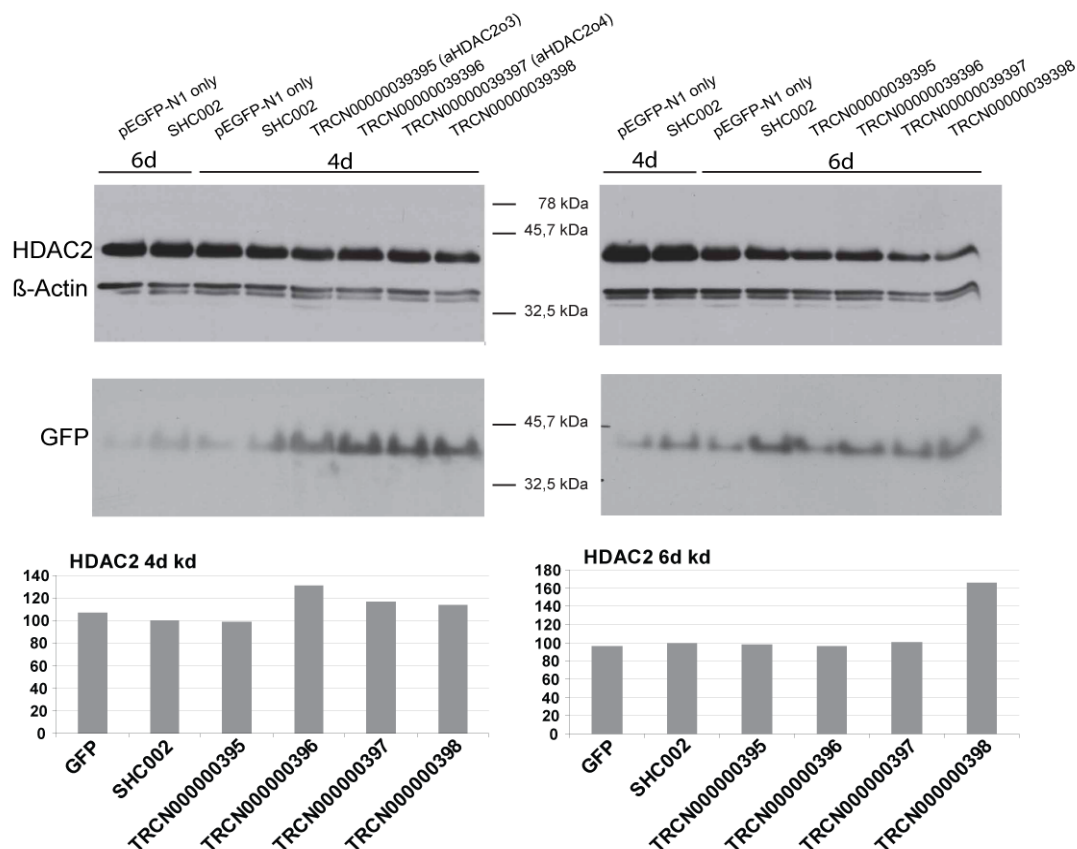

Figure 4.26. Western blot anaylsis of HDAC2 expression in lentivirus infected neurosphere cultures. A dose-dependet reduction of HDAC2 protein levels could be observed in cultures infected with aHDACs oligo 3 after 7 days of infection.

4.1.3.2.1.3 Knockdown of endogenous HDAC2 in 293T cells

To test the original plasmids bought from Sigma for their knockdown capacity, they were transfected into HEK293T cells. The cells were cultured for 4 d respectively 6 days after transfection. Lysates were prepared and subjected to western blot analysis. A cotransfection with GFP served as a control for transfection.

No reduction of protein levels could be observed with the Mission plasmids alone (Figure 4.27). This could be due to a low transfection efficiency. To be able to draw a sound conclusion, the experiment should be repeated.

Figure 4.27. Western blot anaylsis of HDAC2 expression in 293T cells transfected with Mission plasmids containing the shRNA sequences generated against HDAC2. Co-transfection with GFP as trasfection control. No reduction of HDAC2 protein level could be observed after 4 days and 6 days of transfection.

4.1.3.2.2 Knockdown of HDAC2 in cell cultures derived from neurospheres

In order to determine whether the shRNA oligos generated against HDAC2 were reducing HDAC2 expression on the protein level, I carried out immunostainings of infected neurosphere cultures plated out for differentiation 4 days after infection and determined fluorescence levels of HDAC2 antibody staining in nuclei.

The cultures were grown and infected on coverslips, then stained and photographed using the same exposure time for each image. Those images were then processed in Metamorph software. The fluorescence intensity of the nuclear HDAC2 staining was determined using Metamorph software. Regions covering the nuclei were determined and average fluorescence determined for each nucleus.

All nuclei showed HDAC2 expression. Overall, the cultures infected with virus supposed to knock down HDAC2 expression antiHDAC2 oligo 3 and antiHDAC2 oligo 4 did not show less HDAC2 expression than the cultures infected with control virus SHC002.

Furthermore, immunostainings with a TuJ1 antibody revealed no differences in numbers of newborn neurons in the cultures where HDAC2 was knocked down compared to scrambled-infected controls (**Figure 4.28**).
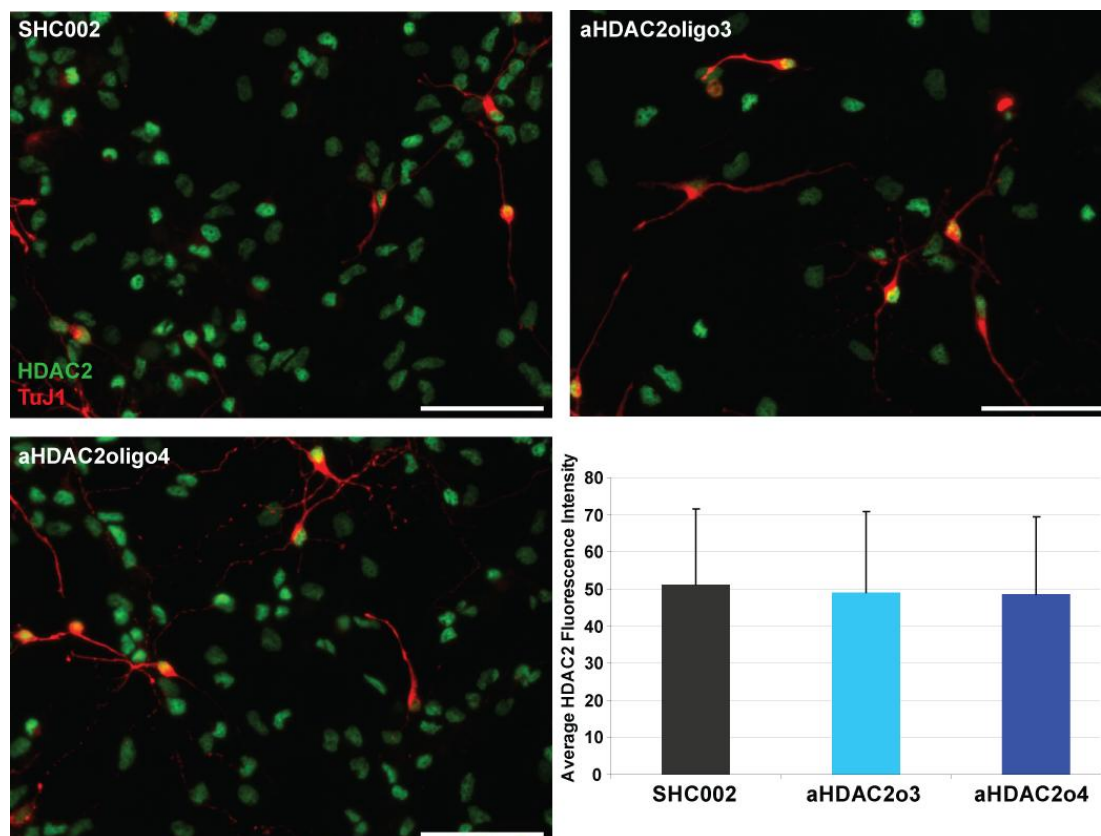
Figure 4.28. Immunostaining of striatal neurosphere derived cells on coverslips. Cells were infected with lentivirus to knock down HDAC2. Antibodies: Tuj1 (neurons) and HDAC2. Scalebar 100 µm. Metamorph Analysis of average HDAC2 immunofluorescence in neurospheres infected with lentivirus to knock down HDAC2 expression. No reduction in HDAC2 protein levels can be detected.

4.1.3.2.3 Knockdown of HDAC2 in hippocampal cell cultures

The same experiment was performed in hippocampal cultures. The cells were infected with lentivirus to knock down HDAC2 expression. The cells were fixed and stained 4

days after infection. The cells were stained with antibodies to detect HDAC2 and GFP to determine the number of infected cells. No reduction in HDAC2 protein levels could be observed in infected cells. The staining for GFP revealed that only very few cells were infected in the cultures and that HDAC2 fluorescence in nuclei of infected cells was not reduced (**Figure 4.29**).
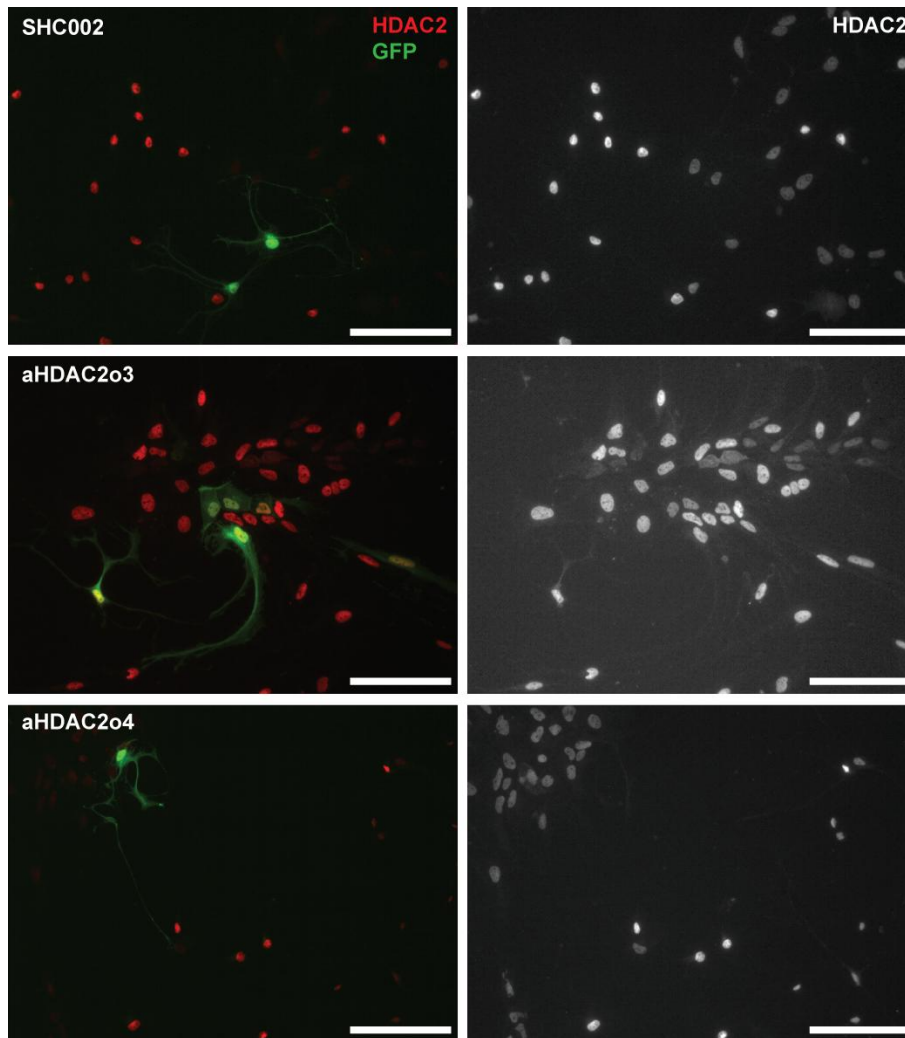

Figure 4.29. Hippocampal cells (DIV 9) infected with lentivirus carrying shRNAs against HDAC2, fixed 4 d after infection. Immunostaining with antibodies against HDAC2 and GFP, revealing that infected cells did not show reduced HDAC2 protein levels. Scalebar 100 µm

4.1.3.2.4 Immunostaining to reveal the progeny of infected precursors

In order to analyze whether infected cells develop specifically to either neurons or astrocytes immunostainings were carried out with antibodies staining the EGFP serving as a reporter of virusinfected cells, TuJ1 to stain for newborn neurons or GFAP to stain astrocytes. The neurosphere cultures were plated out to differentiate, infected and then cultured for 7 days to allow for differentiation to occur.

No neurons could be detected to express GFP, but even only few cells were shown to express both GFP and GFAP. In general, the rate of infected cells in the culture was very low (**Figure 4.30**).
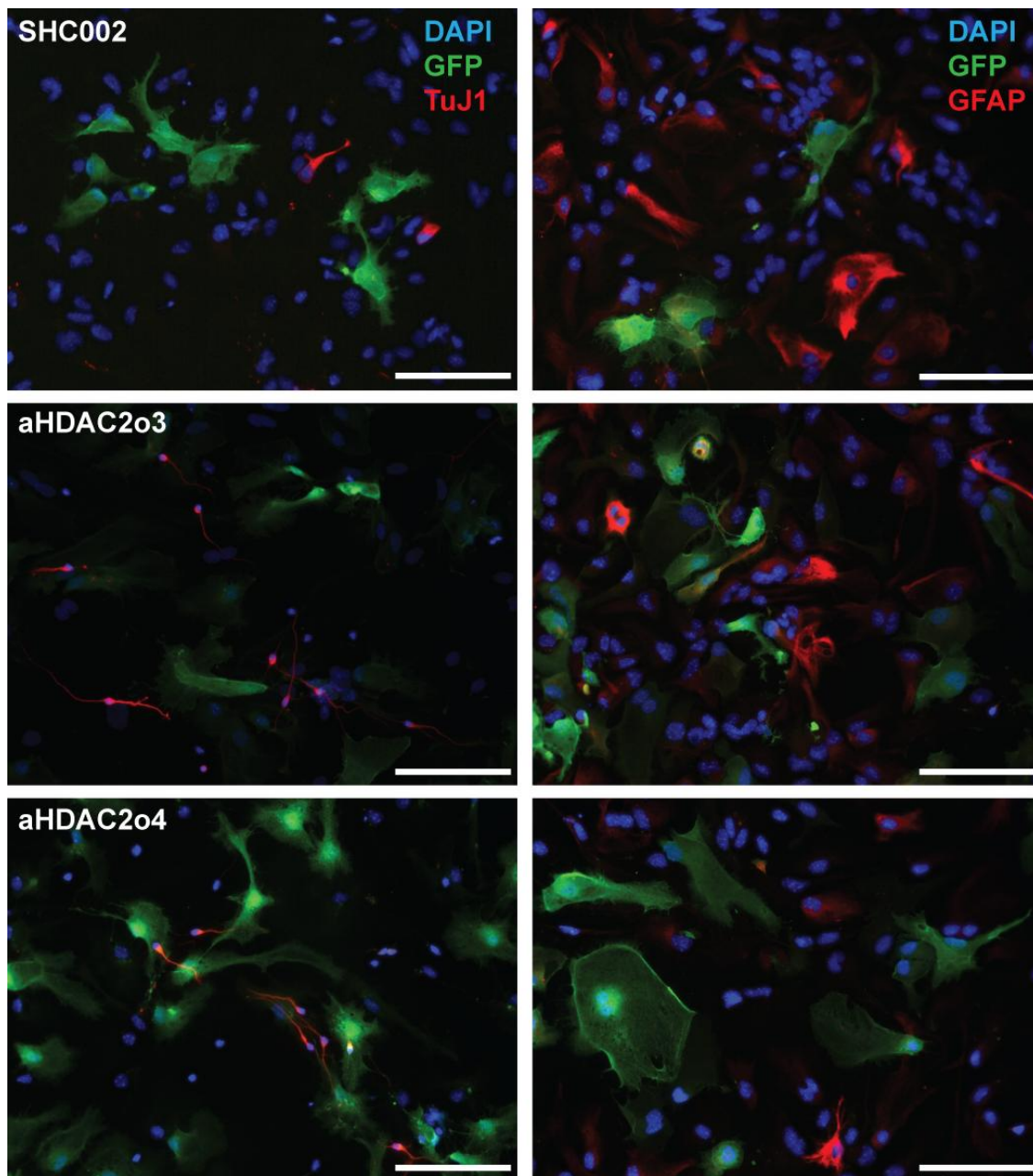
Figure 4.30. Neurosphere cultures infected with lentivirus containing shRNA to knock down HDAC2 were allowed to differentiate for 7 days, then fixed and stained for GFP to detect infected cells and either TuJ1 or GFAP to determine their progeny

None of the neurons seemed to be an infected cell according to the immunostaining against GFP. This could hint to a role of HDAC2 in neurogenesis, but has to be investigated further.

4.1.3.3   Analysis of the outcome of differentiation in cultures infected with lentivirus to knock down HDAC2

4.1.3.3.1 Differentiation of precursor cells 4 days after infection with lentivirus

4 days after infection with virus to knock down HDAC2, neurosphere cultures were fixed and stained with antibodies against TuJ1 to determine the number of neurons or GFAP to investigate the number of astrocytes in the cultures. No change could be detected in the numbers of neurons generated in the cultures (**Figure 4.31**). However, this could be expected because the expression of the shRNA and subsequent knock-down takes some time to occur and might not have exceeded any effect on the cellular composition of the cultures.
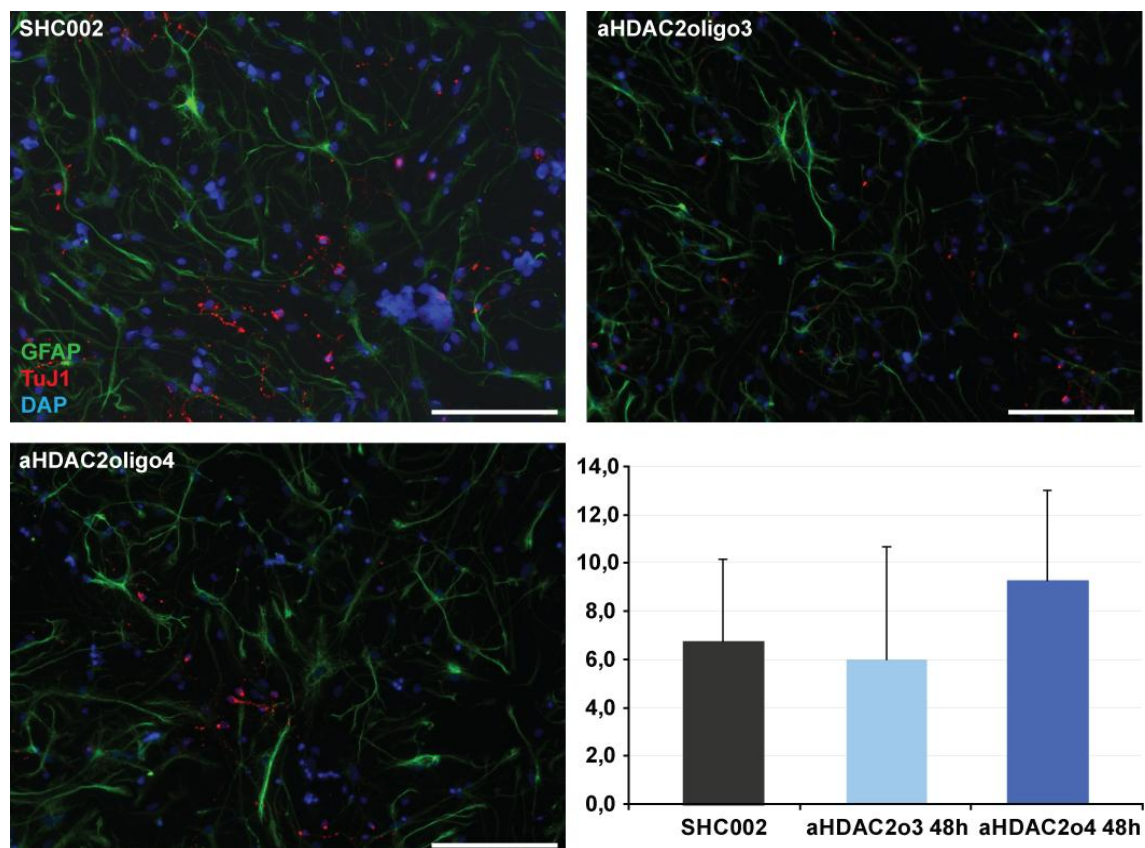

Figure 4.31. Neurosphere cultures infected with lentivirus containing shRNA to knock down HDAC2 were allowed to differentiate for 4 days, then fixed and stained for TuJ1 or GFAP to determine the ratio of neuro-and astrogliogenesis in the cultures. Quantification of the number of neurons in cultures infected with control (SHC002) or shRNA against HDAC2. Scalebar 100 μm

4.1.3.3.2 Differentiation of precursor cells after 7 days of shRNA knockdown of HDAC2

7 days after infection with virus to knock down HDAC2, neurosphere cultures were fixed and stained with antibodies against TuJ1 to determine the number of neurons or GFAP to investigate the number of astrocytes in the cultures. No change could be observed in the cellular composition of the culture (**Figure 4.32**). This could either be because HDAC2 does not influence neuro- or gliogenesis or because infection rates were so low, that eventual, subtle changes in the cellular composition could not be measured.
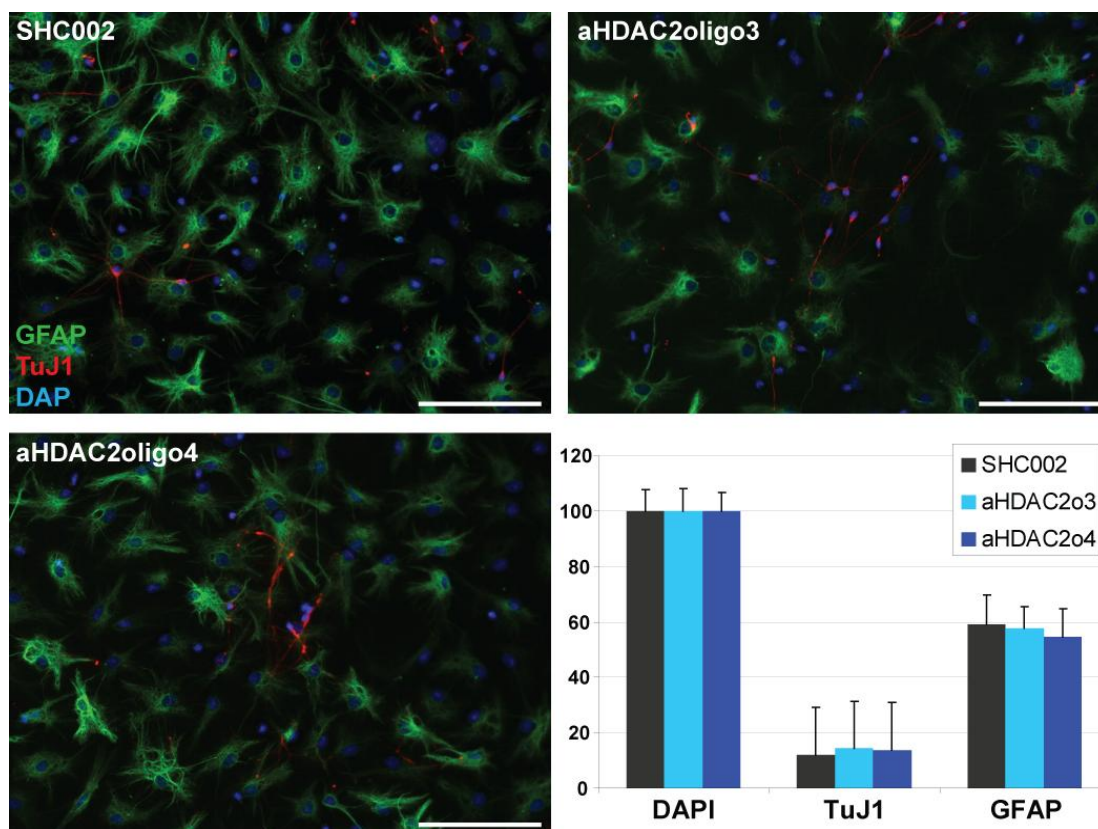

Figure 4.32. Neurosphere cultures infected with lentivirus containing shRNA to knock down HDAC2 were allowed to differentiate for 7 days, then fixed and stained for TuJ1 or GFAP to determine the ratio of neuro-and astrogliogenesis in the cultures. Quantification of the number of neurons in cultures infected with control (SHC002) or shRNA against HDAC2. Scalebar 100 µm

4.2   Developmental phenotype of the CNS of HDAC4 and HDAC5 transgenic mice

4.2.1   Expression analysis of HDAC4 and HDAC5 in embryonic brain

### 4.2.1.1   In situ hybridization to reveal HDAC4 and HDAC5 expression patterns

4.2.1.1.1 Expression of Ngn2 and Dlx2 in embryonic mouse brain

Expression of all HDACs in embryonic brain tissue had been examined via a quantitative real time RT-PCR analysis. Expression of HDAC4 and HDAC5 was also examined via in situ hybridization. To test the protocol, probes for Ngn2 and Dlx2 were used which were known to function well with the protocol applied.

The in situ hybridization was carried out on coronal sections of E15.5 mouse brain which had been embedded in paraffin. Both Dlx2 and Ngn2 probes gave a distinct and specific staining, showing that the experimental procedure worked (**Figure 4.33**). To test the specificity of the HDAC4 and -5 antisense probes, the corresponding sense probes were also generated. Those should not bind to the tissue specifically and can therefore be used to determine whether the staining seen with antisense probes is specific or due to unspecific background staining.

Both probes showed an intense staining in the appropriate brain areas. Ngn2 is highly expressed in embryonic cortex; the transcription factor shows a clear expression pattern in embryonic cortical ventricular zone. Dlx2 is a marker expressed in the ventral forebrain; it is expressed as expected in the VZ and SVZ of the ganglionic eminences (**Figure 4.33**).

I therefore conclude that the in situ protocol works well and that results I obtain with the newly generated probes for HDAC4 and HDAC5 probably show the true distribution of the RNA in embryonic brain.
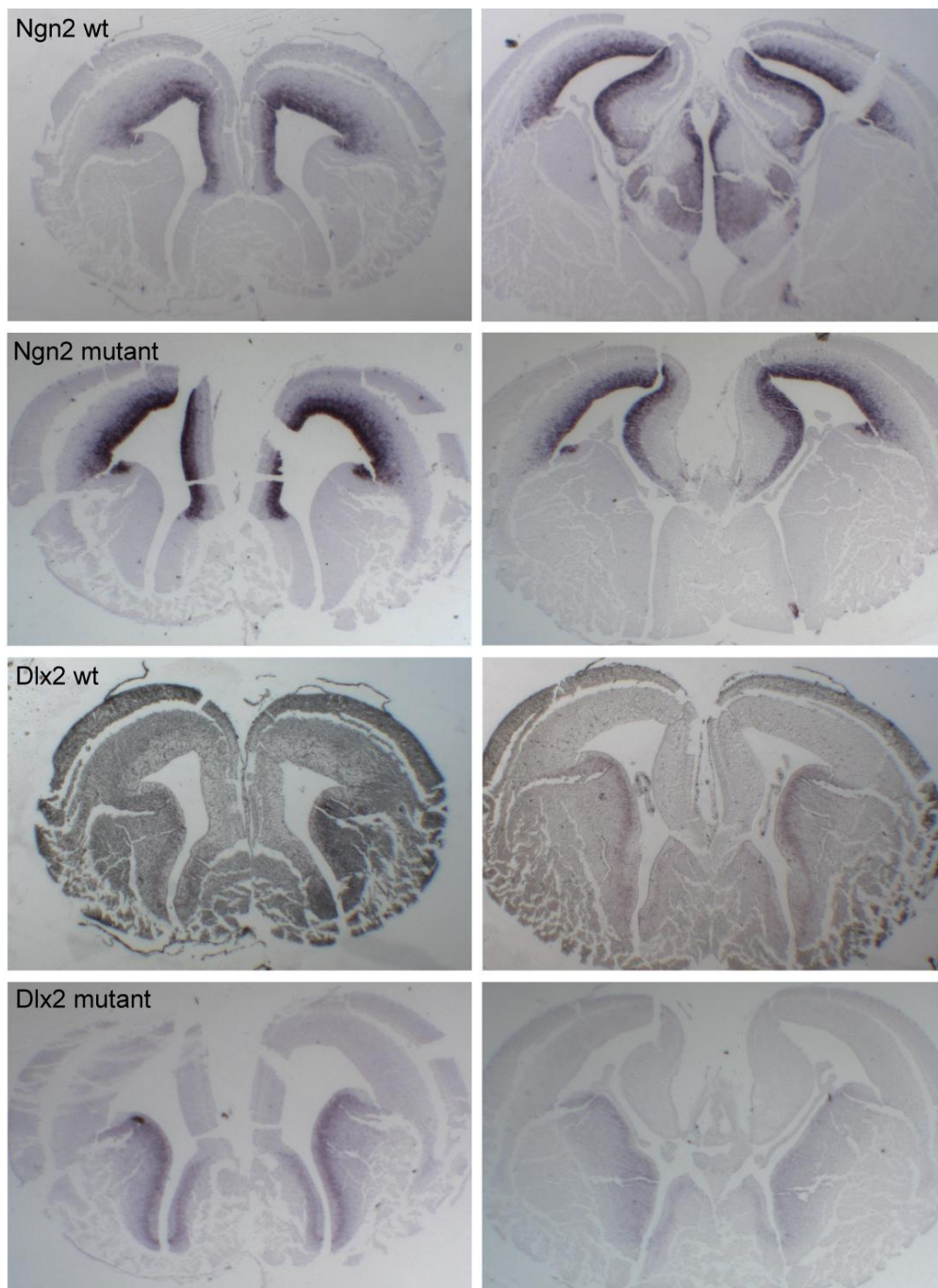
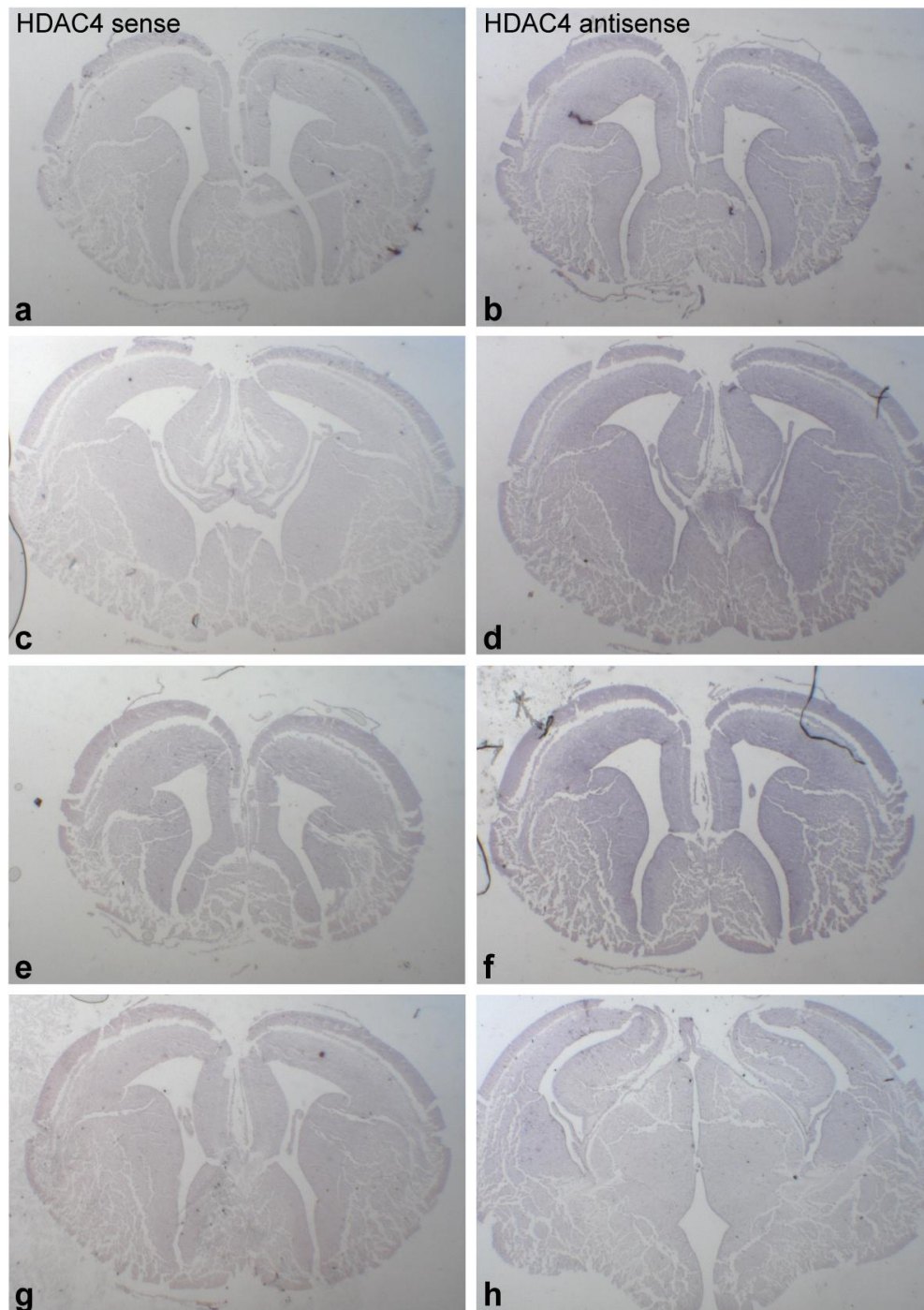**Figure 4.33. In situ hybridization on E 15.5 coronal brain sections**. Ngn2 and Dlx2 probes were chosen to confirm the protocol functioning properly

4.2.1.1.2 HDAC4 is present in neurogenic regions of the developing brain (In situ hybridization of HDAC4)

The HDAC4 sense probe showed a weak overall staining, which can be interpreted as an overall background signal on the sections. The HDAC4 antisense probe led also to a

staining on the entire section; however, several areas were stained more intensely. The cortical plate and the ventricular zone and subventricular zone of the cortex were stained by the HDAC4 antisense probe, as well as ventricular zone and subventricular zone of the lateral and medial ganglionic eminences (LGE and MGE). This can hint to a stronger expression of HDAC4 in those neurogenic areas, but might also be due to the fact that there are more cell bodies in those areas and the staining in the grey matter appears weaker because there are less cell bodies present (**Figure 4.34**).
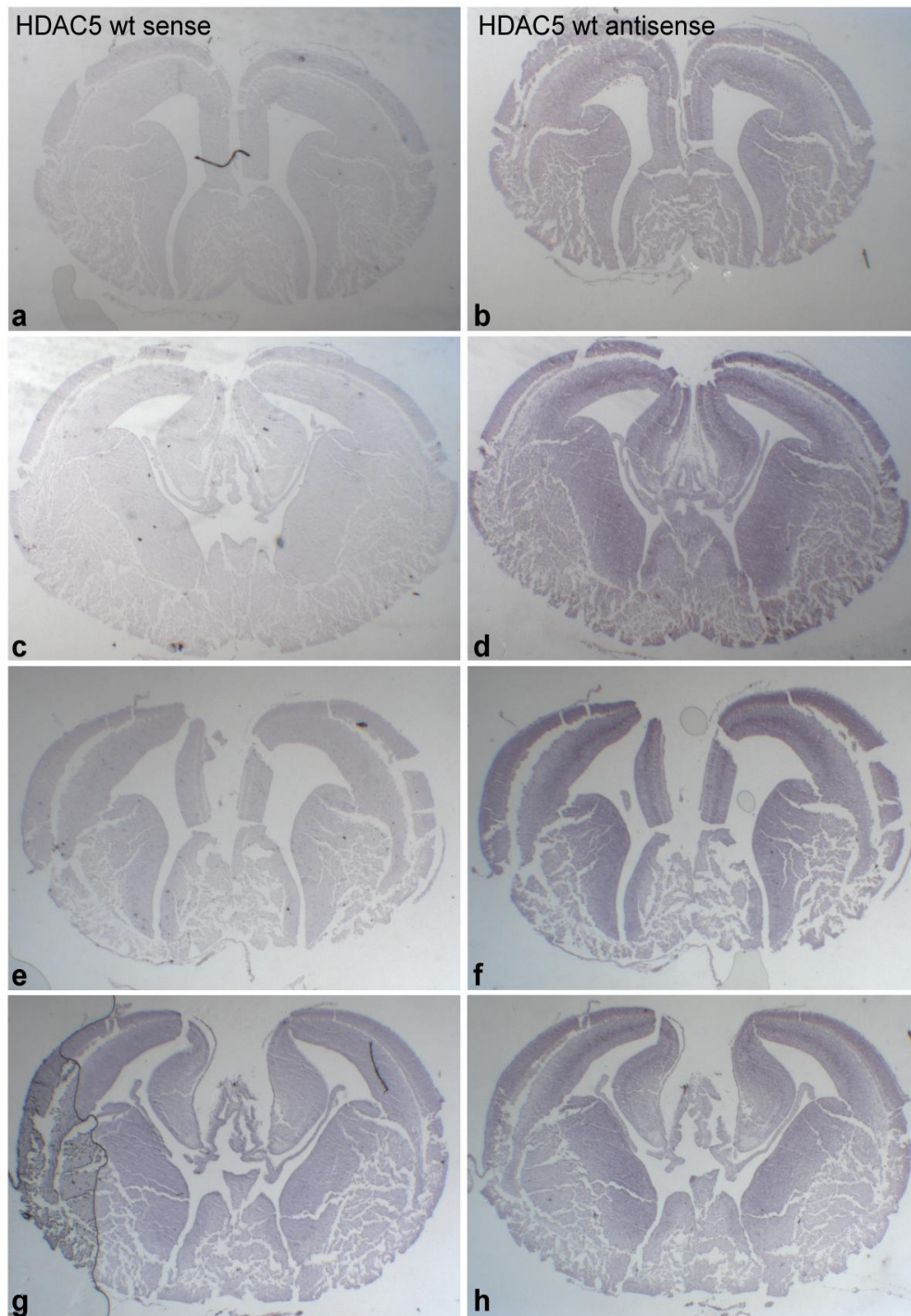
Figure 4.34. In situ hybridization of HDAC4 on E 15.5 coronal brain sections. Sections from anterior (a, b) to more posterior (g, h) brain areas. a and b, c and d, e and f and g and h are sections corresponding in anterior-posterior position.

4.2.1.1.3 HDAC 5 is present in areas important for cortical layering and neurogenesis in the embryonic mouse brain (In situ hybridization of HDAC5)

The HDAC5 sense probe resulted in barely any staining at all on all examined slides, the background signal was very low. The HDAC5 antisense probe treated brain sections showed an overall staining, just like with HDAC4 antisense, but in some areas the staining was also distinctively stronger. The cortical plate showed a strong staining, subplate and white matter a less intensive expression and the subventricular zone (SVZ) of the cortex again a strong staining. The ventricular zone (VZ) was stained less than the SVZ, indicating a stronger expression of HDAC5 in the SVZ. In the case of HDAC4, both VZ and SVZ showed the same strong level of staining, which shows the different expression patterns of HDAC4 and -5. In the SVZ and VZ of both LGE and MGE, I could also observe a very strong staining with HDAC5 antisense.

Again, the stronger staining for HDAC5 corresponds partly with areas with a high density of cell bodies, however, the difference in staining levels in VZ and SVZ of the cortex shows that there is a difference in the expression pattern which cannot be caused only by differences in cell density (**Figure 4.35**)

HDAC5 wt sense

HDAC5 wt antisense

Figure 4.35. In situ hybridization of HDAC5 on E 15.5 coronal brain sections. Sections from anterior (a, b) to more posterior (g, h) brain areas. a and b, c and d, e and f and g and h are sections corresponding in anterior-posterior position.

4.2.1.2   Analysis of HDAC 4 and -5 expression pattern using X-Gal staining

To determine the expression pattern of HDAC4 and -5 in embryonic brain, I also used mutant mice deficient in those genes (Chang 2004, Vega et al 2004b). In both cases a *LacZ* cassette was knocked into the gene sequence, thereby providing a transgene as a marker for the expression of the individual HDAC.

The bacterial enzyme β-galactosidase (gene *LacZ*) is an enzyme which catalyzes the hydrolysis of ß-galactosides into monosaccharides. The enzyme is knocked into the gene locus of the respective HDACs and is then expressed under the control of the promoter of the individual HDAC. When the enzyme cleaves the artificial substrate X-gal, it turns blue and thereby one can identify areas of tissue where the HDACs would be expressed by a blue stain.

I examined brains of mutant embryos at 13.5 dpc and 15.5 dpc. The heads were dissected, fixed in 0.2% glutaraldehyde, embedded in tissue freezing medium and sectioned. 7 µm thin coronal sections were prepared and used for the staining procedure.

4.2.1.2.1 Expression of HDAC4 in embryonic brain

At 13.5 dpc I observed a weak overall staining of HDAC4 throughout the brain. In posterior sections, a stronger staining could be observed in the hippocampus (**Figure 4.36**c,c'). The trigeminus ganglion showed a particularly strong staining at E13.5 dpc (**Figure 4.36**c').
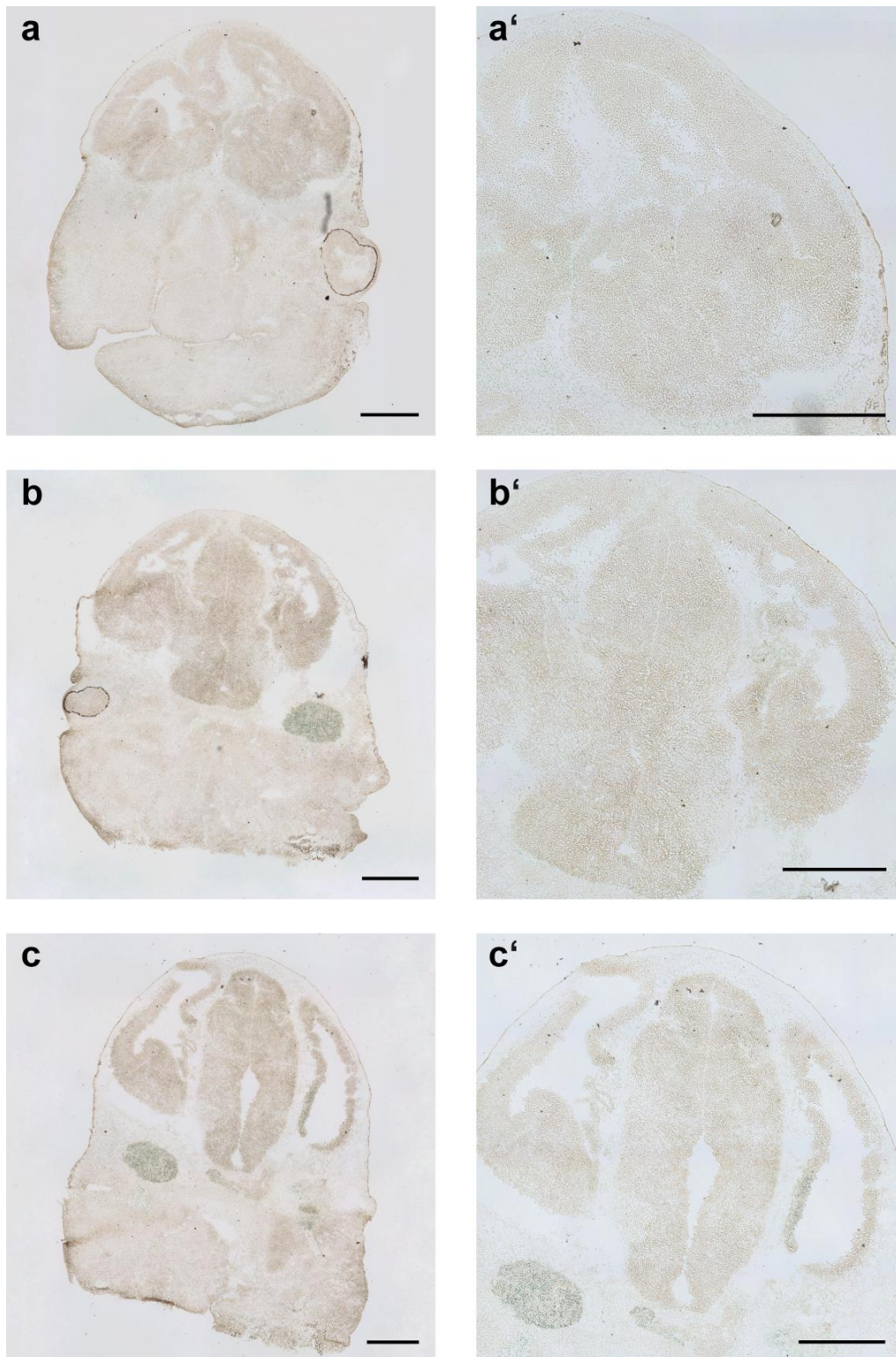
Figure 4.36. *LacZ* **staining on E13.5 coronal brain sections of a HDAC4 mutant embryo** to determine the subcellular localization of HDAC4 expression in embryonic brain. Scalebar 500 µm

Brains of 15.5 dpc embryos showed a weak staining in the anterior sections, with some cells being stained in the olfactory bulb area in the glomerular layer (**Figure 4.37**a'). I also observed staining in the cortical plate and frontal part of the corpus callosum (**Figure 4.37**b', a', b', c' and d' are enlargements of a, b, c and d respectively). The more posterior sections showed a strong staining in the lateral ventricular zone and subventricular zone of the cortex (**Figure 4.37**c,d). However, also the region of the cortical plate showed a stronger staining than the underlying layers of the cortex. The ventricular zone of the LGE and MGE was also stained, as well as the lateral and medial septal nucleus (**Figure 4.37**c',d').
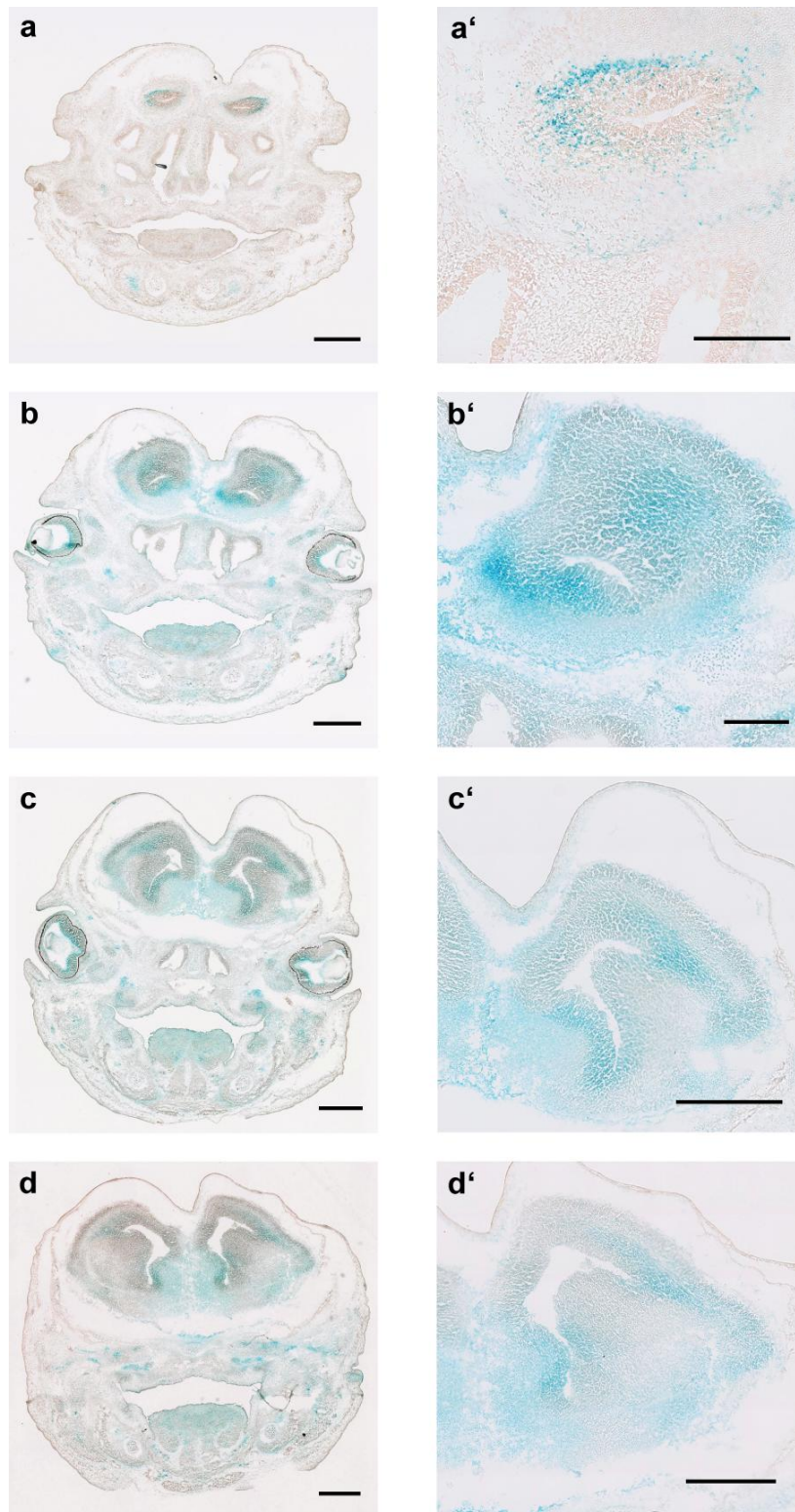
Figure 4.37. *LacZ* **staining on E15.5 coronal brain sections of a HDAC4 mutant embryo** to determine the subcellular localization of HDAC4 expression in embryonic brain. Scalebar 500 µm

4.2.1.2.2 Expression of HDAC5 in embryonic brain

X-Gal staining was also performed on coronal sections of HDAC5 mutant mice. The experiment was performed with brain of developmental stage E13.5 and E15.5.

At E13.5 the embryonic brains showed a distinct staining in the cortical plate which also remains at E15.5. (**Figure 4.38**) The cortical plate is the only region of the brain which is stained at this age. At E15.5 I could observe staining in the cortical plate and the subplate (**Figure 4.39**). Because the cortical plate is known to be crucial in the control of the correct development of cortical layers, I decided to investigate whether there were differences in cortical layering in HDAC5 mutant mice.

Figure 4.38. *LacZ* **staining on E13.5 coronal brain sections of a HDAC5 mutant embryo** to determine the subcellular localization of HDAC5 expression in embryonic brain. Scalebar 500 µm
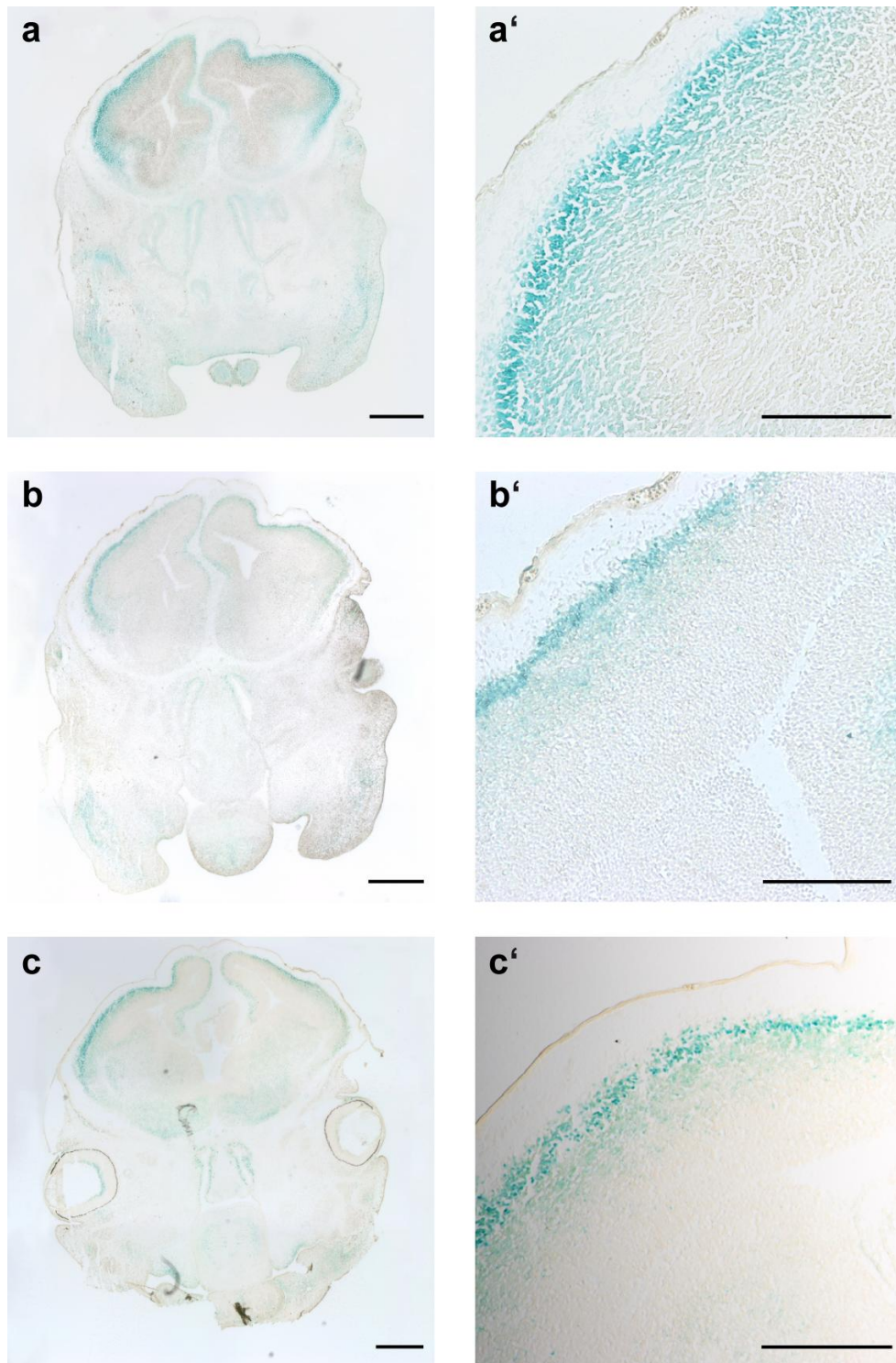
Figure 4.39. *LacZ* **staining on E15.5 coronal brain sections of a HDAC5 mutant embryo** to determine the subcellular localization of HDAC5 expression in embryonic brain. Scalebar 500 µm

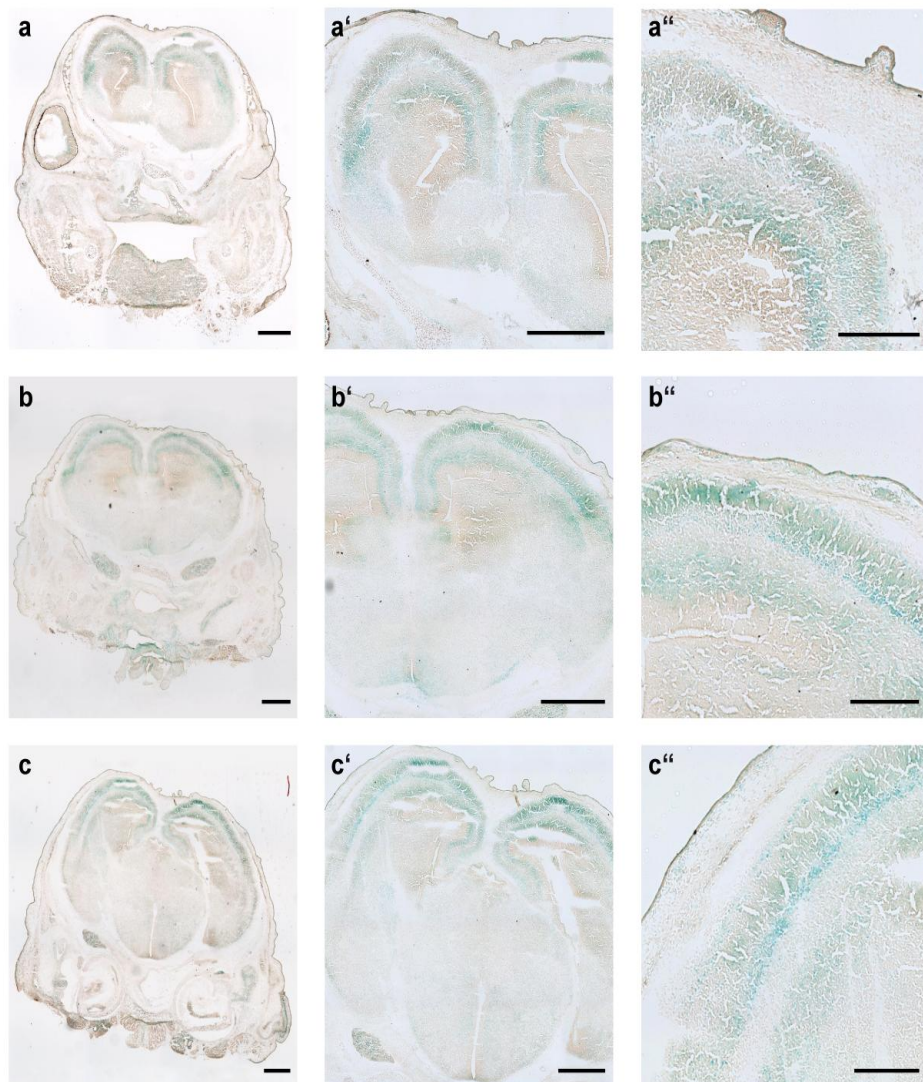Comparing both analyses to each other (*in situ* hybridization and X-Gal staining), overall the same expression pattern for HDAC4 emerges. At E15.5, neurogenic regions of the embryonic brain express HDAC4, the ventricular and subventricular zones of the cortex and the striatum. HDAC4 is also expressed in the cortical plate which might hint to a role in layer formation

Comparing in situ hybridization and X-Gal staining for HDAC5 expression, both methods show a strong expression of HDAC5 in the cortical plate, both at E 13.5 and

E15.5. This hints to a role of HDAC5 in cortical layer formation or perhaps cell migration during layer formation.

4.2.2   Generation and analysis of conditional mutant animals for HDAC4

HDAC4 null mice die within two weeks after birth, they show several changes in their CNS compared to wildtype animals, a reduced brain size and a degeneration of Purkinje neurons to name a few. However, since they show severe malformations of the skeleton and the skull, which could also influence the development of the brain, we decided to generate mice in which HDAC4 is specifically removed from the CNS. We therefore bred HDAC4 flox mice (Potthoff et al 2007) with mice expressing Cre through a nestin promoter (Tronche et al 1999). This should lead to a deletion of HDAC4 in neural progenitor cells and their lineage (neurons and microglia).

Surprisingly, the conditional knock-out animals survived normally and did not show any aberrant behaviour as far as we could observe without applying behavioural tests. They also bred normally.

4.2.2.1   HDAC4 immunoblot to confirm absence of HDAC4 protein in mutant embryonic CNS

To determine to what extent the HDAC4 or -5 protein expression was diminished in transgenic animals already in embryonic stages, immunoblot experiments were carried out with E13.5 or E15.5 dpc brain and spinal cord tissue.

4.2.2.1.1 HDAC4 protein level is decreased in embryonic brain of HDAC4 conditional knockout animals at E 13.5

At 13.5 dpc HDAC4 protein was still detectable brains of conditional HDAC4 mutant embryos, however, the protein levels were drastically reduced compared to heterozygous or wildtype littermates (**Figure 4.40**). The reduction of HDAC4 protein was found to be dose-dependent, a stronger reduction could be seen in homozygous animals with two conditionally deleted alleles compared to heterozygotes with only one

allele. In heterozygous animals, the amount was reduced to about half of the one of wildtype, in homozygous mutants the protein amount was only 2% of wildtype.
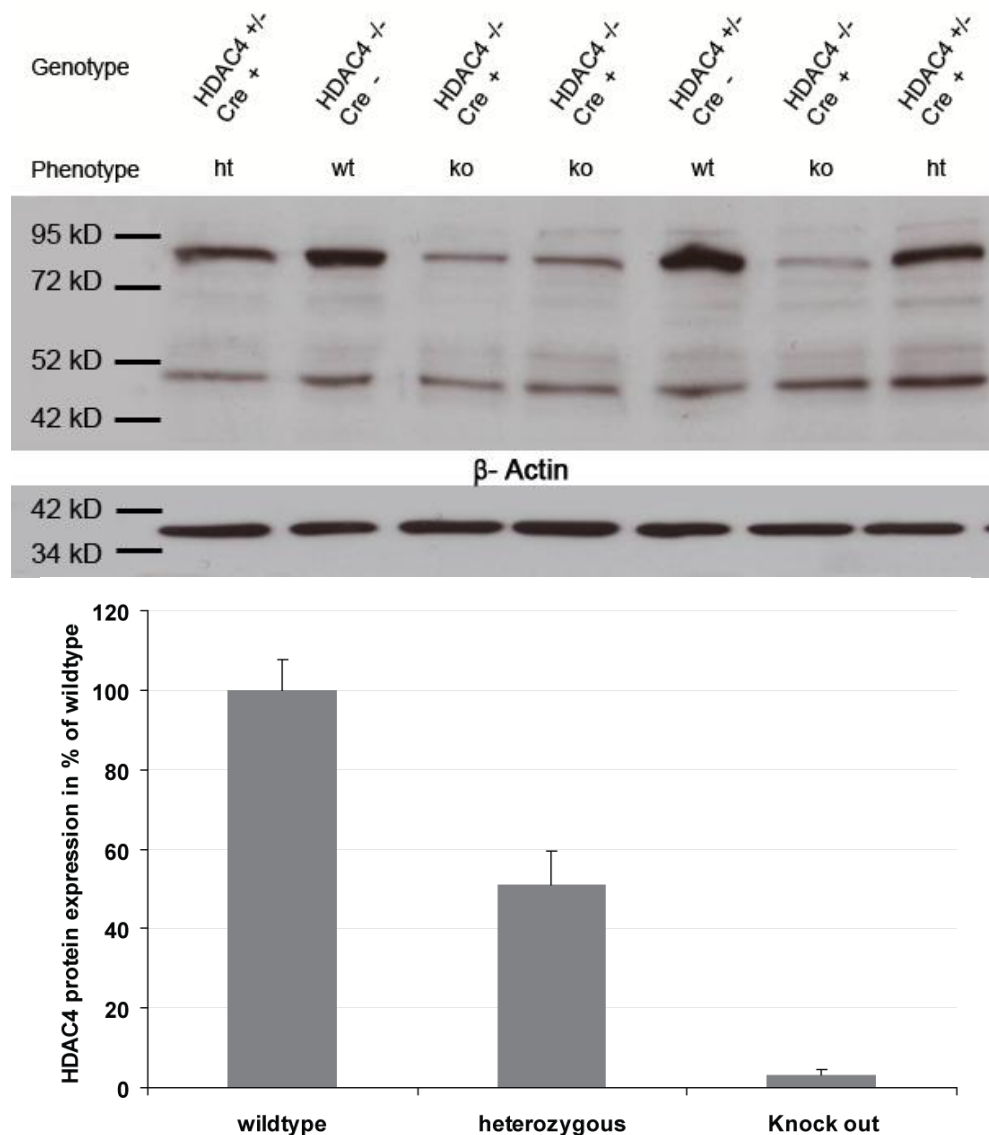
Figure 4.40. HDAC4 immunoblot of E13.5 brain tissue of the CIMH4 mouse line. Antibodies: HDAC4 (Santa Cruz), ß-Actin (Sigma). Quantification of immunoblot results through pixel density.

4.2.2.1.1 Strong reduction of HDAC4 protein levels in embryonic brain and spinal cord of HDAC4 conditional knock-out animals at E 15.5

In E 15.5 animals, both in spinal cord and brain, the amount of HDAC4 protein was clearly reduced in conditional mutant animals in a dose-dependent fashion. Unfortunately there were no wildtype littermates to compare the mutant animals to, but

the reduction in a full mutant to a wildtype is still obvious. The amount of protein is less drastically reduced than in E13.5 brain (**Figure 4.41**), but this can be due to dissecting differences between brain and spinal cord. If there was more meningeal tissue left on the dissected spinal cord, this could already explain the higher content of HDAC4 protein compared to brain.

Figure 4.41. HDAC4 immunoblot of E15.5 spinal cord tissue of the CIMH4 mouse line. Antibodies: HDAC4 (Santa Cruz), ß-Actin (Sigma). Quantification of immunoblot results through pixel density.

A clear reduction of HDAC4 protein levels could also be observed in brains of E 15.5 mutant animals, compared to wildtypes (**Figure 4.42**). The quantification of the blot seems to reveal elevated protein levels in heterozygous embryos, this is however an

artefact due to a very weak actin staining in two of the heterozygous samples, which can be caused for instance by an inhomogeneous distribution of antibody of ECL detection solution.

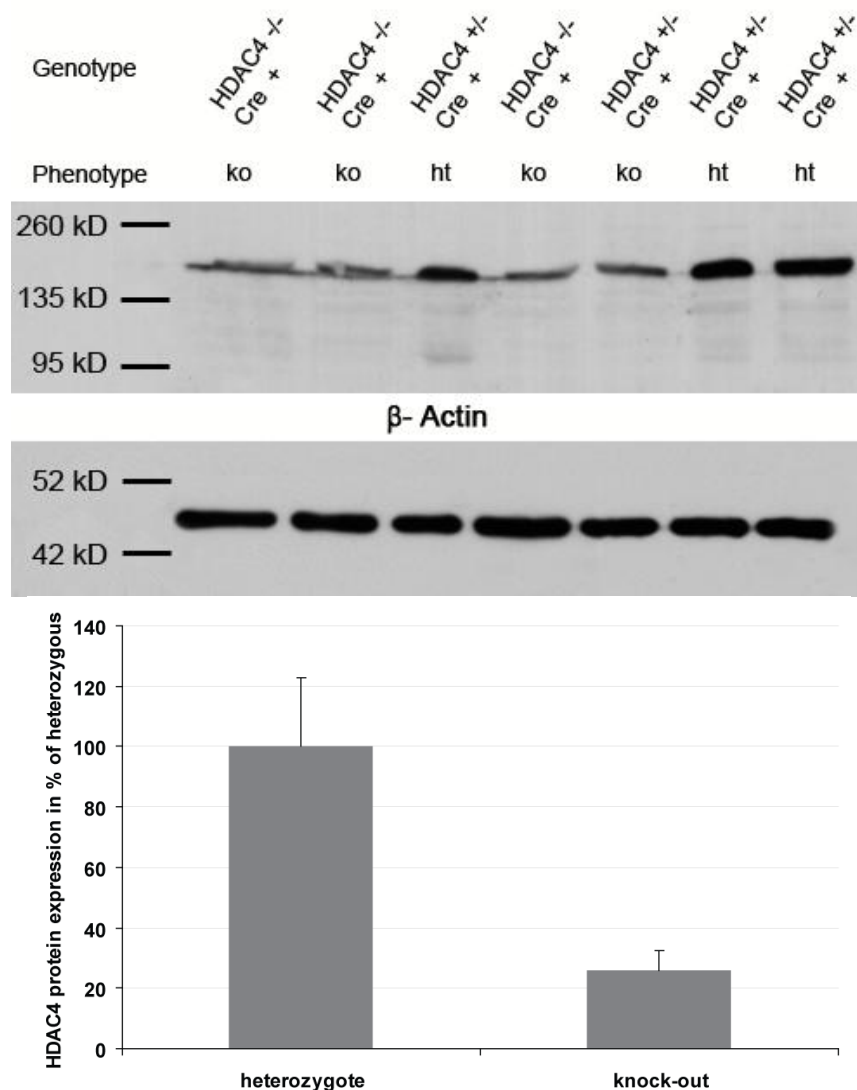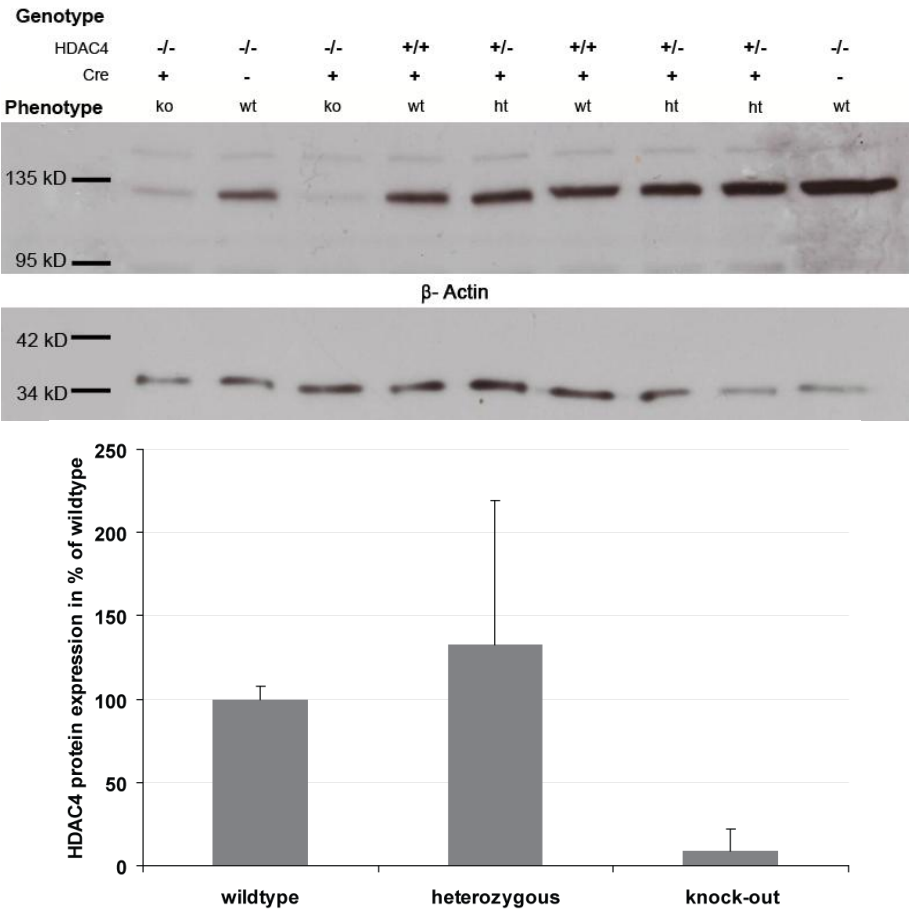**Figure 4.42. HDAC4 immunoblot of E15.5 brain tissue of the CIMH4 mouse line.** Antibodies: HDAC4 (Santa Cruz), ß-Actin (Sigma). Quantification of immunoblot results through pixel density.

4.2.2.2   Effect of HDAC4 knock out on proliferation in the ventricular zone of the cortex

Since the expression analysis of HDAC4 in embryonic brain revealed that HDAC4 is present mainly in neurogenic regions of the forebrain, I decided to investigate the effect on cell proliferation in mutant embryos. To investigate this, cryo-sections derived from wildtype and knock-out embryos for HDAC4 were immunostained with an antibody for the mitosis marker pH3 and the subsequent counting of cells in the cortical ventricular zone (**Figure 4.43**).
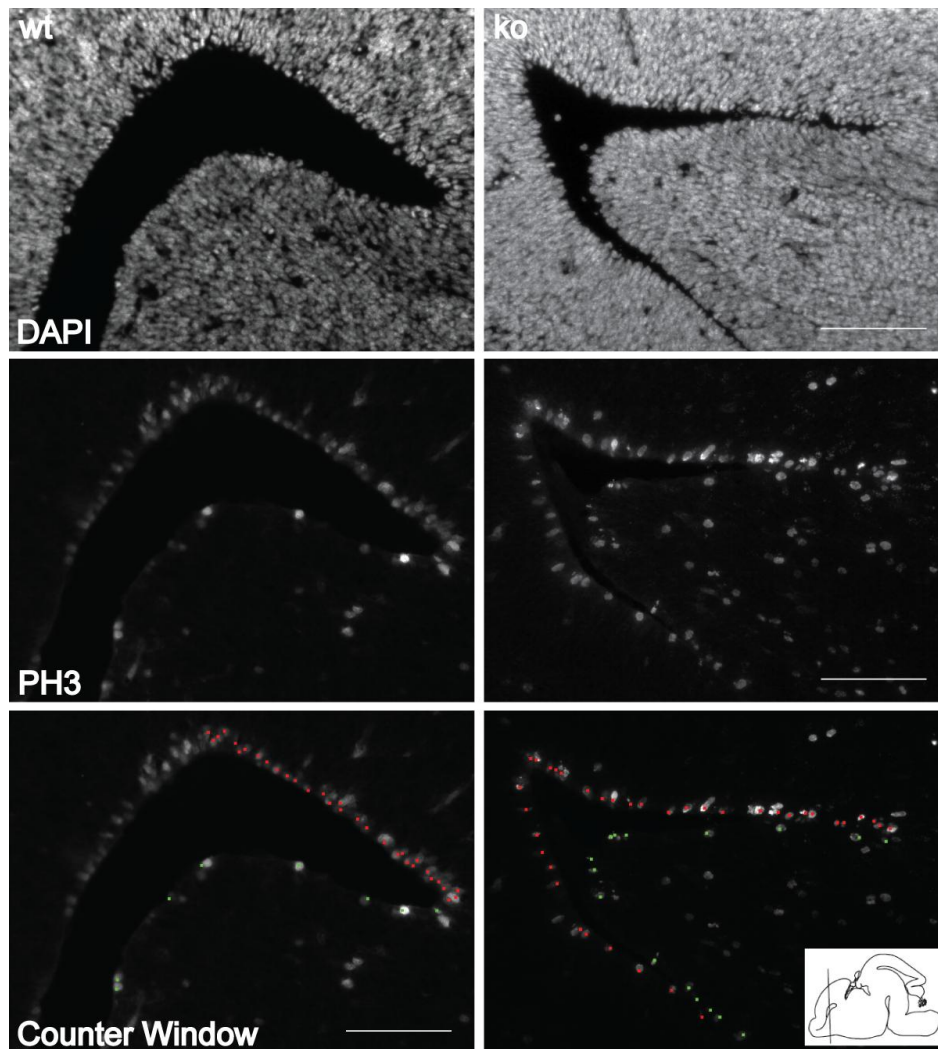
Figure 4.43. Immunostaining for PH3 positive cells on coronal hemisections of HDAC4 mutant mice and wt littermates at E 15.5. Mitotically active cells line the ventricle. Small orientational image from (Ohtsuka et al 2001). Scalebar 100 μm

I observed a decrease in PH3 positive cells in the HDAC4 conditional mutant mice in the anteriormost region that I examined. The difference cannot be observed in the more posterior sections of the brain.

4.2.2.3   Effect of the HDAC4 conditional knock-out on cell proliferation of *non-surface dividing* cells

Intermediate progenitor cells of the subventricular zone of the developing cortex are progenitors for both neurons and macroglia. They specifically express the transcription factor Tbr2. In order to analyse the impact of the conditional knock-out of HDAC4 on intermediate progenitor cells, sections of mutant and wildtype brains were stained for Tbr2 and ß-tubulin III (TuJ1).

The results of these stainings are presented in **Figure 4.44** to **Figure 4.46** which represent different coronal planes of examination from rostral (**Figure 4.44**) to caudal (**Figure 4.46**).
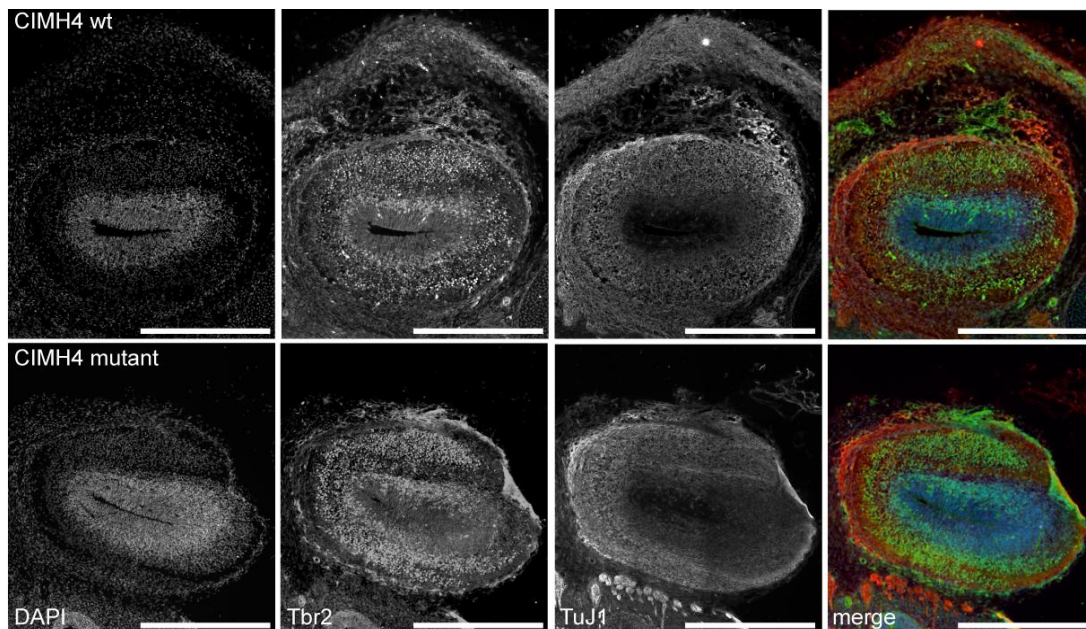
Figure 4.44. Hemicoronal sections of E15.5 HDAC4 wildtype and mutant brain. Immunostaining with antibodies for Tbr2 and TuJ1, nuclear stain with DAPI. Scalebar 500 µm
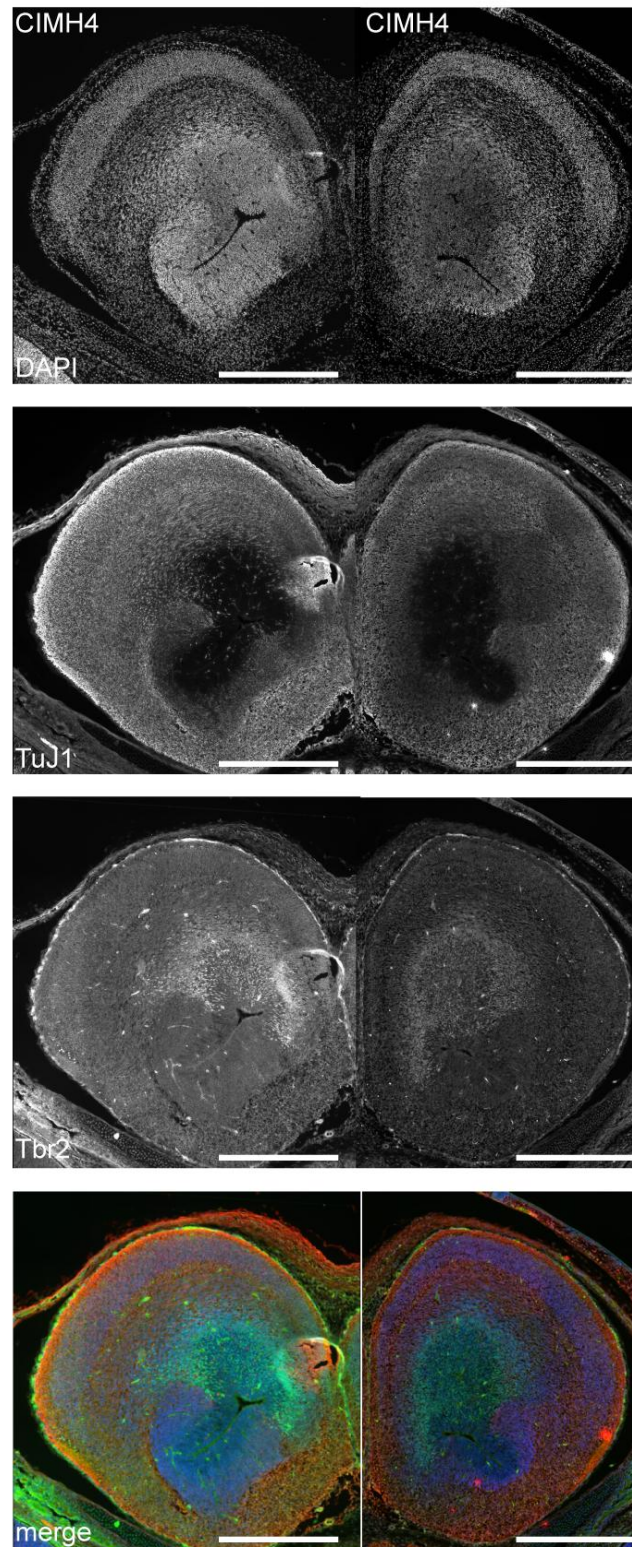
Figure 4.45. Hemicoronal sections of wildtype and HDAC4 mutant brain stained for Tbr2 (intermediate progenitors) and TuJ1 (neurons) Scalebar 500 μm
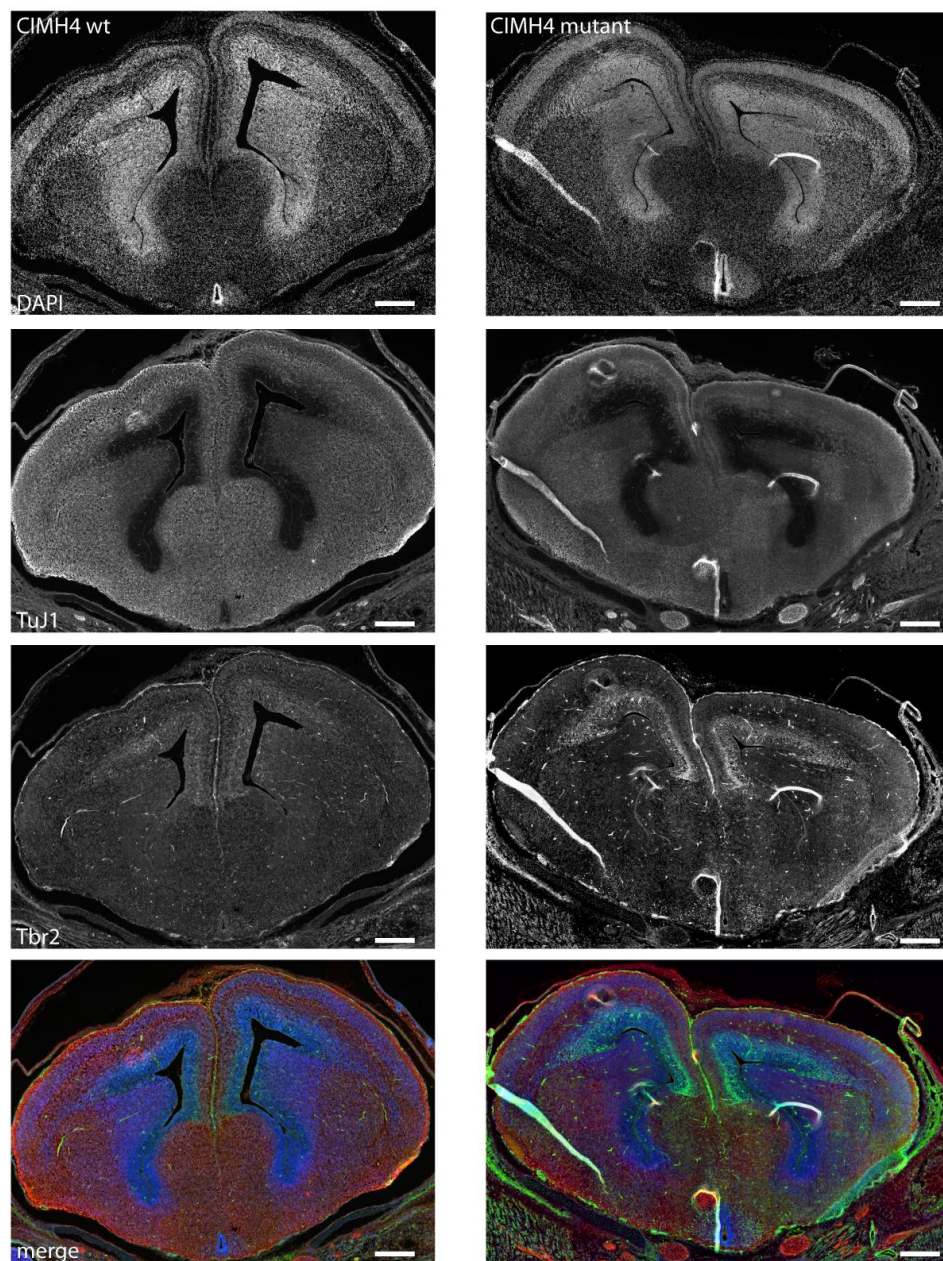
Figure 4.46. Hemicoronal sections of wildtype and HDAC4 mutant brain stained for
Tbr2 (intermediate progenitors) and TuJ1 (neurons). Scalebar 500 μm

No changes could be observed in expression pattern of Tbr2 or Tuj1 or in the number of
cells stained. This was however not quantified in any way, which should be done in
order to get a conclusive result. The location of the staining was equal in both wildtype
and mutant as well as the amount of cells stained. It seems that there is no difference in
the pool of basal progenitors in HDAC4 conditional mutants.

4.2.3   Analysis of HDAC5 mutant mice

4.2.3.1   X-Gal staining for HDAC5 to confirm absence of HDAC5 protein in mutant embryonic brain

Absence of HDAC5 in transgenic embryos could not be determined via immunoblotting. The *LacZ* cassette knocked into the HDAC5 locus impairs the expression of intact protein, but provides a marker for cells in which the protein would normally be expressed. Heterozygote animals show a far less intense staining than homozygous mutants. Staining is only shown in the absence of functioning HDAC5 protein, therefore the staining in HDAC5 null mice is stronger than in heterozygous animals with one HDAC5 allele still intact (**Figure 4.47**). Comparing different coronal sections from E 15.5 brains, heterozygous animals show indeed weaker staining than mutants. The subcellular distribution of HDAC5 expression has already been discussed previously.
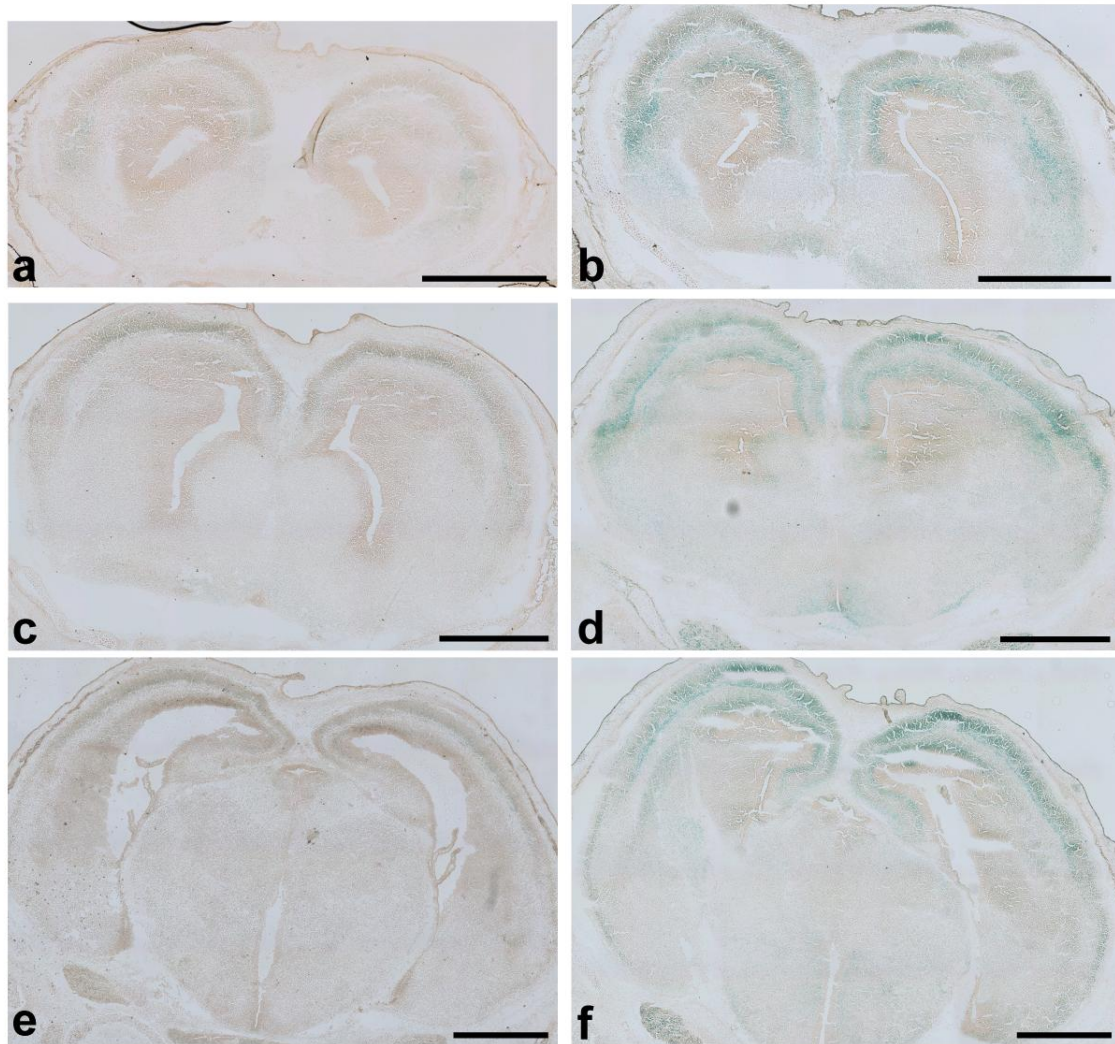
Figure 4.47. X-Gal staining on coronal brain sections of E 15.5 HDAC5 heterozygote (a,c,e) versus mutant (b, d,f) embryos confirms absence of HDAC5 in mutant brains Scalebar 500 µm

4.2.3.2   Investigation of layer formation in HDAC5 mutant mice

In our expression analysis of the subcellular distribution of HDAC5 expression in embryonic brain, the cortical plate showed high expression levels of HDAC5. Therefore we were curious whether there were any changes in cortical layering that could be observed in mutants of HDAC5. The cortical plate is known for its instructive role for the formation of the laminar structure of the cerebral cortex (Frotscher et al 2009,

Sekine et al 2011). Therefore we decided to investigate cortical layering early postnatal stages of HDAC5 null mice.

To this end, the brains of early postnatal mice (P8) were sectioned coronally and stained with markers for different cortical layers.

The transcription factor Pax6 is highly expressed in apical progenitors residing in the VZ from the earliest stages of corticogenesis. Therefore, its expression can be a marker for this layer in developing cortex. Unfortunately the Pax staining has not worked out, so that there is only an overall background signal to be observed (**Figure 4.48**).
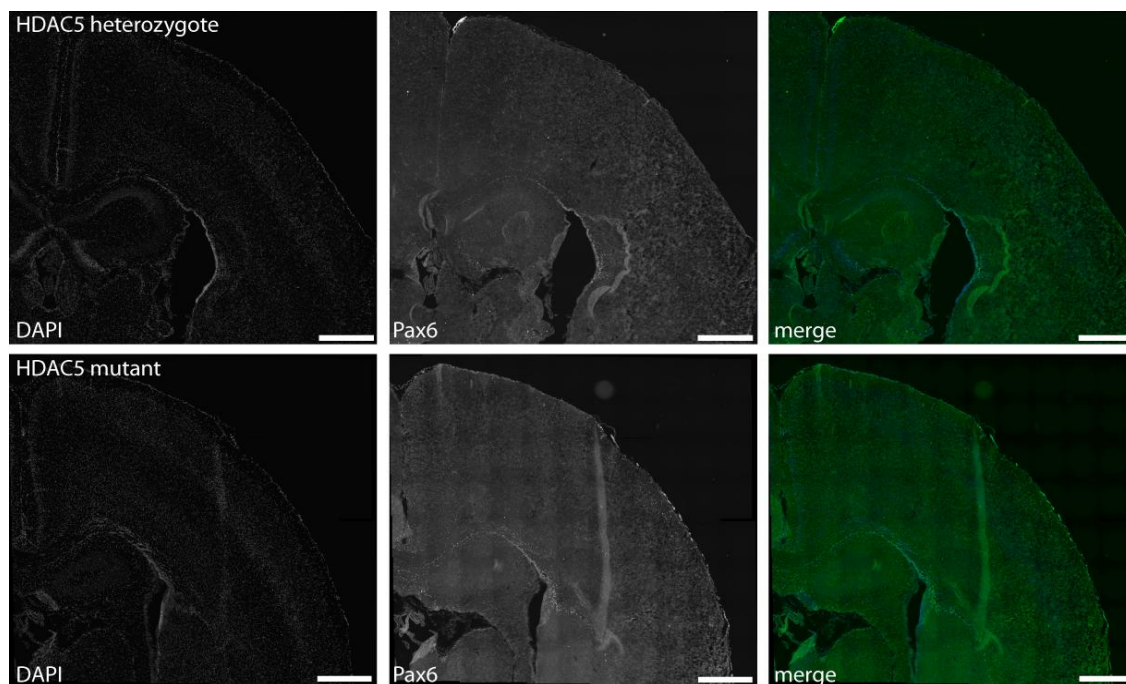
Figure 4.48. Immunostaining for Pax6 to reveal the impact of the absence of HDAC5 on apical layers of the cortex. Scalebar 100 µm

The zinc-finger transcription factor Ctip2 is a marker for the outer layers of the cortex. It is expressed by subcortically projecting neurons in layer 5. Here, a strong staining was only observed in hippocampus. Both heterozygous and mutant brain did not show a strong an discrete staining of the outer layers (**Figure 4.49**). Since no wildtype littermate was available for comparison, it is now unclear whether the lack of staining is a relevant effect of the absence of HDAC5 or due to experimental conditions. All stainings should be repeated with a wildtype brain as control.
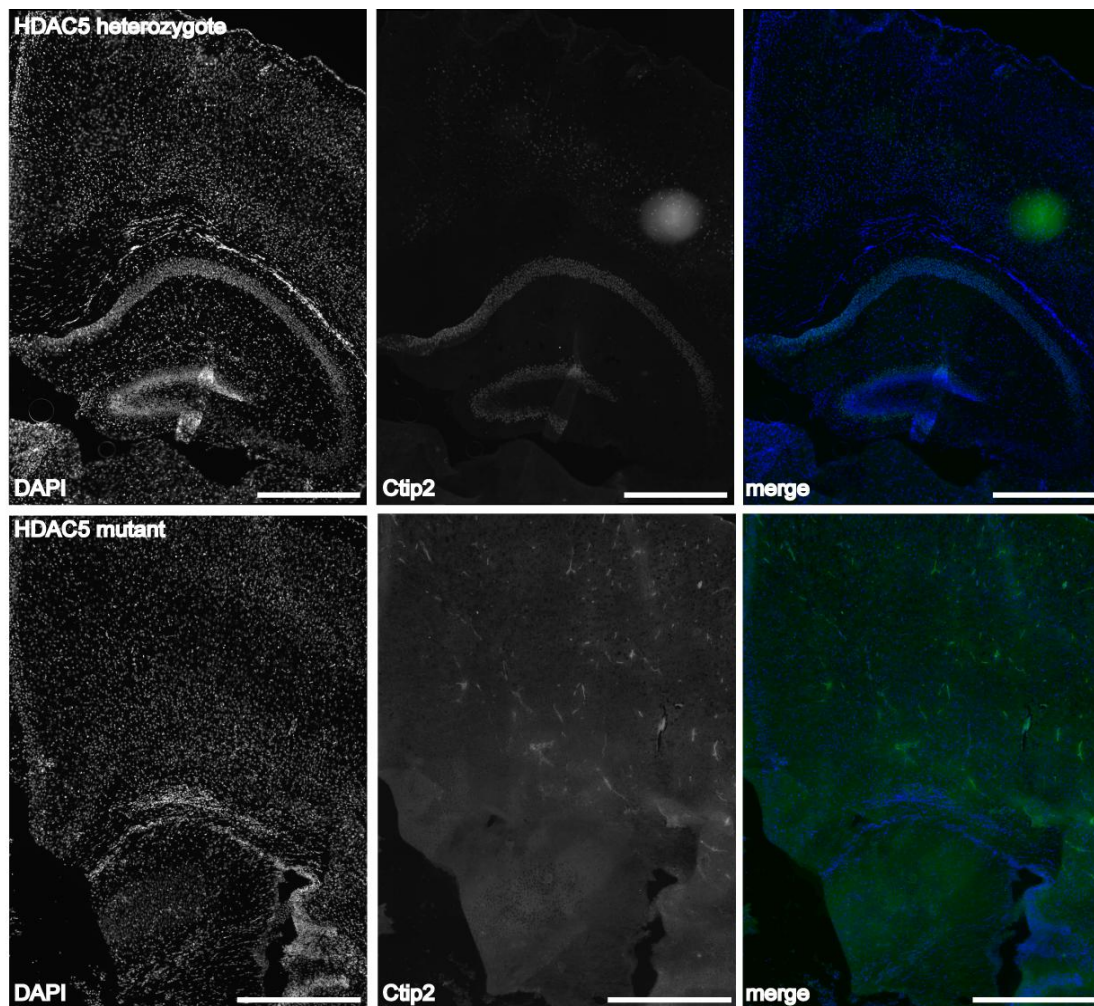
Figure 4.49. Immunostaining of Ctip2 in coronal hemisections of HDAC5 heterozygote and mutant mice. Scalebar 500 μm

SatB2 (Special AT-rich sequence-binding protein 2) is expressed in upper cortical layers. The staining for SatB2 did not differ between wildtype and mutant brain (**Figure 4.50**).
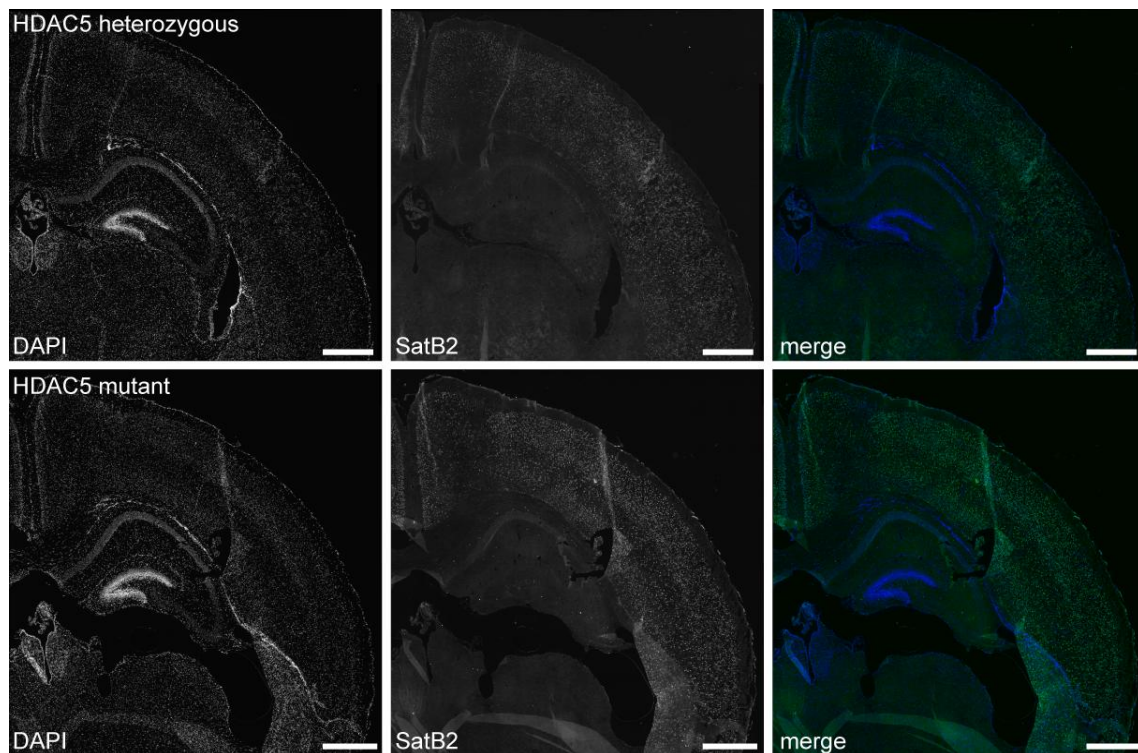
Figure 4.50. Immunostaining of SatB2 in coronal hemisections of HDAC5 heterozygote and mutant mice. Scalebar 500 µm

Reelin is a large secreted glycoprotein of the extracellular matrix. It is secreted by Cajal-Retzius cells in hippocampus and developing cortex. In the prenatal and early postnatal brain, reelin is expressed in the marginal zone. A staining of the outermost layer of the cortex could be observed in both wildtype and mutant. The staining did not differ between wildtype and mutant (**Figure 4.51**).
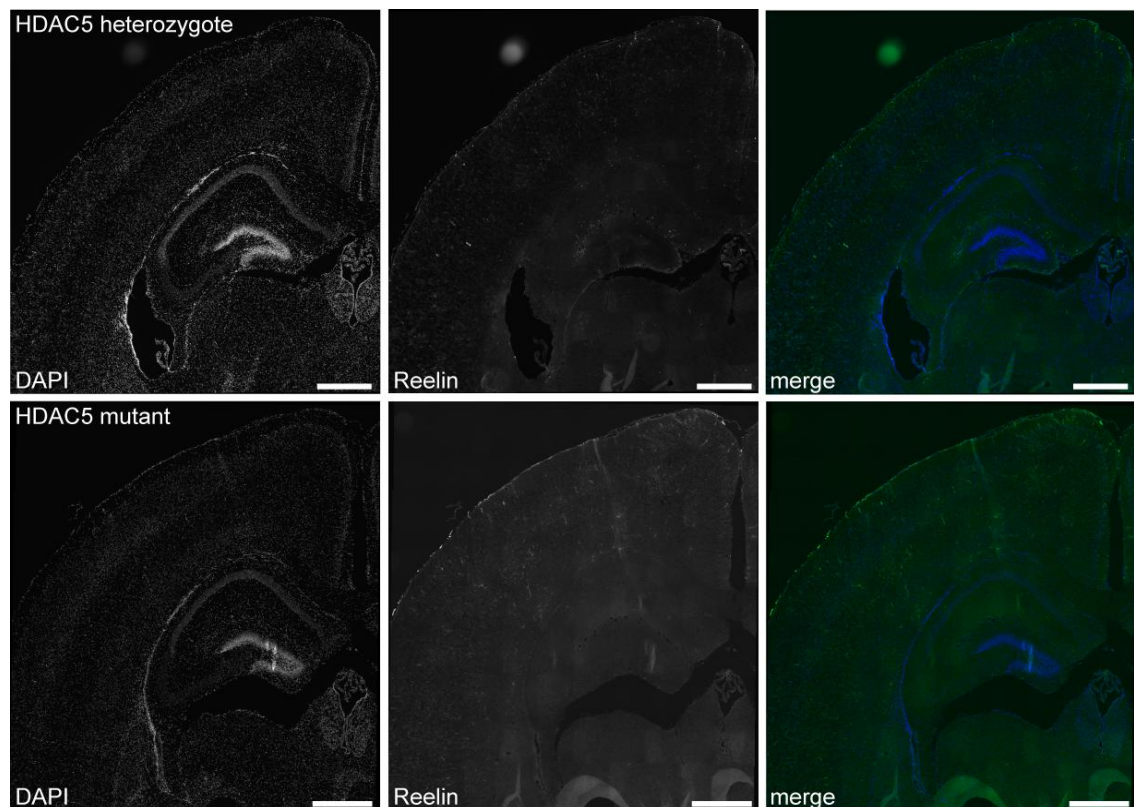
Figure 4.51. Immunostaining of Reelin in coronal hemisections of HDAC5 heterozygote and mutant mice. Scalebar 500 μm

Taken together, the immunostainings on early postnatal brain sections of HDAC5 mutant mice did not reveal any difference in layer formation between mutant and wildtype mice. This could be due to the bad quality of the stainings and images or barely to the fact that absence of HDAC5 does not have an impact on cortical layer formation.

5   Discussion

5.1   Analysis of the role of class I and II HDACs in neuro- and gliogenesis in embryonic mouse brain *in vitro*

We had previously shown that a large number of HDACs is expressed in neural progenitor cultures prepared from E 15.5 GE. However, it was not clear which HDACs are expressed *in vivo* in different brain regions and whether there was any change in HDAC expression over time. Therefore, quantitative real time RT-PCR analysis was performed on total RNA lysates from embryonic brain regions dissected at two different developmental ages to analyze expression of HDAC1, -2, -3, -4, -5, 7a, -8 and -9. Expression of all examined HDACs could be confirmed at both E 13.5 and E 15.5, but there were obviously differences in expression levels.

At E 13.5 HDAC2 showed the highest expression in all brain tissues, HDAC3 the second highest and HDAC1 the lowest. When comparing the expression level not only among the individual HDACs, but also between brain regions, HDAC1 showed to have a much higher expression in hippocampus than in cortex and GE. This might hint to a specific role of HDAC1 in the hippocampus. Although HDAC1 and -2 show very high sequence similarities, they were found to be expressed in different patterns in the brain (MacDonald & Roskams 2008).. At the same time, expression of HDAC5 is more than 3-fold higher in striatum and almost 3-fold higher in the cortex than in the hippocampus.

At E 15.5 HDAC3 showed the highest expression level in cortex and hippocampus, in striatum both HDAC2 and -3 were highly expressed. In line with the E 13.5 data, HDAC1 and -2 expression was higher in the hippocampus than in cortex and GE. Also, HDAC5 expression was higher in the cortex than in the hippocampus. Although the standard deviations are high and it is difficult to draw a conclusion, this could also point to a role for HDAC5 in cortex and hippocampus.

This analysis provides a summary of HDAC expression in different regions of the developing brain. Individual differences in expression levels might hint to a specific role of the respective enzyme in the area of high expression.

5.2   Inhibition of HDACs *in vitro* to determine their role in neuro- and gliogenesis

5.2.1   Reduction of neurogenesis in culture upon HDAC inhibition wih TSA

Neurosphere cultures from the developing mammalian forebrain provide a relatively uniform population of neural precursor cells, from which both neurons and microglia can be derived. Here, neurosphere cultures generated from the medial and lateral ganglionic eminences of E15.5 C57BL/6 mice were used to study the effect of HDAC inhibition on neurogenesis *in vitro*. The cultures were plated out to differentiate and treated with 10 nM or 50 nM trichostatin A for different time intervals (3 – 24 h) before collection of RNA or protein or fixing the cells for immunocytochemistry or FACS. TSA belongs to the hydroxamic acid group of HDAC inhibitors and inhibits all class I and II HDACs by binding reversibly to their deacetylase domain. .

When cells were treated with TSA for 12 h (DIV 1.5 to 2.5) and left to differentiate for other 5 days, neurogenesis was reduced to less than 50% of the control. This corresponds to our previous findings both *in vitro* and *in vivo*. TSA had the same effect on embryonic neurogenesis *in vivo* when it was injected in pregnant females from E13.5 to E14.5. Along with the reduction of neurogenesis in the GE, also the number of GABA-positive cells derived from GE and undergoing tangential migration in the cortex was reduced (Shaked et al 2008). In previous *in vitro*-experiments, neurogenesis in GE was shown to be drastically reduced; possibly, the smaller extent of reduction shown here is due to experimental variation. However, the reduction could be verified *in vitro*.

The increase in astrogliogenesis we reported previously could not be observed in these experiments although it showed to be a very robust and reproducible effect (Shaked et

al. 2008). This also speaks for an unexpected variation in these experiments and that they should be repeated.

5.2.2   Quantification of neurogenesis in adherent neurosphere cultures by FACS analysis

In order to quantify neurogenesis more efficiently and in an unbiased manner, a FACS protocol for fixed cells was established. The protocol allows for culturing neural progenitors in adherent cultures, then detaching them from the surface, fixing and staining them with a ß-tubulin III antibody. The protocol proved to be very robust and reliable in quantifying neurogenesis in differentiated neuroshere cultures. It confirmed the results of the conventional immunostainings and subsequent counting of stained cells on coverslips. Also with FACS, a dose-dependent effect of TSA treatment on neurogenesis could be observed. It is a novelty to quantify neurogenesis with an internal antibody staining in fixed cells by FACS; usually surface epitopes are chosen as markers and live cells are used for cytometry. The FACS protocol provides an efficient tool to analyze neurogenesis in our culture system and could perhaps also be applied for other experimental questions and markers.

5.2.3   HDACs influence neurogenesis on a transcriptional level

In order to elucidate by which signaling mechanism HDACs influence the generation of neurons and glia in the embryonic brain, we investigated signaling pathways known to be involved in these processes. Since we expected HDACs to influence neuro- and gliogenesis on a transcriptional level, real time RT-analysis was performed to examine transcription of genes known to be involved in neuro- and astrogliogenic developmental programs. BMPs had been shown to promote astroglial lineage commitment *in vitro* (Gross et al 1996) and *in vivo* (Bonaguidi et al 2005); therefore I measured gene expression of a number of genes involved in this pathway in TSA-treated neurosphere cultures. Also, we saw previously that adding inhibitors of BMP2/4 signaling (Noggin and Alk3-ECD) to differentiating neurosphere cultures, did not show any effect on neurogenesis. However, in the TSA treated cultures, these inhibitors restored normal levels of neuro- and astrogliogenesis (Shaked et al 2008).

Upon inhibition of HDACs Bmp2 was transcriptionally upregulated, especially after 6 h of treatment, while Bmp4 showed a downregulation. No changes could be observed in the transcription levels of Bmp receptors 1a, 1b and 2. Smad7, however, which negatively regulates Bmp2/4 signaling, showed a drastic downregulation. Both the upregulation of Bmp2 and the downregulation of Smad7 point to the possibility that inhibition of BMP signaling is released by TSA. I could also observe a robust upregulation of the transcription of Stat1 and Stat3, which was more prominent at later time points of observation (12 h treatment). Stat3 is an upstream regulator of Bmp expression (Fukuda et al 2007) and co-regulates astrocyte-specific genes through the formation of a STAT3-p300-Smad complex (Nakashima et al 1999). The increase in Stat3 expression therefore corresponds to our observation of an increase in premature astrogliogenesis in TSA-treated cultures along with the decrease in neurogenesis. Expression of Ngn1 is also upregulated up to 3-fold upon HDAC inhibition. Ngn1 is known to promote cortical neurogenesis.

Neurosphere cultures were also treated with 10 ng/ml BMP2, to determine the effect of BMP2 on transcription levels. BMP2 did not increase its own expression, but decreased the one of Bmp4 as TSA did. In contrast to TSA which was downregulating Smad7 expression, BMP2 strongly upregulates the negative regulator of BMP2/4 signaling. Stat3 was upregulated with TSA and BMP2 treatment at all observed time points. This effect could also be observed in luciferase assays. A Smad binding motif drives the expressiong of firefly luciferase. BMP2 treatment led to a strong luciferase signal reflecting a strong upregulation of BMP2/4 signaling. TSA however first decreased the activity and subsequently upregulated it. The response to BMP2 treatment also occurred much earlier than the one of TSA, suggesting an indirect effect of HDACs on BMP2/4 signaling.

We could show that different levels of acetylation upon HDAC inhibition can promote different transcriptional outcomes.

5.2.4   Protein translation is necessary to upregulate BMP2 expression upon TSA treatment

To elucidate which genes' expression levels are directly or indirectly regulated by HDACs, additionally to the differentiation protocol and treatment with TSA, protein translation was blocked in neurosphere cultures and the expression of Bmp2, Bmp4 and Stat3 determined again through real time RT-PCR after 3 h of treatment with TSA. Cycloheximide (5 µg/ml) was used to block translation and added 1 h before TSA treatment was started. Bmp2 expression was not upregulated as strongly in the presence of cycloheximide (CHX). This implies that HDACs influence transcription of Bmp2 via a factor which has to be transcribed in order to act upon Bmp2 expression. Also the downregulation of Bmp4 did not occur as observed before without inhibition of translation, so the same holds true for Bmp4 expression. Interestingly, CHX did not inhibit the upregulation of Stat3 expression upon HDAC inhibition. Probably the expression of Stat3 is regulated by HDACs directly on the chromatin level; perhaps Stat3 expression is repressed through deacetylation of the Stat3 promoter. It could be that Stat3 is upstream of Bmp2 in mediating the effect of HDACs on neurogenesis.

5.2.5   Microarray analysis of pathways potentially involved in HDAC influence on neurogenesis

To elucidate the signalling involved between HDACs and neurogenesis, we have performed microarray expression profiling on BMP2- and TSA-treated cultures, followed by validation of the findings with quantitative RT-PCR and protein analysis. Since this work was done in collaboration with Dr. Catharina Scholl and she performed much of the data analysis, I will not discuss the findings in detail (Scholl, Weissmuller et al. 2012).

TSA- and BMP-treated cultures showed different transcriptional responses, which would also be expected. However, we observed an overlap in genes regulated by the treatments, especially when comparing not the same treatment intervals but BMP2 6h and 24 h with TSA 24 h for example. Many genes involved in Bmp2/4 signaling could be observed at this intersection (e.g. Bmp4, Smad7, Follistatin and Bambi). BMP2 and TSA treatment resulted in independent gene expression profiles, the downregulation of

genes seems to reflect the similar phenotype seen after both treatments. Only few primary target genes of TSA and BMP2 clustered together, but many genes involved in neural development were present.

We assume that genes regulated after 6 h of treatment directly reflected the well-established activity of HDAC inhibition on gene regulation, but that after 24 h already a secondary biological effect might have been observed. The stronger correlation in the 24 h gene expression data set between TSA- and BMP2-treated cultures reveals that even if the early gene expression response to the treatment differs dramatically, similar downstream processes are involved which lead to a similar change in the cell fate of treated cells. As observed in real time RT-PCR previously, an upregulation of Stat3 and its active, phosphorylated form could be observed at the protein level. This corresponds to the increase in astrogliogenesis observed in our experiments as well.

5.3 RNA interference to dissect which HDAC family member(s) influence neuro- and astrogliogenesis

5.3.1 Real time RT-PCR analysis of shRNA-mediated knockdown of HDAC1, -2, -4, and -5

RNA interference was used to dissect which of the class I and II HDAC family members inhibited by TSA mediate the effect on neuro- and astrogliogenesis. For HDAC 1, -2, -4, and -5 five shRNA oligos were bought from Sigma Aldrich to knock down expression of the individual enzymes. Effective knockdown of the expression of HDACs 1, 2, 4 and 5 was observed at the mRNA level; however, all examined oligos against the HDACs also influence expression of other non-target HDACs. This is obviously not a good starting point to examine the role one individual enzyme plays. It is still unclear why the shRNA oligos directed against one HDAC showed a broad and rather unspecific effect also on other family members. It would have perhaps been not surprising if HDACs with high sequence similarities and which might have similar redundant roles in the CNS were influenced by each other's knockdown. Here, all shRNA oligos generated against one HDAC also up- or downregulated more than one

other, not always closely related HDAC. It is known that siRNAs can have off-target effects totally unrelated to their actual target mRNA (Scacheri et a. 2004). Those off-target effects are speculated to be due to partial sequence matches to other sequences and a microRNA-like regulation (Scacheri et al. 2004). There are also many sensor motifs recognizing foreign RNA molecules in cells which could initiate subsequent off-target effects (Olejniczak et al. 2010). In this case, I believe that the changes could also be explained by unfavorable conditions in the cells due to the viral infection. Many improvements to the protocol were made in order to reduce unfavorable conditions as much as possible, but with very limited success. The cells usually displayed a different morphology compared to untreated cultures and had an unhealthy appearance. Purification of the virus preparation with a sucrose pellet, using an endotoxin-free plasmid preparation kit did not seem to have a large impact on the cells. Coating of the culture dishes with poly-L-lysine reduced detachment of cells after the first round of virus harvesting.

5.3.2 Confirming HDAC2 knockdown on the protein and the cellular level

For further investigations, HDAC2 was chosen as a candidate gene because of its high expression levels in embryonic brain, especially in GE and cortex, and because it was shown to play a role in several brain functions. HDAC2 negatively regulates memory formation (Guan et al 2009) and is found at higher expression levels in the brain and spinal cord of patients suffering from amyotrophic lateral sclerosis (ALS) (Janssen et al. 2010).

We analyzed knockdown of HDAC2 because we knew HDAC2 to be ubiquitously expressed in brain, especially in GE and cortex, and since it was shown to play a role in several brain functions. It negatively regulates memory formation (Guan et al 2009) and can be found in higher levels in the brain and spinal cord of patients suffering from amyotrophic lateral sclerosis (ALS) (Janssen et al 2010).

5.3.2.1 Knockdown of endogenous HDAC2 in neurospheres –immunoblot analysis 4 days after infection

Knockdown of HDAC2 was assessed in neurosphere cultures and in a permanent cell line (293T) to determine the efficiency of the shRNA oligos for knocking down HDAC2. Neurosphere cultures were infected with lentivirus carrying shRNA against HDAC2 and cell lysates prepared 4 days or 7 days after infection. The protein was separated by PAGE and subsequently analyzed though western blotting.

HDAC2 protein levels were decreased in infected cultures in a dose-dependent manner both after 4 and 7 days. However, in cultures infected with scrambled shRNA virus, HDAC2 protein level was also decreased compared to uninfected cultures. According to this result, knockdown of HDAC2 in neurosphere cultures leads to a reduction of protein levels to 50% or even 30% of control; at the same time the viral infection itself already decreases the expression of the protein, probably because the cell is in a stressed, unfavorable state.

5.3.2.2 Knockdown of endogenous HDAC2 in 293T cells

In order to control the knockdown capacity of the lentivirus generated, I went back to the original pLKO.1-puro plasmids purchased from Sigma. These were transfected into HEK293T cells which were cultured for 4 or 6 days. Lysates were prepared and subjected to western blot analysis. A co-transfection with GFP served as a control for transfection. In this experiment no reduction of HDAC2 protein could be observed. This could be due to low transfection efficiency and a therefore not detectable change in protein levels. According to GFP fluorescence in the cultures, the transfection efficiency did not seem to be low. To be able to draw a sound conclusion, the experiment should be repeated.

5.3.2.3 Knockdown of HDAC2 in neurosphere-derived cultures

To determine knockdown of HDAC2 on protein level, immunocytochemistry was applied. Neurosphere cultures were plated out for differentiation and infected with lentivirus. Cells were fixed and stained 4 days after infection, photographs taken and the fluorescence intensity of HDAC2 in nuclei measured with Metamorph software.

Although all nuclei were positive for HDAC2, no reduction in HDAC2 fluorescence intensity could be observed in infected cultures with shRNA against HDAC2 compared to control. However, since I measured the overall HDAC2 fluorescence in all nuclei in the cultures, this could dilute a knockdown effect seen on the individual cell level. In order to determine the knockdown on the cellular level only cells which are actually infected should be analyzed. Therefore, the experiment should be repeated using a reporter for infected cells and the degree of knockdown determined only in those.

The amount of neurons in the cultures did not change between HDAC2 knockdown and controls. This would also be expected because no difference in HDAC2 protein levels could be observed.

5.3.2.4   Knockdown of HDAC2 in hippocampal cell cultures

Knockdown of HDAC2 was also assessed in hippocampal cultures. The cells were infected, then fixed and stained 4 days after infection. Immunocytochemistry was performed using antibodies to detect HDAC2 and GFP to determine the number of infected cells. HDAC2 fluorescence levels were measured with Metamorph. Just as in neurospheres, no reduction in HDAC2 protein levels could be observed in the cultures. Since the GFP staining revealed that only very few cells were infected in the cultures, this is not surprising and also supports the assumption that in the neurosphere experiment the same was true and very few cells were infected.

5.3.3   Immunostaining to reveal the progeny of infected precursors

I wanted to assess whether the reduction in HDAC2 protein level had a consequence on the cellular composition of the cultures after differentiation. If HDAC2 knockdown led to a change in neuro- and gliogenesis, the cellular composition of the culture should reflect this difference. Immunocytochemistry stainings were performed with antibodies against EGFP to detect infected cells, TuJ1 to stain for newborn neurons or GFAP to stain astrocytes. The neurospheres were cultured for 4 days or 7 days to allow for differentiation to occur.

The infection rate in the cultures was very low also in this experiment. Very few infected cells were co-stained for GFAP, none of the infected cells was positive for TuJ1. This could suggest that HDAC2, in infected cells, shifts the developmental outcome towards glia instead of neurons. However, since the infection rate was so low, it is difficult to draw any conclusion and further experiments should be carried out.

At both time points, 4 days and 7 days after transfection, no change could be observed in the cellular composition of the cultures compared to controls. This could either be because HDAC2 does not influence neuro- or gliogenesis or because infection rates were so low, that eventual, subtle changes in the cellular composition could not be measured.

To conclude the HDAC2 knockdown experiments it can be said that shRNA against HDAC2 led to a knockdown both on transcriptional and protein level. On protein level, the knockdown was shown to be dose-dependent. The highest concentration of lentivirus led to a reduction of HDAC2 protein to about 30% of controls. On the RNA level an unspecific influence on the expression of non-target HDACs was observed. It is not clear whether this is the result of off-target effects of the shRNA sequence or, what is perhaps more probable, that virus infection leads to detrimental effects on the cells thus leading to the observed variability in the expression of non-target family members.

On a cellular level, it was observed that none of the infected cells co-stained for TuJ1, but some were positive both for EGFP and GFAP. This could suggest that inhibition of HDACs prevents the cells from becoming neurons. This would be corresponding to the finding of MacDonald et al. that HDAC2 expression is initiated in a subset of mitotic stem/progenitor cells and appears to be up-regulated as the progenitors commit to a neuronal lineage. HDAC2 expression could not be detected, however, in the majority of glia (MacDonald and Roskams 2008). This could suggest a role of HDAC2 in the fate decision of progenitor cells towards neurogenesis. However, assessment of the progeny of infected precursor cells did not reveal any change in cell fate decision. This could be due to the low infection rate which might prevent subtle changes from being detected, but it also could just be due to the fact that reduction of HDAC2 protein levels does not

have an influence on the decision of a progenitor cell to become a neuron or an astrocyte.

5.4   Developmental phenotype of the CNS of HDAC4 and HDAC5 transgenic mice

The recent generation of knockout models for different HDACs has opened up new possibilities to investigate their function *in vivo*. Transgenic mice provide a powerful tool to study the role of the enzymes in the organism and at different developmental stages.

The class II family members HDAC4 and HDAC5 were found to be highly expressed in brain (Grozinger at al. 1999, Majdzadeh et al. 2008). As opposed to class I HDACs, class II HDACs are expressed in more restricted patterns. They are assumed to influence protein deacetylation by binding to class I HDACs. HDAC4- and -5 null mice were recently generated in the group of Eric N. Olson and extensive analyses of the postnatal phenotype carried out. Majdzadeh and colleagues found that the brains of HDAC4 null mice were 40% smaller than the ones of wildtype littermates. The cortical hemispheres as well as the cerebellum were reduced in size (Majdzadeh et al. 2008).

HDAC4 was found to protect cerebellar granule neurons against low potassium-induced apoptosis and to particularly protect cortical neurons from 6-hydroxydopamine-induced neurotoxicity. The neuroprotective effect is independent of the deacetylase activity of the enzyme (Majdzadeh et al 2008).

Since the Hdac4 null mice displayed severe malformations of skeleton and skull, the changes in brain morphology could also result from the premature ossification of the skull which does not allow the brain to develop normally. For this reason, we generated conditonal mutants where HDAC4 is only lacking in the CNS by crossing Hdac4 $^{flox/flox}$ mice with a nestin::Cre line.

HDAC5 null mice are viable in contrast to HDAC4 mutants which die within 2 weeks of birth. Since Hdac5 was knocked out by inducing a *LacZ* expression cassette into the gene, mutant mice could be observed for onset and localization of HDAC5 expression

in embryos. Already at E10.5, HDAC5 was observed to be strongly expressed in the CNS (Chang et al. 2004).

5.4.1 Embryonic brain phenotype of HDAC4 mutant mice

5.4.1.1 HDAC4 is expressed in neurogenic regions of the embryonic brain

Before analyzing the expression pattern in embryonic brains of mutant mice, the expression was determined on coronal sections through in situ hybridization and *LacZ* staining.

In situ hybridization was performed on coronal sections of E15.5 mouse brains which had been embedded in paraffin. To test the specificity of the newly generated HDAC4 antisense probe, the corresponding sense probes were used. The Sense probe did not produce but a faint background staining and therefore proved the specificity of the staining.

The HDAC4 sense probe showed a weak overall staining, which can be interpreted as an overall background signal on the sections. The HDAC4 antisense probe led also to a staining on the entire section; however, several areas were stained more intensely. The cortical plate, the ventricular zone and subventricular zone of the cortex were specifically stained by the HDAC4 antisense probe, as well as the ventricular zone and subventricular zone of the lateral and medial ganglionic eminences (LGE and MGE). The stronger expression of the protein in neurogenic areas of the brain might suggest a role of the protein in those areas and perhaps in neurogenesis.

The expression data collected with in situ hybridization was further confirmed through X-Gal staining. E 13.5 and E 15.5 coronal sections of mutant and heterozygous brain were subjected to X-Gal staining. At 13.5 an overall staining of the sections could be observed. Areas with stronger signal were the hippocampus and the trigeminus ganglion. At E15.5 the cortical plate and frontal part of corpus callosum were stained, as well as the ventricular zone and subventricular zone of the cortex and GE.

Both in situ hybridization and X-Gal staining showed the same expression pattern of HDAC4 which I therefore believe to be specific. E15.5 embryonic brains reveal

190

HDAC4 to be localized to the VZ and SVZ of cortex and GE. Moreover, a strong expression could also been observed in cortical plate, which suggests a role in neuronal migration and layer formation.

5.4.1.2 Generation and analysis of conditional mutant animals for HDAC4

Hdac4 null mice show several changes in their CNS compared to wildtype animals, a reduced brain size and a degeneration of Purkinje neurons, to name a few. However, the brain phenotype might also derive from the fact that the prematurely ossified skull is smaller in size and prevents normal brain development. Therefore a conditional knockout line was generated by breeding Hdac4 $^{flox/flox}$ mice (Potthoff et al 2007) with mice expressing Cre through a nestin promoter (Tronche et al 1999). This removes HDAC4 selectively from neural progenitor cells and their lineage (neurons and microglia).

Western blot confirmed the absence of HDAC4 protein from embryonic spinal cord and brain at E13.5 and E15.5. At both embryonal ages, the protein amount in mutant animals corresponded to 2 – 3% of the one in wildtypes.

The nestin::Cre mouse line was generated by oocyte injection. Therefore neither the copy number nor the location of the insertion site of the transgene in the genome are known. It cannot be excluded that Cre copy number variations led to differences in the extent of Hdac4 knockdown. However, the Cre copy number does not necessarily reflect the recombinase activity of the transgene (O'Gorman et al., 1997).

Since neurogenic regions of the developing forebrain showed high expression levels of HDAC4, proliferation in the VZ of the cortex was examined. The VZ is the main source of excitatory cortical neurons. Coronal sections of wildtype and mutant brains of E15.5 mice were stained for phospho-histone H3 (PH3). Sections of corresponding position along the rostro-caudal axis of the embryo were compared to each other. In the anteriormost sections, a decrease in PH3 positive cells could be detected in mutant animals. This finding corresponds with the previous one that when all class I and II HDACs were inhibited in the embryonic brain, an increase in cell proliferation was detected in the ganglionic eminences, but not in the cortex (Shaked et al 2008). The

detailed analysis in this study revealed a slight change in proliferation in rostral telencephalon. Here, the absence of HDAC4 seems to reduce mitotic activity. A mechanism which is believed to have an important function in the context of cell proliferation is the ability of HDAC4 to repress CDK1 activity, thereby suppressing cell cycle progression (Majdzadeh et al 2008)

When non-surface dividing cells, basal progenitors in the subventricular zone, were examined through immunohistochemistry for their marker Tbr2 and costaining for TuJ1 to visualize newborn neurons, no differences in Tbr2 expressing cells or newborn neurons could be observed in mutant animals compared to wildtypes at E15.5. The pool of basal progenitors in the mutants does not seem to be different in HDAC4 conditional mutants. It must, however, be kept in mind that this analysis was by no means quantitative and that a quantitative analysis will be indispensable to draw a sound conclusion on the basal progenitor population.

This study confirms the conditional knockout of HDAC4 specifically in embryonic brain and spinal cord. Expression analysis reveals localization of in all embryonic brain regions, but especially in VZ and SVZ of the cortex and basal ganglia. The preliminary experiment to investigate the basal progenitor pool in mutant brains did not show any changes, but should be repeated in a quantitative fashion. Also gliogenesis should be examined further, possibly by immunohistochmistry to detect GFAP. Since HDAC4 was also localized to the cortical plate, changes in cell migration or layer formation would not be surprising.

Interestingly, Price and colleagues recently published a study in which the same conditional knock-out mice were generated crossing the Hdac4 $^{flox/flox}$ line (Potthoff et al. 2007) with mice expressing Cre recombinase through a nestin promoter. Their experiments revealed no gross abnormalities that could be detected based on basic histological and immunohistological analyses in conditional knock out mice of HDAC4. They also carried out locomotor tests which did not reveal any abnormalities (Price et al. 2013). This would support the finding in this study that the conditional knockout animals were viable, behaved and bred normally and did not show any obvious changes in either VZ proliferation or basal progenitors.

5.4.2   Embryonic brain phenotype of HDAC5 mutant mice

5.4.2.1   HDAC 5 is present in areas important for cortical layering and neurogenesis in the embryonic mouse brain

In situ hybridization of HDAC5 revealed that the enzyme is present ubiquitously in the embryonic brain. However, the cortical plate and the subventricular zone of the cortex showed a more intense staining. Since the cortical plate is important for cortical layer formation, the presence of HDAC5 in the structure could suggest a role in the formation of layers or neuronal migration. In the basal ganglia, both VZ and SVZ showed strong HDAC5 expression.

X-Gal staining of HDAC5 mutant mice could confirm the absence of HDAC5 from mutant tissue. A dose-dependent effect could be seen, since heterozygotes showed a weaker X-Gal staining than homozygous mutants in which X-Gal is expressed from both Hdac5 alleles. Mutant and heterozygous brains of E13.5 and E15.5 embryos were cut coronally and subjected to *LacZ* staining.

At E13.5 and E15.5 cortical plate showed a strong staining of HDAC5. At E15.5 also the subplate was stained. Presence of HDAC5 in these areas suggests a role of the enzyme in cortical layer formation. Therefore, I decided to examine cortical layer formation in early postnatal animals.

Comparing in situ hybridization and X-Gal staining for HDAC5 expression, both methods show a strong expression of HDAC5 in the cortical plate, both at E13.5 and E15.5. This hints to a role of HDAC5 in cortical layer formation or perhaps cell migration during cortical layer formation.

In order to access potential changes in cortical layer formation in HDAC5 mutant mice compared to wildtypes, coronal sections of early postnatal brains (P8) were subjected to immunohistochemistry for different cortical layer markers.

To this end, the brains of early postnatal mice (P8) were sectioned coronally and stained with markers for different cortical layers. The following markers were examined: Pax6 as a marker for apical progenitors in the VZ, Ctip2 and SatB2 as markers for outer

cortical layers, and Reelin as a marker of the marginal zone. Pax6 staining has not functioned properly, but also stainings for the other markers did not reveal distinct changes between wildtype and HDAC5 mutants.

The fact that no changes could be observed most probably reflects the insufficient quality of the staining, but could in principle also be due to the fact that HDAC5 does not have an impact on cortical layer formation.

6   Outlook

To complement the studies on signalling pathways mediating the influence of histone deacetlyases on neuro- and gliogenesis, chromatin immunoprecipitation should be carried out to reveal changes in chromatin structure upon HDAC inhibition and identify direct targets of histone deacetylases. We could show that the change in expression of Stat3 upon HDAC inhibition was not dependent on translational activity. Therefore, the promoter of Stat3 could be a direct target of acetylation. To generate a broader range of information on HDAC targets, a genome-wide approach would be appropriate. ChIP-sequencing might be a sensitive approach to identify putative target sequences.

Given that transgenic animals for HDACs are available, I would not consider continuing the RNA interference studies to analyze the effect of individual HDACs on neuro- and gliogenesis. The off-target effects were considerable and the *in vitro* system also does not reflect the situation *in vivo*.

The analysis of the brain phenotype of embryonic mutants of HDAC4 and HDAC5 is very preliminary in this study. Many aspects of brain development still need to be addressed, especially since HDAC4 and -5 have been implicated in several changes in brain function, for instance the function of HDAC4 as a neuroprotective agent.

It should be determined at which developmental stage the conditional knock-out of HDAC4 can be first observed; western blot would be a feasible approach to look into this. Cre is known to be expressed in mouse embryos as early as 10.5 dpc, therefore it should be tested at what age HDAC4 is found to be absent.

Initial experiments concerning proliferation in the cortical VZ should be repeated and also other areas, like the GE, should be investigated, where HDAC4 was also shown to be expressed.

To further investigate the developmental switch from neuro- to astrogliogenesis, basal progenitors should be examined also in immunohistochemistry for Pax6 and Tbr1 (Englund et al. 2005).

Astrogliogenesis needs to be examined more closely, especially since HDACs have been shown to influence BMP2/4 signaling which in turn in known to induce astrocytic differentiation *in vitro* (Fukuda and Taga 2005).

It would also be very interesting to investigate HDAC4/5 double knockouts for changes in brain architecture and development. Although HDAC4 and -5 have a very high sequence similarity, they seem to be expressed differentially and play different roles in the CNS.
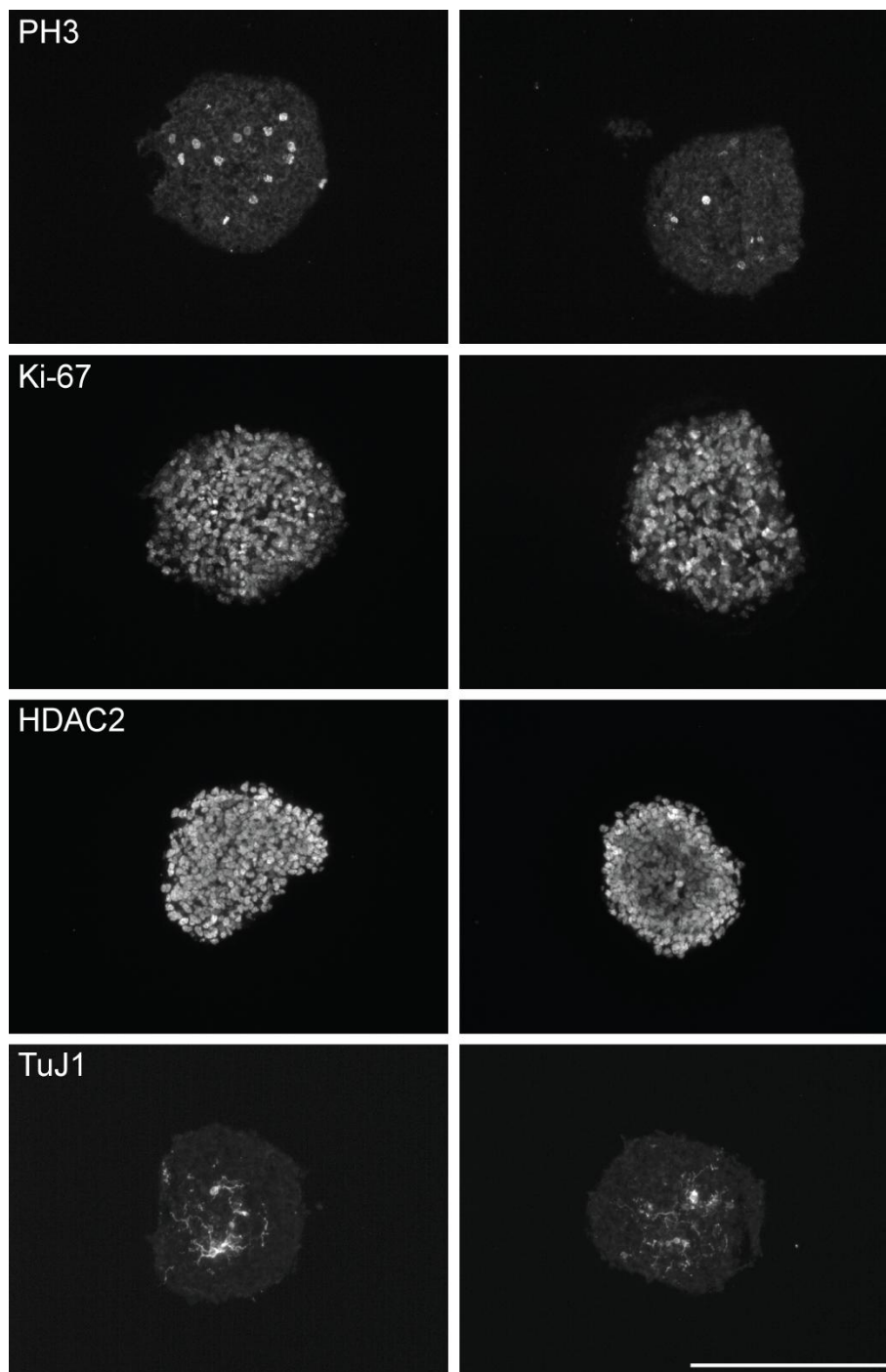
7   Appendix

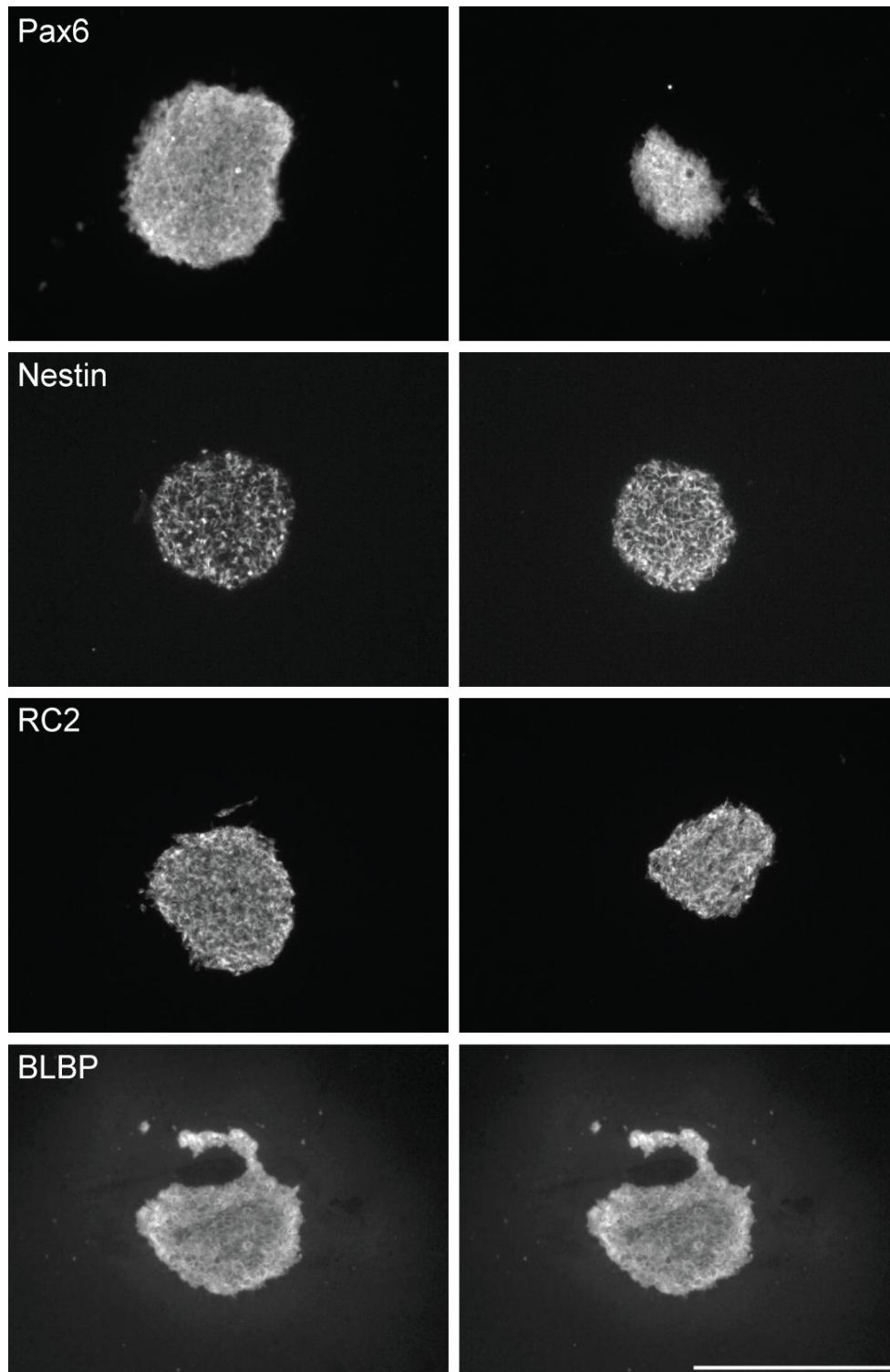## 7.1   Plasmid maps

pLKO.1-puro
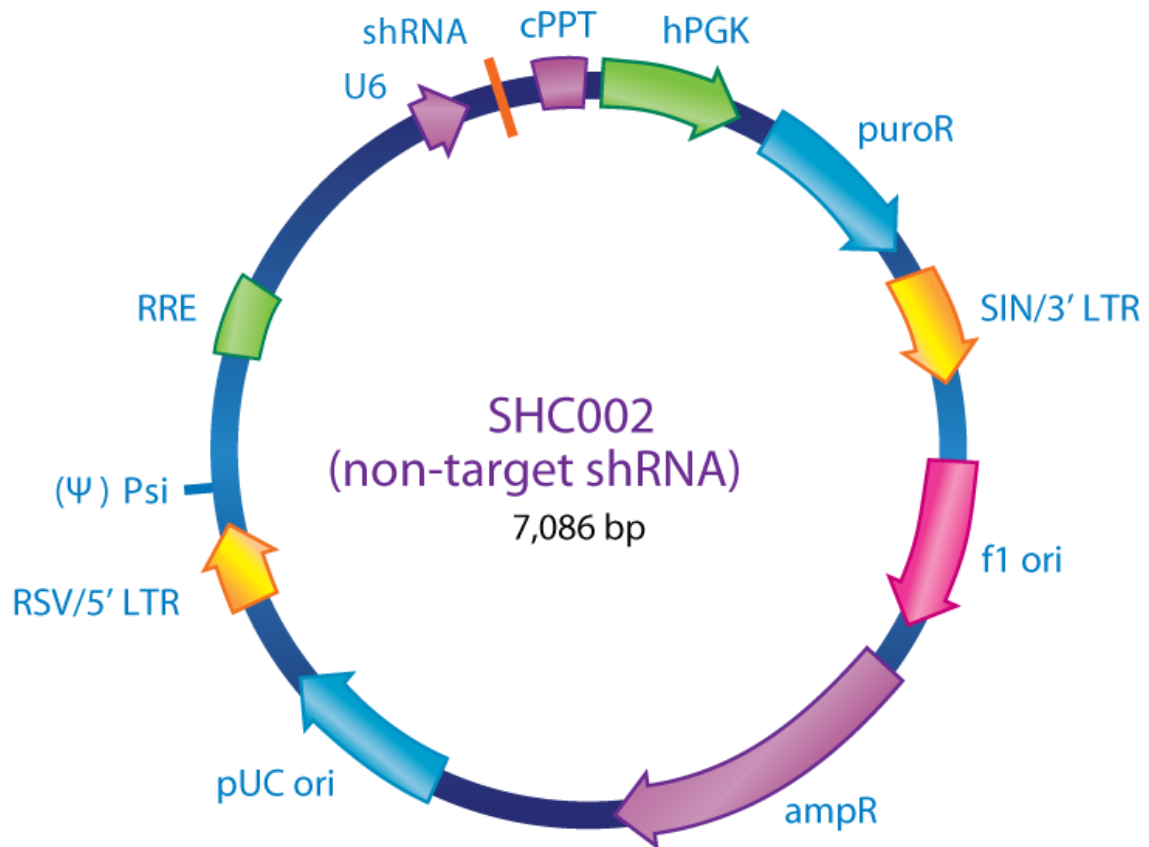
pSHC002
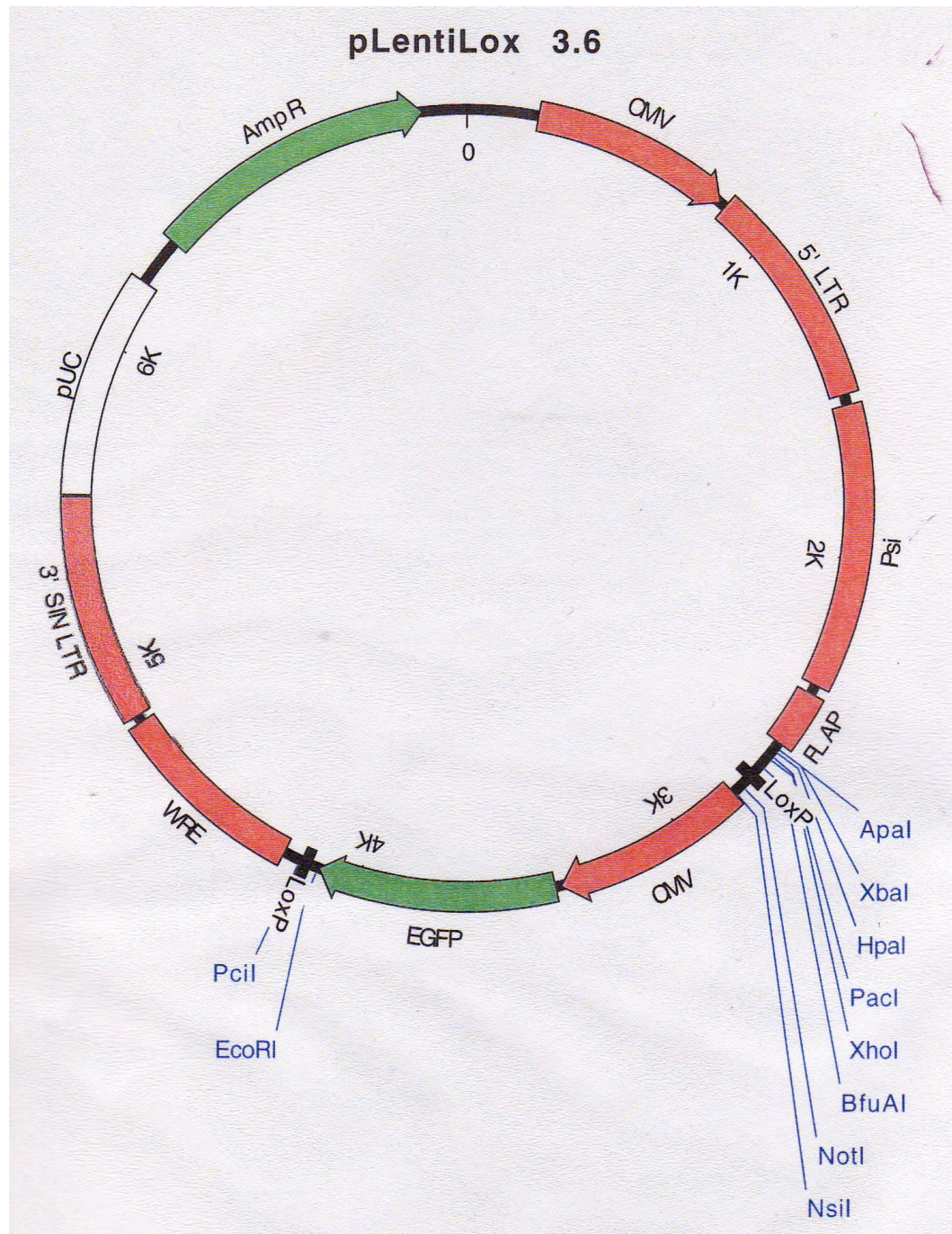
pLentiLox3.6

7.2 Immunocytochemistry of neurosphere cross-sections

Neurospheres cultured for 7 days in suspension, 10 μm cryosections. Scalebar 100 μm

Neurospheres cultured for 7 days in suspension, 10 µm cryosections. Scalebar 100 µm

Acknowledgements

I would like to express my sincere gratitude to the following people:

PD Dr. Kerry Lee Tucker for giving me the opportunity to work on this project and for helpful advice, criticism and suggestions during my project, sometimes peculiar conversation topics and gourmet lab dinners.

Prof. Dr. Achim Kirsch for providing a wonderful working environment and scientific support as well as an introduction into insect model organisms.

Prof. Dr. Hilmar Bading for evaluating this thesis, suggestions and help, as well as for serious and humorous advice.

Prof. Dr. Stefan Wölfl for our collaboration on the signaling project, a very positive approach and a great and truly collaborative atmosphere, furthermore for allowing me to use the FACSCalibur system.

Dr. Catharina Scholl for an excellent and harmonical collaboration on the signaling pathway project, interesting discussions and suggestions and excellent scientific contribution.

Dr. Johannes Backs for the Hdac4 null, Hdac4$^{flox/flox}$ and Hdac5 null mouse lines and helpful discussions.

Prof. Dr. Klaus Unsicker for allowing me to use the ABIprism sequence detection system.

Dr. Markus Islinger for expert help and support with protein biochemistry and RNA work, as well as general scientific discussions, for sharing his vast knowledge generously and above all for personal support.

Dr. Stefanie Schumacher for being a great friend and colleague, for guiding my first steps into western blotting and the great time we had together in and out of the lab.

References

Agis-Balboa RC, Pavelka Z, Kerimoglu C, Fischer A. 2013. Loss of HDAC5 impairs memory function: implications for Alzheimer's disease. *Journal of Alzheimer's disease : JAD* 33: 35-44

Allfrey VG, Faulkner R, Mirsky AE. 1964. Acetylation and Methylation of Histones and Their Possible Role in the Regulation of Rna Synthesis. *Proceedings of the National Academy of Sciences of the United States of America* 51: 786-94

Alvarez-Buylla A, Theelen M, Nottebohm F. 1990. Proliferation "hot spots" in adult avian ventricular zone reveal radial cell division. *Neuron* 5: 101-9

Anderson SA, Marin O, Horn C, Jennings K, Rubenstein JL. 2001. Distinct cortical migrations from the medial and lateral ganglionic eminences. *Development* 128: 353-63

Anthony TE, Klein C, Fishell G, Heintz N. 2004. Radial glia serve as neuronal progenitors in all regions of the central nervous system. *Neuron* 41: 881-90

Arlotta P, Molyneaux BJ, Chen J, Inoue J, Kominami R, Macklis JD. 2005. Neuronal subtype-specific genes that control corticospinal motor neuron development in vivo. *Neuron* 45: 207-21

Berger SL. 2007. The complex language of chromatin regulation during transcription. *Nature* 447: 407-12

Berger SL, Kouzarides T, Shiekhattar R, Shilatifard A. 2009. An operational definition of epigenetics. *Genes & development* 23: 781-3

Bertrand N, Castro DS, Guillemot F. 2002. Proneural genes and the specification of neural cell types. *Nature reviews. Neuroscience* 3: 517-30

Birnboim HC, Doly J. 1979. A rapid alkaline extraction procedure for screening recombinant plasmid DNA. *Nucleic acids research* 7: 1513-23

Bonaguidi MA, McGuire T, Hu M, Kan L, Samanta J, Kessler JA. 2005. LIF and BMP signaling generate separate and discrete types of GFAP-expressing cells. *Development* 132: 5503-14

Bult CJ, Eppig JT, Kadin JA, Richardson JE, Blake JA, Mouse Genome Database G. 2008. The Mouse Genome Database (MGD): mouse biology and model systems. *Nucleic acids research* 36: D724-8

Casper KB, McCarthy KD. 2006. GFAP-positive progenitor cells produce neurons and oligodendrocytes throughout the CNS. *Molecular and cellular neurosciences* 31: 676-84

Chandler VL. 2007. Paramutation: from maize to mice. *Cell* 128: 641-5

Chang S, McKinsey, T. A., Zhan, C. L., Richardson, J. A., Hill, J. A., Olson, E. N, . 2004. Histone Deacetylases 5 and 9 govern responsiveness of the heart to a subset of stress signals and play redundant roles in heart development. *Molecular and Cellular Biology* 24: 8467-76

Chen Y, Wang H, Yoon SO, Xu X, Hottiger MO, et al. 2011. HDAC-mediated deacetylation of NF-kappaB is critical for Schwann cell myelination. *Nature neuroscience* 14: 437-41

Cheung WL, Briggs SD, Allis CD. 2000. Acetylation and chromosomal functions. *Current opinion in cell biology* 12: 326-33

Cunliffe VT. 2004. Histone deacetylase 1 is required to repress Notch target gene expression during zebrafish neurogenesis and to maintain the production of motoneurones in response to hedgehog signalling. *Development* 131: 2983-95

Cunliffe VT, Casaccia-Bonnefil P. 2006. Histone deacetylase 1 is essential for oligodendrocyte specification in the zebrafish CNS. *Mechanisms of development* 123: 24-30

Doetsch F, Caille I, Lim DA, Garcia-Verdugo JM, Alvarez-Buylla A. 1999. Subventricular zone astrocytes are neural stem cells in the adult mammalian brain. *Cell* 97: 703-16

Drummond DC, Noble CO, Kirpotin DB, Guo Z, Scott GK, Benz CC. 2005. Clinical development of histone deacetylase inhibitors as anticancer agents. *Annual review of pharmacology and toxicology* 45: 495-528

Edlund T, Jessell TM. 1999. Progression from extrinsic to intrinsic signaling in cell fate specification: a view from the nervous system. *Cell* 96: 211-24

Englund C, Fink A, Lau C, Pham D, Daza RA, et al. 2005. Pax6, Tbr2, and Tbr1 are expressed sequentially by radial glia, intermediate progenitor cells, and postmitotic neurons in developing neocortex. *The Journal of neuroscience : the official journal of the Society for Neuroscience* 25: 247-51

Finnin MS, Donigian JR, Cohen A, Richon VM, Rifkind RA, et al. 1999. Structures of a histone deacetylase homologue bound to the TSA and SAHA inhibitors. *Nature* 401: 188-93

Fogarty M, Richardson WD, Kessaris N. 2005. A subset of oligodendrocytes generated from radial glia in the dorsal spinal cord. *Development* 132: 1951-9

Frotscher M, Chai X, Bock HH, Haas CA, Forster E, Zhao S. 2009. Role of Reelin in the development and maintenance of cortical lamination. *J Neural Transm* 116: 1451-5

Fukuda S, Abematsu M, Mori H, Yanagisawa M, Kagawa T, et al. 2007. Potentiation of astrogliogenesis by STAT3-mediated activation of bone morphogenetic protein-Smad signaling in neural stem cells. *Mol Cell Biol* 27: 4931-7

Graff J, Mansuy IM. 2009. Epigenetic dysregulation in cognitive disorders. *The European journal of neuroscience* 30: 1-8

Graff J, Tsai LH. 2013. The Potential of HDAC Inhibitors as Cognitive Enhancers. *Annual review of pharmacology and toxicology* 53: 311-30

Gritti A, Galli R, Vescovi AL. 2001. Cultures of stem cells of the central nervous system. In *Fedoroff, S, Richardon, A, eds. Protocols for Neuronal Cell Culture*, ed. R Galli, Vescovi, AL, pp. 173-97. Totowa, N.J.: Humana Press

Gross RE, Mehler MF, Mabie PC, Zang Z, Santschi L, Kessler JA. 1996. Bone morphogenetic proteins promote astroglial lineage commitment by mammalian subventricular zone progenitor cells. *Neuron* 17: 595-606

Grozinger CM, Hassig CA, Schreiber SL. 1999. Three proteins define a class of human histone deacetylases related to yeast Hda1p. *Proceedings of the National Academy of Sciences of the United States of America* 96: 4868-73

Grunstein M. 1997. Histone acetylation in chromatin structure and transcription. *Nature* 389: 349-52

Gu W, Roeder RG. 1997. Activation of p53 sequence-specific DNA binding by acetylation of the p53 C-terminal domain. *Cell* 90: 595-606

Guan JS, Haggarty SJ, Giacometti E, Dannenberg JH, Joseph N, et al. 2009. HDAC2 negatively regulates memory formation and synaptic plasticity. *Nature* 459: 55-60

Haberland M, Montgomery RL, Olson EN. 2009. The many roles of histone deacetylases in development and physiology: implications for disease and therapy. *Nature reviews. Genetics* 10: 32-42

Hartfuss E, Galli R, Heins N, Gotz M. 2001. Characterization of CNS precursor subtypes and radial glia. *Developmental biology* 229: 15-30

Hata A, Seoane J, Lagna G, Montalvo E, Hemmati-Brivanlou A, Massague J. 2000. OAZ uses distinct DNA- and protein-binding zinc fingers in separate BMP-Smad and Olf signaling pathways. *Cell* 100: 229-40

He F, Sun YE. 2007. Glial cells more than support cells? *The international journal of biochemistry & cell biology* 39: 661-5

Heinzel T, Lavinsky RM, Mullen TM, Soderstrom M, Laherty CD, et al. 1997. A complex containing N-CoR, mSin3 and histone deacetylase mediates transcriptional repression. *Nature* 387: 43-8

Hevner RF. 2006. From radial glia to pyramidal-projection neuron: transcription factor cascades in cerebral cortex development. *Molecular neurobiology* 33: 33-50

Hevner RF, Daza RA, Rubenstein JL, Stunnenberg H, Olavarria JF, Englund C. 2003. Beyond laminar fate: toward a molecular classification of cortical projection/pyramidal neurons. *Developmental neuroscience* 25: 139-51

Holliday R. 1990. Mechanisms for the control of gene activity during development. *Biological reviews of the Cambridge Philosophical Society* 65: 431-71

Huang Y, Myers SJ, Dingledine R. 1999. Transcriptional repression by REST: recruitment of Sin3A and histone deacetylase to neuronal genes. *Nature neuroscience* 2: 867-72

Hubbert C, Guardiola A, Shao R, Kawaguchi Y, Ito A, et al. 2002. HDAC6 is a microtubule-associated deacetylase. *Nature* 417: 455-8

Ish-Horowicz D, Burke JF. 1981. Rapid and efficient cosmid cloning. *Nucleic acids research* 9: 2989-98

Janssen C, Schmalbach S, Boeselt S, Sarlette A, Dengler R, Petri S. 2010. Differential histone deacetylase mRNA expression patterns in amyotrophic lateral sclerosis. *Journal of neuropathology and experimental neurology* 69: 573-81

Juan LJ, Shia WJ, Chen MH, Yang WM, Seto E, et al. 2000. Histone deacetylases specifically down-regulate p53-dependent gene activation. *The Journal of biological chemistry* 275: 20436-43

Kovacs JJ, Murphy PJ, Gaillard S, Zhao X, Wu JT, et al. 2005. HDAC6 regulates Hsp90 acetylation and chaperone-dependent activation of glucocorticoid receptor. *Molecular cell* 18: 601-7

Kriegstein A, Alvarez-Buylla A. 2009. The glial nature of embryonic and adult neural stem cells. *Annual review of neuroscience* 32: 149-84

Lahm A, Paolini C, Pallaoro M, Nardi MC, Jones P, et al. 2007. Unraveling the hidden catalytic activity of vertebrate class IIa histone deacetylases. *Proceedings of the National Academy of Sciences of the United States of America* 104: 17335-40

Lee KK, Workman JL. 2007. Histone acetyltransferase complexes: one size doesn't fit all. *Nature reviews. Molecular cell biology* 8: 284-95

Lu J, McKinsey TA, Zhang CL, Olson EN. 2000. Regulation of skeletal myogenesis by association of the MEF2 transcription factor with class II histone deacetylases. *Molecular cell* 6: 233-44

Luger K, Mader AW, Richmond RK, Sargent DF, Richmond TJ. 1997. Crystal structure of the nucleosome core particle at 2.8 A resolution. *Nature* 389: 251-60

MacDonald JL, Roskams AJ. 2008. Histone deacetylases 1 and 2 are expressed at distinct stages of neuro-glial development. *Developmental dynamics : an official publication of the American Association of Anatomists* 237: 2256-67

Majdzadeh N, Wang L, Morrison BE, Bassel-Duby R, Olson EN, D'Mello SR. 2008. HDAC4 inhibits cell-cycle progression and protects neurons from cell death. *Developmental neurobiology* 68: 1076-92

Malatesta P, Hack MA, Hartfuss E, Kettenmann H, Klinkert W, et al. 2003. Neuronal or glial progeny: regional differences in radial glia fate. *Neuron* 37: 751-64

Malatesta P, Hartfuss E, Gotz M. 2000. Isolation of radial glial cells by fluorescent-activated cell sorting reveals a neuronal lineage. *Development* 127: 5253-63

Marin-Husstege M, Muggironi M, Liu A, Casaccia-Bonnefil P. 2002. Histone deacetylase activity is necessary for oligodendrocyte lineage progression. *The Journal of neuroscience : the official journal of the Society for Neuroscience* 22: 10333-45

Marin O, Valiente M, Ge X, Tsai LH. 2010. Guiding neuronal cell migrations. *Cold Spring Harbor perspectives in biology* 2: a001834

McGhee JD, Felsenfeld G. 1980. Nucleosome structure. *Annual review of biochemistry* 49: 1115-56

McKinsey TA, Zhang CL, Lu J, Olson EN. 2000. Signal-dependent nuclear export of a histone deacetylase regulates muscle differentiation. *Nature* 408: 106-11

Miller CA, Campbell SL, Sweatt JD. 2008. DNA methylation and histone acetylation work in concert to regulate memory formation and synaptic plasticity. *Neurobiology of learning and memory* 89: 599-603

Miller TA, Witter DJ, Belvedere S. 2003. Histone deacetylase inhibitors. *Journal of medicinal chemistry* 46: 5097-116

Miyata T, Kawaguchi A, Saito K, Kawano M, Muto T, Ogawa M. 2004. Asymmetric production of surface-dividing and non-surface-dividing cortical progenitor cells. *Development* 131: 3133-45

Molyneaux BJ, Arlotta P, Menezes JR, Macklis JD. 2007. Neuronal subtype specification in the cerebral cortex. *Nature reviews. Neuroscience* 8: 427-37

Nakashima K, Takizawa T, Ochiai W, Yanagisawa M, Hisatsune T, et al. 2001. BMP2-mediated alteration in the developmental pathway of fetal mouse brain cells from neurogenesis to astrocytogenesis. *Proceedings of the National Academy of Sciences of the United States of America* 98: 5868-73

Nakashima K, Yanagisawa M, Arakawa H, Kimura N, Hisatsune T, et al. 1999. Synergistic signaling in fetal brain by STAT3-Smad1 complex bridged by p300. *Science* 284: 479-82

Naryzhny SN, Lee H. 2004. The post-translational modifications of proliferating cell nuclear antigen: acetylation, not phosphorylation, plays an important role in the regulation of its function. *The Journal of biological chemistry* 279: 20194-9

Nieto M, Monuki ES, Tang H, Imitola J, Haubst N, et al. 2004. Expression of Cux-1 and Cux-2 in the subventricular zone and upper layers II-IV of the cerebral cortex. *The Journal of comparative neurology* 479: 168-80

Nowakowski RS, Caviness VS, Jr., Takahashi T, Hayes NL. 2002. Population dynamics during cell proliferation and neuronogenesis in the developing murine neocortex. *Results and problems in cell differentiation* 39: 1-25

Nusinzon I, Horvath CM. 2005. Histone deacetylases as transcriptional activators? Role reversal in inducible gene regulation. *Science's STKE : signal transduction knowledge environment* 2005: re11

Ohtsuka T, Sakamoto M, Guillemot F, Kageyama R. 2001. Roles of the basic helix-loop-helix genes Hes1 and Hes5 in expansion of neural stem cells of the developing brain. *The Journal of biological chemistry* 276: 30467-74

Olejniczak M, Galka P, Krzyzosiak WJ. 2010. Sequence-non-specific effects of RNA interference triggers and microRNA regulators. *Nucleic acids research* 38: 1-16

Olsson M, Bjorklund A, Campbell K. 1998. Early specification of striatal projection neurons and interneuronal subtypes in the lateral and medial ganglionic eminence. *Neuroscience* 84: 867-76

Passier R, Zeng H, Frey N, Naya FJ, Nicol RL, et al. 2000. CaM kinase signaling induces cardiac hypertrophy and activates the MEF2 transcription factor in vivo. *The Journal of clinical investigation* 105: 1395-406

Petryniak MA, Potter GB, Rowitch DH, Rubenstein JL. 2007. Dlx1 and Dlx2 control neuronal versus oligodendroglial cell fate acquisition in the developing forebrain. *Neuron* 55: 417-33

Phiel CJ, Zhang F, Huang EY, Guenther MG, Lazar MA, Klein PS. 2001. Histone deacetylase is a direct target of valproic acid, a potent anticonvulsant, mood stabilizer, and teratogen. *The Journal of biological chemistry* 276: 36734-41

Potthoff MJ, Wu H, Arnold MA, Shelton JM, Backs J, et al. 2007. Histone deacetylase degradation and MEF2 activation promote the formation of slow-twitch myofibers. *The Journal of clinical investigation* 117: 2459-67

Powell LM, Jarman AP. 2008. Context dependence of proneural bHLH proteins. *Current opinion in genetics & development* 18: 411-7

Rakic P. 1974. Neurons in rhesus monkey visual cortex: systematic relation between time of origin and eventual disposition. *Science* 183: 425-7

Renthal W, Maze I, Krishnan V, Covington HE, 3rd, Xiao G, et al. 2007. Histone deacetylase 5 epigenetically controls behavioral adaptations to chronic emotional stimuli. *Neuron* 56: 517-29

Reynolds BA, Weiss S. 1992. Generation of neurons and astrocytes from isolated cells of the adult mammalian central nervous system. *Science* 255: 1707-10

Reynolds BA, Weiss S. 1996. Clonal and population analyses demonstrate that an EGF-responsive mammalian embryonic CNS precursor is a stem cell. *Developmental biology* 175: 1-13

Rick B. Vega KM, Junyoung Oh, Ana C. Barbosa, Xiangli Yang, Eric Meadows, John McAnally, Chris Pomajzl, John M. Shelton, James A. Richardson, Gerard Karsenty, and Eric N. Olson. 2004. Histone Deacetylase 4 Controls Chondrocyte Hypertrophy during Skeletogenesis. *Cell* 119: 555-66

Scacheri PC, Rozenblatt-Rosen O, Caplen NJ, Wolfsberg TG, Umayam L, et al. 2004. Short interfering RNAs can induce unexpected and divergent changes in the levels of untargeted proteins in mammalian cells. *Proceedings of the National Academy of Sciences of the United States of America* 101: 1892-7

Scholl C, Weissmuller K, Holenya P, Shaked-Rabi M, Tucker KL, Wolfl S. 2012. Distinct and overlapping gene regulatory networks in BMP- and HDAC-controlled cell fate determination in the embryonic forebrain. *BMC genomics* 13: 298

Sekine K, Honda T, Kawauchi T, Kubo K, Nakajima K. 2011. The outermost region of the developing cortical plate is crucial for both the switch of the radial migration mode and the Dab1-dependent "inside-out" lamination in the neocortex. *The Journal of neuroscience : the official journal of the Society for Neuroscience* 31: 9426-39

Shahbazian MD, Grunstein M. 2007. Functions of site-specific histone acetylation and deacetylation. *Annual review of biochemistry* 76: 75-100

Shaked M, Weissmuller K, Svoboda H, Hortschansky P, Nishino N, et al. 2008. Histone deacetylases control neurogenesis in embryonic brain by inhibition of BMP2/4 signaling. *PloS one* 3: e2668

Shen S, Li J, Casaccia-Bonnefil P. 2005. Histone modifications affect timing of oligodendrocyte progenitor differentiation in the developing rat brain. *The Journal of cell biology* 169: 577-89

Shogren-Knaak M, Ishii H, Sun JM, Pazin MJ, Davie JR, Peterson CL. 2006. Histone H4-K16 acetylation controls chromatin structure and protein interactions. *Science* 311: 844-7

Shute RE, Dunlap B, Rich DH. 1987. Analogues of the cytostatic and antimitogenic agents chlamydocin and HC-toxin: synthesis and biological activity of chloromethyl ketone and diazomethyl ketone functionalized cyclic tetrapeptides. *Journal of medicinal chemistry* 30: 71-8

Spassky N, Goujet-Zalc C, Parmantier E, Olivier C, Martinez S, et al. 1998. Multiple restricted origin of oligodendrocytes. *The Journal of neuroscience : the official journal of the Society for Neuroscience* 18: 8331-43

Tarabykin V, Stoykova A, Usman N, Gruss P. 2001. Cortical upper layer neurons derive from the subventricular zone as indicated by Svet1 gene expression. *Development* 128: 1983-93

Tekki-Kessaris N, Woodruff R, Hall AC, Gaffield W, Kimura S, et al. 2001. Hedgehog-dependent oligodendrocyte lineage specification in the telencephalon. *Development* 128: 2545-54

Tomita A, Towatari M, Tsuzuki S, Hayakawa F, Kosugi H, et al. 2000. c-Myb acetylation at the carboxyl-terminal conserved domain by transcriptional co-activator p300. *Oncogene* 19: 444-51

Tronche F, Kellendonk C, Kretz O, Gass P, Anlag K, et al. 1999. Disruption of the glucocorticoid receptor gene in the nervous system results in reduced anxiety. *Nature genetics* 23: 99-103

Tsankova NM, Berton O, Renthal W, Kumar A, Neve RL, Nestler EJ. 2006. Sustained hippocampal chromatin regulation in a mouse model of depression and antidepressant action. *Nature neuroscience* 9: 519-25

Tucker KL. 2001. Methylated cytosine and the brain: a new base for neuroscience. *Neuron* 30: 649-52

Tucker KL, Meyer M, Barde YA. 2001. Neurotrophins are required for nerve growth during development. *Nature neuroscience* 4: 29-37

Urdinguio RG, Sanchez-Mut JV, Esteller M. 2009. Epigenetic mechanisms in neurological diseases: genes, syndromes, and therapies. *Lancet neurology* 8: 1056-72

Vecsey CG, Hawk JD, Lattal KM, Stein JM, Fabian SA, et al. 2007. Histone deacetylase inhibitors enhance memory and synaptic plasticity via CREB:CBP-dependent transcriptional activation. *The Journal of neuroscience : the official journal of the Society for Neuroscience* 27: 6128-40

Vega RB, Harrison BC, Meadows E, Roberts CR, Papst PJ, et al. 2004a. Protein kinases C and D mediate agonist-dependent cardiac hypertrophy through nuclear export of histone deacetylase 5. *Mol Cell Biol* 24: 8374-85

Vega RB, Matsuda K, Oh J, Barbosa AC, Yang X, et al. 2004b. Histone deacetylase 4 controls chondrocyte hypertrophy during skeletogenesis. *Cell* 119: 555-66

Vescovi AL, Reynolds BA, Fraser DD, Weiss S. 1993. bFGF regulates the proliferative fate of unipotent (neuronal) and bipotent (neuronal/astroglial) EGF-generated CNS progenitor cells. *Neuron* 11: 951-66

Waterston RH, Lindblad-Toh K, Birney E, Rogers J, Abril JF, et al. 2002. Initial sequencing and comparative analysis of the mouse genome. *Nature* 420: 520-62

Wichterle H, Turnbull DH, Nery S, Fishell G, Alvarez-Buylla A. 2001. In utero fate mapping reveals distinct migratory pathways and fates of neurons born in the mammalian basal forebrain. *Development* 128: 3759-71

Yamaguchi M, Tonou-Fujimori N, Komori A, Maeda R, Nojima Y, et al. 2005. Histone deacetylase 1 regulates retinal neurogenesis in zebrafish by suppressing Wnt and Notch signaling pathways. *Development* 132: 3027-43

Zhang CL, McKinsey TA, Chang S, Antos CL, Hill JA, Olson EN. 2002. Class II histone deacetylases act as signal-responsive repressors of cardiac hypertrophy. *Cell* 110: 479-88

Zimmerman L, Parr B, Lendahl U, Cunningham M, McKay R, et al. 1994. Independent regulatory elements in the nestin gene direct transgene expression to neural stem cells or muscle precursors. *Neuron* 12: 11-24